



Brejevs, Vitalijs (2021) *On slice alternating 3-braid closures and Stein-fillable genus one open books*. PhD thesis.

<https://theses.gla.ac.uk/82659/>

Copyright and moral rights for this work are retained by the author

A copy can be downloaded for personal non-commercial research or study, without prior permission or charge

This work cannot be reproduced or quoted extensively from without first obtaining permission in writing from the author

The content must not be changed in any way or sold commercially in any format or medium without the formal permission of the author

When referring to this work, full bibliographic details including the author, title, awarding institution and date of the thesis must be given

Enlighten: Theses

<https://theses.gla.ac.uk/>  
[research-enlighten@glasgow.ac.uk](mailto:research-enlighten@glasgow.ac.uk)

---

# On slice alternating 3-braid closures and Stein-fillable genus one open books

---

by  
**Vitalijs Brejevs**

A thesis submitted in fulfilment of the requirements  
for the degree of

Doctor of Philosophy

at the

School of Mathematics & Statistics  
College of Science & Engineering  
University of Glasgow



September 2021

*To my mother and grandmother*

# Abstract

This thesis consists of two parts, each concerning a different question about the relationship of 3- and 4-manifolds. The first part is devoted to a generalisation of the slice–ribbon conjecture to non-zero determinant links that can be obtained as closures of alternating 3-braids, while the second investigates the connection between Stein fillings of contact manifolds and positive monodromy factorisations of supporting open books.

In the first part, we obtain a conditional classification of alternating 3-braid closures whose double branched covers are unobstructed from bounding rational homology 4-balls by Donaldson’s theorem. This result has been independently superseded by Jonathan Simone who provided an unconditional classification that consists of five infinite families. Based on Simone’s work, we confirm the generalised slice–ribbon conjecture for four of these families by explicitly constructing ribbon surfaces via band moves. We also show that the remaining family contains infinitely many ribbon links and employ twisted Alexander polynomials to conclude the enumeration of smoothly slice knots that can be given as closures of alternating 3-braids with at most 20 crossings.

In the second part, we apply the theory of surface mapping class groups to the study of symplectic fillings of contact manifolds. For a contact manifold supported by a genus zero open book, there exists a correspondence between Stein fillings of the manifold and factorisations of the monodromy of the open book into positive Dehn twists; this correspondence is known to fail in genera greater than one. We present the results of joint work with Andy Wand in which we exhibit an infinite family of Stein-fillable contact manifolds supported by open books with two-holed torus pages whose monodromies do not admit positive factorisations. These are the first known such examples of genus one, and their existence implies that the above correspondence only holds in the planar case. Our proof crucially relies on transverse contact surgery tools developed by James Conway and observations about lantern relations in the mapping class group of the two-holed torus.

# Contents

---

<b>1</b>	<b>Introduction</b>	<b>1</b>
1.1	The slice–ribbon conjecture for alternating 3-braid closures . . . . .	2
1.1.1	Classification of lattice embeddings . . . . .	5
1.1.2	Ribbon surfaces . . . . .	6
1.1.3	Twisted Alexander polynomials . . . . .	7
1.2	Stein-fillable genus one open books . . . . .	8
<b>I</b>	<b>On slice alternating 3-braid closures</b>	<b>11</b>
<b>2</b>	<b>Preliminaries</b>	<b>12</b>
2.1	Alternating links and 3-braids . . . . .	12
2.2	Surfaces bounded by links . . . . .	15
2.3	Goeritz matrices and Tait graphs . . . . .	16
2.4	Lattice obstructions to $\chi$ -sliceness . . . . .	22
<b>3</b>	<b>Classification of embeddable ABCs</b>	<b>24</b>
3.1	Lattice embeddings as labelled Tait graphs . . . . .	24
3.2	Operations on labelled Tait graphs . . . . .	29
3.3	Properties of embeddable ABCs . . . . .	30
3.4	Contraction classes of embeddable ABCs . . . . .	34
3.4.1	Case I: $p_1 > 0$ . . . . .	34
3.4.2	Case II: $p_1 = 0$ . . . . .	36
3.5	Relation to Simone’s classification . . . . .	45
<b>4</b>	<b>Ribbon surfaces for ABCs</b>	<b>48</b>
4.1	Ribbon surfaces for $\mathcal{S}_{2a} \cup \mathcal{S}_{2b} \cup \mathcal{S}_{2d} \cup \mathcal{S}_{2e}$ . . . . .	48
4.2	The case of $\mathcal{S}_{2c} \setminus (\mathcal{S}_{2a} \cup \mathcal{S}_{2b} \cup \mathcal{S}_{2d} \cup \mathcal{S}_{2e})$ . . . . .	55
<b>5</b>	<b>TAPs of some ABC knots</b>	<b>60</b>
5.1	Main definitions and the sliceness obstruction . . . . .	60
5.2	Computing TAPs for $K_1$ , $K_2$ and $K_3$ . . . . .	63

5.2.1	Seifert matrices . . . . .	64
5.2.2	Structure of $H_1(\Sigma_3(K_i))$ . . . . .	64
5.2.3	Blanchfield and linking forms . . . . .	66
5.2.4	Metabolisers of $H_1(\Sigma_3(K_i))$ . . . . .	67
5.2.5	Characters vanishing on the metabolisers . . . . .	68
5.2.6	Representations of knot groups . . . . .	68
5.2.7	Calculating TAPs . . . . .	70
5.2.8	Obstructing sliceness . . . . .	72
<b>II</b>	<b>On Stein-fillable genus one open books</b>	<b>74</b>
<b>6</b>	<b>Preliminaries</b>	<b>75</b>
6.1	Mapping class groups and open books . . . . .	76
6.2	Contact structures . . . . .	77
6.3	Giroux correspondence . . . . .	80
6.4	Symplectic fillability . . . . .	81
<b>7</b>	<b>Non-positive Stein-fillable open books of genus one</b>	<b>84</b>
7.1	The family $(Y_n, \xi_n)$ . . . . .	84
7.1.1	Transverse contact surgery . . . . .	85
7.1.2	Open books for transverse-surgered manifolds . . . . .	85
7.1.3	Transverse +5–surgery on a right-handed trefoil . . . . .	86
7.2	Non-positivity of $\varphi_n$ . . . . .	87
<b>A</b>	<b>Script for computing lattice embeddings for ABCs</b>	<b>94</b>
<b>B</b>	<b>Scripts for computing TAPs for <math>K_1</math>, <math>K_2</math> and <math>K_3</math></b>	<b>103</b>
<b>C</b>	<b>Reduced TAPs for <math>K_1</math>, <math>K_2</math> and <math>K_3</math></b>	<b>116</b>

# List of Figures

---

Figure 1.1	An infinite family of non-positive Stein-fillable open books . . . . .	9
Figure 2.1	Ribbon surface for the square knot . . . . .	17
Figure 2.2	Incidence number of a crossing . . . . .	18
Figure 2.3	Generic alternating 3-braid closure . . . . .	19
Figure 2.4	Chessboard colouring of an alternating 3-braid closure . . . . .	20
Figure 3.1	Effect of a contraction on the link diagram . . . . .	30
Figure 4.1	Moves for cancellation of dual sub-braids . . . . .	50
Figure 4.2	Example of cancelling dual sub-braids . . . . .	50
Figure 4.3	Ribbon surfaces for the $\mathcal{S}_{2a}$ family . . . . .	51
Figure 4.4	Ribbon surfaces for the $\mathcal{S}_{2b}$ family . . . . .	52
Figure 4.5	Ribbon surfaces for the $\mathcal{S}_{2d}$ family . . . . .	53
Figure 4.6	Ribbon surfaces for the $\mathcal{S}_{2e}$ family . . . . .	54
Figure 4.7	Ribbon surfaces for an infinite subfamily of $\mathcal{S}_{2e}^\dagger$ . . . . .	59
Figure 5.1	Seifert surface for $K_1$ . . . . .	65
Figure 5.2	Arc labels for a Wirtinger presentation of $\pi_1(X_1)$ . . . . .	71
Figure 6.1	Positive Dehn twist . . . . .	76
Figure 6.2	Standard and overtwisted contact structures on $\mathbb{R}^3$ . . . . .	78
Figure 7.1	Open books for $(S^3, \xi_{\text{std}})$ and $(Y_0, \xi_0)$ . . . . .	86
Figure 7.2	Topological +5-surgery on a right-handed trefoil . . . . .	88
Figure 7.3	Lantern relation on $\Sigma_{0,4}$ . . . . .	89
Figure 7.4	Seifert fibred manifold $M(e_0; r_1, r_2, r_3)$ . . . . .	90
Figure 7.5	Inadmissible transverse +2-surgery on a right-handed trefoil . . . . .	91
Figure 7.6	Topological +2-surgery on a right-handed trefoil . . . . .	92

## Acknowledgements

I would like to express my deep gratitude to my supervisors Brendan Owens and Andy Wand for their patient support, tactful guidance and invaluable advice about both mathematics and not. I have greatly benefited from the environment at the University of Glasgow, and I am thankful for the wealth of opportunity to grow as a student, a researcher and a person that I have been afforded over the eight years I have spent here so far.

I also wish to thank my fellow PhD students who always made it a pleasure to come into the office when it was possible, and to log on to Zoom when it was not. Of them, I am particularly grateful to James for the unyielding spirit, Ross for the contagious enthusiasm (and help with some algebra), Niall for the light touch, and Okke for being a great friend and flatmate. More thanks are due to Dave, Jamie, Kellan, Luke, Mikel, Sarah, and everyone else.

I am endlessly indebted for my family's unfailing trust and encouragement over these long years.

This work would not have been possible without the generous support and accommodation of the Carnegie Trust for the Universities of Scotland.

## **Author's declaration**

I declare that, except where explicit reference is made to the contribution of others, this dissertation is the result of my own work and has not been submitted for any other degree at the University of Glasgow or any other institution.

# Introduction

---

The overarching theme of this thesis is the relationship between 4-manifolds and their 3-manifold boundaries along with its connection to the theory of links and surface mappings. Understanding how topological and geometrical properties of 4-manifolds impose constraints on their boundaries can often shed light on the objects of lower dimension that determine said boundaries. Conversely, manipulations of intuitively tangible one- and two-dimensional objects can be a way to obtain deep insight into the wild world of 4-manifolds.

We study this relationship for two categories of 4-manifolds: smooth and symplectic. In the first case, we are concerned with *rational homology 4-balls* that are bounded by 3-manifolds associated to a class of links called *alternating 3-braid closures*. Common techniques for investigating the existence of said rational homology 4-balls ultimately rely on the gauge-theoretic *Donaldson's theorem*, though in practice they amount to combinatorial analysis of lattice embeddings. This approach enables us to make progress towards proving a generalisation of the enduring *slice-ribbon conjecture*, which relates different ways of how a link in the 3-sphere can bound a properly embedded surface in the 4-ball. Our methods include explicit constructions of surfaces via *band moves* on link diagrams, coupled with applications of a deep homological obstruction to the existence of such surfaces arising from *twisted Alexander polynomials*.

In the second case, we turn our attention to *contact 3-manifolds*, namely, 3-manifolds equipped with *contact structures*. Such manifolds admit supporting *open book decompositions*, characterised by a surface with boundary, called the *page*, and its self-diffeomorphism, called the *monodromy*. Contact manifolds occur naturally as boundaries of symplectic 4-manifolds, and there exist various notions of compatibility between contact and symplectic manifolds; one strong such notion is called *Stein fillability*. Stein fillings of a given contact manifold have been conjectured to correspond with positive factorisations of monodromies of supporting open book decompositions, which is indeed the case for decompositions with planar pages. However, counterexamples have been discovered showing that this correspondence fails for page genera greater than one. By considering self-diffeomorphisms of the two-holed torus, we extend this line of counterexamples to genus one open book decompositions.

## Thesis structure

In Chapter 1, we give a more detailed overview of the contents of the thesis, including some historical background and a summary of our main results. The rest of the thesis is divided into two independent parts, with Chapters 2 to 5 comprising Part I and Chapters 6 and 7 comprising Part II.

In Chapter 2 we present basic material on alternating links and 3-braids, enabling the reader to follow Chapter 3 that culminates in a partial classification of alternating 3-braid closures whose double branched covers are unobstructed by Donaldson’s theorem from bounding rational homology 4-balls. In Chapter 4, we use Jonathan Simone’s full classification to resolve the generalised slice–ribbon conjecture for several infinite families of alternating 3-braid closures by constructing ribbon surfaces bounded by those families. Using twisted Alexander polynomials, in Chapter 5 we prove that three particular alternating 3-braid closure knots are not slice; this concludes the enumeration of slice knots that can be obtained by taking closures of alternating 3-braids with up to 20 crossings. Chapters 4 and 5 are independent from the technical Chapter 3.

Chapter 6 focusses on the basics of contact topology, such as contact structures, open book decompositions and symplectic fillings. Finally, Chapter 7 contains a construction of an infinite family of Stein-fillable contact manifolds whose supporting open books have pages of genus one and non-positive monodromies.

The work in Chapter 3 has been carried out independently and then largely superseded by [Sim20]; we discuss the relationship between the two classifications in Section 3.5. Chapters 4 and 5 are based on the preprint [Bre20] by the author. Original results in Chapter 7 have first appeared in the joint work [BW21] by the author and Andy Wand.

## § 1.1 | The slice–ribbon conjecture for alternating 3-braid closures

Recall that a knot  $K \subset S^3$  is called *smoothly slice* (henceforth, just *slice*) if there exists a smooth proper embedding  $\psi : D^2 \hookrightarrow D^4$  such that  $K$  is the boundary of  $S := \psi(D^2)$ , where  $S$  is called a *slice disc* of  $K$ . Recall also that  $K$  is *ribbon* if  $\psi$  may be chosen such that the radial distance function  $r : D^4 \rightarrow [0, 1]$  induces a handle decomposition of  $S$  with only 0- and 1-handles, in which case  $S$  is called a *ribbon disc*. A long-standing question of Fox [Fox62] asks whether every slice knot is, in fact, ribbon; ultimately, this question concerns our basic understanding of surface knotting in 4-manifolds. The answer has been shown to be affirmative for some familiar classes of knots, for example, 2-bridge knots by Lisca [Lis07], certain 3-strand pretzel knots by Greene and Jabuka [GJ11], and various Montesinos knots by Lecuona [Lec12; Lec15]. Common to all of this work is the use of Donaldson’s ‘Theorem A’ [Don87] to obstruct sliceness, detailed in the following.

It is well-known that the double cover of  $S^3$  branched over a slice knot  $K$ , de-

noted  $\Sigma_2(S^3, K)$ , is the boundary of a *rational (homology) ball*  $B$ , that is, a 4-manifold  $B$  that has the same homology with  $\mathbb{Q}$ -coefficients as  $D^4$  (for example, see [Kau87, Lemma 17.2]). If  $\Sigma_2(S^3, K)$  branched over a putatively slice knot is known to also bound some 4-manifold  $X$  with definite intersection form  $Q_X$ , then one can glue  $X$  and  $-B$  together along  $\Sigma_2(S^3, K)$  to obtain a smooth closed manifold  $Y$  with intersection form  $Q_Y$ . It then follows from a Mayer–Vietoris argument and Donaldson’s theorem that there exists an embedding of the lattice  $\Lambda := (H_2(X; \mathbb{Z})/\text{Tors}, Q_X)$  into the standard integral lattice of the same rank; by a *lattice* we always mean a freely finitely generated abelian group with an integral-valued symmetric bilinear pairing. Donald and Owens [DO12] have shown that an analogous procedure applies when  $K$  is replaced in the above discussion by a link  $L$  that bounds a properly embedded surface  $S \subset D^4$  of Euler characteristic one ( $\chi(S) = 1$ ) with no closed components, in which case we say that  $L$  is  $\chi$ -*slice* and  $S$  is a *slice surface*. Similarly, if  $S$  only has 0- and 1-handles, then we say that  $L$  is  $\chi$ -*ribbon* and  $S$  is a *ribbon surface*. The definitions of ‘ $\chi$ -slice’ and ‘ $\chi$ -ribbon’ coincide with the definitions of ‘slice’ and ‘ribbon’ in the case of knots, thus allowing a natural generalisation of Fox’s question: we refer to the presumed equality of ‘ $\chi$ -slice’ and ‘ $\chi$ -ribbon’ as the *slice–ribbon conjecture*. No counterexamples to this generalisation are currently known to exist, making it an attractive and logical continuation of the slice–ribbon pursuit.

Our interest lies in *alternating links*, that is, links admitting diagrams in which over- and undercrossings alternate as one traverses along any of the components. To any diagram  $D$  of a link  $L$  one can associate a pair of surfaces, called *black* and *white surfaces* and denoted  $F_b$  and  $F_w$ , respectively. Both  $H_1(F_b; \mathbb{Z})$  and  $H_1(F_w; \mathbb{Z})$  are presented by *Goeritz matrices*  $G_b$  and  $G_w$  that are adjacency matrices of the *black* and *white Tait (multi-)graphs* constructed from  $D$ . If  $D$  is an alternating diagram, then, subject to choosing appropriate conventions, both Goeritz matrices are negative-definite.<sup>1</sup> Also, the determinants of both Goeritz matrices are equal and independent of the choice of  $D$ , hence we can speak of the *determinant* of  $L$ .

Given an alternating diagram  $D$  of a link  $L$  with a choice of black and white surfaces, definite 4-manifolds bounded by  $\Sigma_2(S^3, L)$  are readily available by the work of Gordon and Litherland [GL78]. Specifically, they have shown that there exists a pair of 4-manifolds  $X_b$  and  $X_w$  both bounded by  $\Sigma_2(S^3, L)$  such that their respective intersection forms are represented by the two Goeritz matrices  $G_w$  and  $G_b$ ; we denote the lattices arising from  $X_b$  and  $X_w$  by  $\Lambda_b$  and  $\Lambda_w$ , respectively. Generators of  $\Lambda_b$  (respectively,  $\Lambda_w$ ) are in bijection with all but one vertex of the white (respectively, black) Tait graph, and pairings between them can also be read off the graph directly. Thus, one strategy of proving the slice–ribbon conjecture for a class of alternating links is to determine the subclass of said links for which both  $\Lambda_w$  and  $\Lambda_b$  embed into the standard negative-definite integral lattice of the same rank, and then construct ribbon

<sup>1</sup>This property fully characterises alternating links, as shown by Greene [Gre17] and Howie [How17].

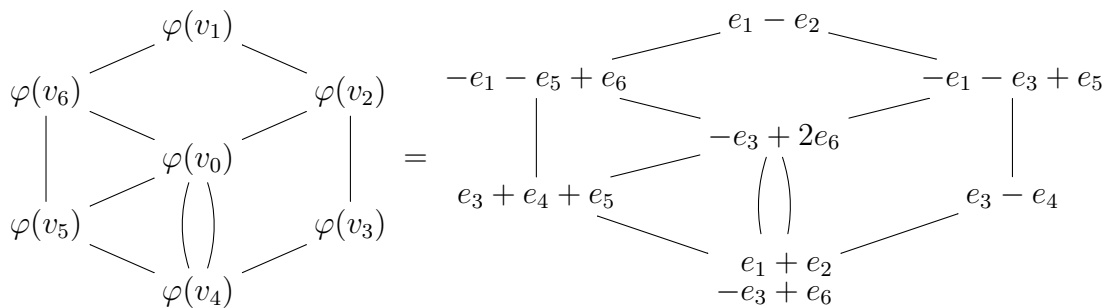
surfaces bounded by all links in that subclass. However, the fact that embeddings of  $\Lambda_w$  and  $\Lambda_b$  for some link  $L$  exist does not a priori guarantee that so do slice and ribbon surfaces bounded by  $L$ .

In this thesis, we are concerned specifically with the slice–ribbon conjecture for *alternating 3-braid closures*, namely, for links that can be obtained by taking closures of alternating braids on three strands (by an *alternating braid* we mean, analogously, a braid such that along any strand, over- and undercrossing alternate). This is an ample and important class of links that contains so-called *Turk’s head knots* whose sliceness is famously unknown except for a few examples, some of which are slice and some are not [Sar10; AMMMPS20]. From a lattice-theoretic perspective, 3-braid closures have been studied by Lisca [Lis17] who classified all 3-braid closure knots of finite concordance order.

It follows from the work of Murasugi [Mur74] that any alternating 3-braid closure with non-zero determinant is isotopic to the closure of precisely one 3-braid in the set

$$\mathcal{A} = \left\{ \sigma_1^{a_1} \sigma_2^{-b_1} \sigma_1^{a_2} \sigma_2^{-b_2} \dots \sigma_1^{a_n} \sigma_2^{-b_n} \mid n \geq 1 \text{ and } a_i, b_i \geq 1 \text{ for all } 1 \leq i \leq n \right\},$$

where  $\sigma_1$  and  $\sigma_2$  are the standard generators of  $B_3$ , the group of braids on three strands. The Tait graphs for such alternating 3-braid closures are *wheel (multi-)graphs*: they consist of a simple cycle (the rim) with an additional vertex placed on the inside that is joined to each vertex in the cycle by multiple (possibly zero) edges (the spokes). Vertices  $v_1, \dots, v_n$  in the rim of the white Tait graph  $\Gamma_w$  of an alternating 3-braid closure  $\hat{\beta}$  can be identified with the generators of the lattice  $\Lambda_b$ , while the central vertex  $v_0$  can be thought of as the negative sum of all generators (analogously for the opposite colour). If  $\text{rk } \Lambda_b = n$ , we can represent an embedding  $\varphi : \Lambda_b \hookrightarrow (\mathbb{Z}^n, -I)$  by *labelling* the vertices of  $\Gamma_w$  with the images  $\varphi(v_i)$  for  $i = 0, \dots, n$ . For example, consider the closure of the 3-braid  $\sigma_1^2 \sigma_2^{-1} \sigma_1^2 \sigma_2^{-2} \sigma_1 \sigma_2^{-1} \sigma_1 \sigma_2^{-1}$  whose white Tait graph  $\Gamma_w$  has six vertices on the rim, and choose a basis  $\{e_1, \dots, e_6\}$  for  $(\mathbb{Z}^6, -I)$  such that  $e_i \cdot e_j = -\delta_{ij}$ . Then one choice of  $\varphi$  is determined by



An important operation that can be applied to labelled Tait graphs of alternating links is called *contraction*. A contraction of a labelled Tait graph corresponding to the lattice  $\Lambda_b$  of rank  $n$  amounts to deleting one of the edges of the graph, contracting another (merging two vertices into one), and then transforming the labels so that

the resulting labelled graph represents an embedding of a lattice  $\Lambda'_b$  of rank  $n - 1$  into  $(\mathbb{Z}^{n-1}, -I)$ . Say that a contraction on a labelled wheel graph is *preserving* if it again yields a labelled wheel graph. Lisca was the first to demonstrate the power of contractions by characterising labellings of linear graphs in his work on 2-bridge knots [Lis07]; Greene and Owens later conjectured that a non-split alternating link  $L$  admits labelled black and white Tait graphs  $\Gamma_b$  and  $\Gamma_w$  that can be reduced to the Tait graphs of the unknot by a sequence of contractions if and only if  $\Sigma_2(S^3, L)$  bounds a rational ball.

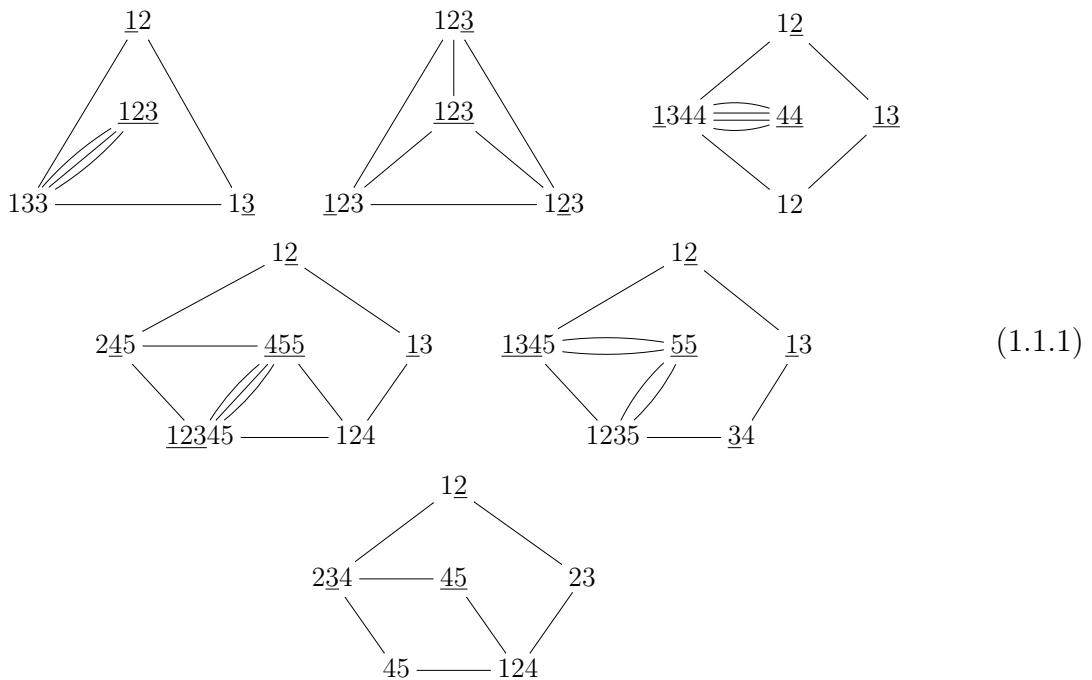
**§ 1.1.1 | Classification of lattice embeddings**

We now sketch our main lattice-theoretic result. Choose  $\beta \in \mathcal{A}$  and consider its closure  $\widehat{\beta}$ . If  $\text{rk } \Lambda_b = \text{rk } \Lambda_w$ , then denote either of them by  $\Lambda$ , otherwise denote by  $\Lambda$  the lattice of higher rank, with  $\text{rk } \Lambda = n$  in either case; write  $\Gamma$  for the Tait graph of colour opposite to  $\Lambda$  and assume that  $\Lambda$  is generated by  $\{v_1, \dots, v_n\}$ . Let  $\{e_1, \dots, e_n\}$  be a *canonical* basis of  $(\mathbb{Z}^n, -I)$  with  $e_i \cdot e_j = -\delta_{ij}$  and suppose there exists an embedding  $\varphi : \Lambda \hookrightarrow (\mathbb{Z}^n, -I)$  given by

$$v_i \mapsto \sum_{j=1}^n \alpha_i^j e_j$$

that satisfies the technical condition we formulate in Conjecture 3.3.2: roughly, it says that  $|\alpha_i^j|$  cannot get too big. If  $\alpha_i^j > 0$ , write the symbol  $j$  on the corresponding vertex of  $\Gamma$  repeated  $|\alpha_i^j|$  times; if  $\alpha_i^j < 0$ , then do the same with the symbol  $\underline{j}$ . With this setup, we have:

**Theorem 1.** If  $n \geq 5$ , then, up to a change of canonical basis of  $(\mathbb{Z}^n, -I)$ , the labelled graph  $\Gamma$  admits a sequence of preserving contractions to exactly one of the base cases in Diagram (1.1.1). Moreover,  $\Gamma$  admits a sequence of (possibly non-preserving) contractions to the labelled graph for the unknot, represented as the closure of  $\sigma_1\sigma_2^{-1}$ .



We posed Conjecture 3.3.2 after directly considering all embeddings of lattices arising from closures of alternating 3-braids with up to 20 crossings; these embeddings were obtained using the SageMath script in Appendix A. The salient implications of the conjecture are that  $|\alpha_i^j| \leq 2$  for all  $i, j = 1, \dots, n$ , and there is at most one  $j$  such that  $\sum_{i=1}^n (\alpha_i^j)^2 > 4$ . These implications enabled us, in particular, to reach the above classification without appealing to [Lis07]. However, the proof of the conjecture itself remained elusive.

### § 1.1.2 | Ribbon surfaces

While we were working on proving Conjecture 3.3.2, Jonathan Simone has independently announced a preprint [Sim20] in which he applied results of Lisca on embeddings of linear lattices to give a full and unconditional classification of all alternating 3-braid closures with non-zero determinant whose double branched covers bound rational balls. Simone’s work implies that every such link gives rise to a lattice that admits an embedding satisfying our conjecture, hence that our classification describes the same subset of alternating 3-braid closures. However, Simone’s classification is not concerned with the properties of embeddings themselves and is phrased in terms of *associated strings* that can be assigned to every alternating 3-braid; we may confuse the associated string of  $\beta \in \mathcal{A}$  with the 3-braid itself or its closure  $\widehat{\beta}$ . Deferring the detailed discussion of associated strings to Chapter 2, we present this classification in an abridged form as follows.

**Theorem** ([Sim20]). If  $\Sigma_2(S^3, \widehat{\beta})$  bounds a rational ball for some  $\beta \in \mathcal{A}$ , then  $\widehat{\beta}$  lies in one of the five infinite families  $\mathcal{S}_{2a}$ ,  $\mathcal{S}_{2b}$ ,  $\mathcal{S}_{2c}$ ,  $\mathcal{S}_{2d}$  and  $\mathcal{S}_{2e}$ .

Write  $\mathcal{S}_2$  for the union of all five families. Each one of  $\mathcal{S}_{2d}$  and  $\mathcal{S}_{2e}$  is disjoint from every other family, but families  $\mathcal{S}_{2a}$ ,  $\mathcal{S}_{2b}$  and  $\mathcal{S}_{2c}$  have non-empty pairwise intersections; we also have  $\mathcal{S}_{2a} \cap \mathcal{S}_{2b} \cap \mathcal{S}_{2c} \neq \emptyset$ .

Thus, with the aim of proving the slice–ribbon conjecture for alternating 3-braid closures, we turned to the question of determining which of them admit ribbon surfaces of Euler characteristic one. A convenient way of building a surface  $S$  properly embedded in the 4-ball and bounded by a given link  $L$  is via *band moves*: operations that amount to fusing small segments of  $L$  and correspond to 1-handle attachments in a handle decomposition of  $S$ . A sequence of  $n$  band moves on  $L$  that results in an  $(n + 1)$ -unlink determines a ribbon surface of Euler characteristic one. Now, families  $\mathcal{S}_{2a}$ ,  $\mathcal{S}_{2b}$  and  $\mathcal{S}_{2e}$  are defined in terms of *linear duals* of substrings, hence it is particularly convenient to construct ribbon surfaces for the links in those families: after a single band move, one can cancel most of the crossings in the diagrams of such links.<sup>2</sup> Links in the family  $\mathcal{S}_{2d}$  also have a simple description, each of them admitting a single band move that reduces it to the two-component unlink. These constructions are illustrated in Figures 4.3 to 4.6. In summary:

<sup>2</sup>Similar observations have been previously made by Lisca [Lis07] and Lecuona [Lec12].

**Theorem 2.** Let  $\widehat{\beta}$  be an alternating 3-braid closure with non-zero determinant. If  $\widehat{\beta} \in \mathcal{S}_{2a} \cup \mathcal{S}_{2d} \cup \mathcal{S}_{2e}$ , then it bounds a ribbon surface with a single 1-handle. If  $\widehat{\beta} \in \mathcal{S}_{2b}$ , then it bounds a ribbon surface with at most two 1-handles.

Known non-slice alternating 3-braid closures in  $\mathcal{S}_2$ , namely the closures  $K_i$  of  $(\sigma_1\sigma_2^{-1})^i$  for  $i \in \{7, 11, 17, 23\}$ , live in the  $\mathcal{S}_{2c}$  family; more precisely, they belong to the complement  $\mathcal{S}_{2c}^\dagger = \mathcal{S}_{2c} \setminus (\mathcal{S}_{2a} \cup \mathcal{S}_{2b} \cup \mathcal{S}_{2d} \cup \mathcal{S}_{2e})$ . Hence, no universal construction of ribbon surfaces would suffice in the  $\mathcal{S}_{2c}$  case. However, we show in Lemma 4.2.3 that there are infinitely many  $\chi$ -ribbon links in  $\mathcal{S}_{2c}^\dagger$ . In addition, we discover three more one-component closures of braids in  $\mathcal{S}_{2c}^\dagger$  with at most 20 crossings for which we could not construct ribbon surfaces: these are the closures of

$$\begin{aligned}\beta_1 &= \sigma_1^2\sigma_2^{-2}\sigma_1^2\sigma_2^{-2}\sigma_1\sigma_2^{-2}\sigma_1^2\sigma_2^{-2}\sigma_1^2\sigma_2^{-1}, \\ \beta_2 &= \sigma_1^3\sigma_2^{-2}\sigma_1\sigma_2^{-1}\sigma_1^2\sigma_2^{-3}\sigma_1^2\sigma_2^{-1}\sigma_1\sigma_2^{-2}, \\ \beta_3 &= \sigma_1^2\sigma_2^{-1}\sigma_1\sigma_2^{-2}\sigma_1\sigma_2^{-1}\sigma_1\sigma_2^{-2}\sigma_1\sigma_2^{-1}\sigma_1^2\sigma_2^{-1}\sigma_1\sigma_2^{-1},\end{aligned}$$

denoted by  $K_1$ ,  $K_2$  and  $K_3$ , respectively.

### § 1.1.3 | Twisted Alexander polynomials

Given how fruitful the band move approach proved to finding ribbon surfaces for alternating 3-braid closures so far, one would suspect that  $K_1$ ,  $K_2$  and  $K_3$  are, in fact, not slice. However, the signature of all links in  $\mathcal{S}_{2a} \cup \mathcal{S}_{2b} \cup \mathcal{S}_{2c}$  vanishes, therefore, if said links are knots, invariants such as Ozsváth and Szabó's  $\tau$  and Rasmussen's  $s$  fail to obstruct sliceness. Tristram–Levine signatures for  $K_1$ ,  $K_2$  and  $K_3$  are identically zero as well, hence do not rule out sliceness. In addition, these knots satisfy the *Fox–Milnor condition* [FM66] on their Alexander polynomials: if  $\Delta(t) = \Delta_{K_i}(t) \in \mathbb{Z}[t^{\pm 1}]$  for  $i = 1, 2, 3$ , then  $\Delta(t) = f(t)f(t^{-1})$  for some  $f(t) \in \mathbb{Z}[t^{\pm 1}]$ , up to multiplication by units. Having exhausted our supply of easily computable obstacles to sliceness, we instead apply the approach of Aceto, Meier, A. N. Miller, M. Miller, J. Park and Stipsicz [AMMMPS20] that uses a refinement of the Fox–Milnor condition to twisted Alexander polynomials, due to Kirk and Livingston [KL99] and explained in the following.

Fix distinct primes  $p$  and  $q$ , let  $\zeta_q$  denote a primitive  $q^{\text{th}}$  root of unity, and consider a character  $\chi : H_1(\Sigma_p(S^3, K); \mathbb{Z}) \rightarrow \mathbb{Z}/q\mathbb{Z}$  for some knot  $K$ . For the purposes of this introduction, the *twisted Alexander polynomial*  $\Delta_K^\chi(t)$  is an element of  $\mathbb{Q}(\zeta_q)[t^{\pm 1}]$ , taken up to multiplication by units, that is fully determined by  $K$ ,  $p$ ,  $q$  and  $\chi$ . Define the *reduced twisted Alexander polynomial*  $\widetilde{\Delta}_K^\chi(t) := \Delta_K^\chi(t)/(1-t)^e$  with  $e = 1$  if  $\chi$  is non-trivial, and  $e = 0$  otherwise. Recall that  $H_1(\Sigma_p(S^3, K); \mathbb{Z})$  admits a non-singular bilinear form called the *linking form*; a square-root order submodule of  $H_1(\Sigma_p(S^3, K); \mathbb{Z})$  w.r.t. the action of  $\mathbb{Z}[t]$ , where  $t$  acts by deck transformations, is called a *metaboliser* if the linking form vanishes on it. Now we can state the Kirk–Livingston obstruction.

**Theorem** ([KL99]). Suppose that  $K$  is slice. Then there exists a metaboliser  $N \subset H_1(\Sigma_p(S^3, K); \mathbb{Z})$  such that the following condition holds: for every character  $\chi :$

$H_1(\Sigma_p(S^3, K); \mathbb{Z}) \rightarrow \mathbb{Z}/q\mathbb{Z}$  that vanishes on  $N$ , the associated reduced twisted Alexander polynomial  $\tilde{\Delta}_K^\chi(t) \in \mathbb{Q}(\zeta_q)[t^{\pm 1}]$  is a *norm*, meaning that  $\tilde{\Delta}_K^\chi(t)$  can be written as

$$\tilde{\Delta}_K^\chi(t) = at^k f(t) \overline{f(t)}$$

for some  $a \in \mathbb{Q}(\zeta_q)$ ,  $k \in \mathbb{Z}$  and  $\overline{f(t)}$  obtained from  $f(t) \in \mathbb{Q}(\zeta_q)[t^{\pm 1}]$  by the involution  $t \mapsto t^{-1}$ ,  $\zeta_q \mapsto \zeta_q^{-1}$ .

In order to show that  $K$  is not slice using this result, one clearly needs to make suitable choices of  $p$  and  $q$ , and of characters  $\chi$ . Moreover, one also needs an understanding of all metabolisers of  $H_1(\Sigma_p(S^3, K); \mathbb{Z})$ , a way of actually computing  $\tilde{\Delta}_K^\chi(t)$  for a given  $\chi$ , and a way of testing whether  $\tilde{\Delta}_K^\chi(t)$  is a norm. We follow the general procedure detailed in [AMMMPS20] with  $p = 3$  and  $q = 7$ , employing SageMath and SnapPy to prove the following.

**Theorem 3.** The knots  $K_1$ ,  $K_2$  and  $K_3$  are not slice. Hence, if a knot  $K$  is obtained as a closure of an alternating 3-braid with up to 20 crossings and  $\Sigma_2(S^3, K)$  bounds a rational ball, then  $K$  is slice unless it is isotopic to  $K_1$ ,  $K_2$ ,  $K_3$ , or the Turk's head knot  $K_7$ .

In particular, this shows for the first time that there exist non-slice alternating 3-braid closures which are not Turk's head knots and whose double branched covers bound rational balls.

## § 1.2 | Stein-fillable genus one open books

An *open book decomposition* (or just *open book*) of a closed 3-manifold  $Y$  is a pair  $(L, \pi)$  where  $L \subset Y$  is an oriented link, called the *binding*, and  $\pi : Y \setminus L \rightarrow S^1$  is a fibration such that for any  $s \in S^1$ ,  $\pi^{-1}(s)$  is the interior of a compact orientable surface  $\Sigma_\pi$  with boundary, called the *page*, such that  $\partial\Sigma_\pi = L$ . The pair  $(L, \pi)$  determines another pair  $(\Sigma, \varphi)$ , where  $\Sigma = \Sigma_\pi$  is the page and the *monodromy*  $\varphi$  is an element of the mapping class group  $\Gamma_\Sigma$  of  $\Sigma$ . In fact,  $(\Sigma, \varphi)$  recovers  $Y$  up to diffeomorphism, so we refer to  $(L, \pi)$  and  $(\Sigma, \varphi)$  interchangeably as open books of  $Y$ . The terminology is suggestive: open books can be thought of as a way to break down a 3-manifold into surfaces bounded by a link that resemble an open rolodex near the link.

Given  $\varphi \in \Gamma_\Sigma$ , we say that  $\varphi$  admits a *positive factorisation*, or simply is *positive*, if it can be written as a product of positive Dehn twists about non-null-homotopic simple closed curves in  $\Sigma$ .

A *contact structure* on a 3-manifold  $Y$  is an oriented plane field  $\xi \subset TY$  given by  $\ker \alpha$  for some 1-form  $\alpha \in \Omega^1(Y)$  satisfying  $\alpha \wedge d\alpha > 0$ ; call  $Y$  equipped with such  $\xi$  a *contact manifold*  $(Y, \xi)$ . Contact manifolds occur organically by restricting symplectic structures on symplectic manifolds to their boundaries. Thus, a natural question when studying contact manifolds is the one of *fillability*, that is, determining when a contact manifold is the boundary of a symplectic manifold, the latter called a *filling*, in some

compatible way. There are many inequivalent notions of compatibility, the strongest of which is called *Stein fillability*.

Open books are closely connected to contact structures in the following way. Say that  $\xi$  is *supported* by an open book decomposition of  $Y$  if  $\alpha > 0$  on the binding and  $d\alpha > 0$  on the interior of the pages. In fact, every open book of  $Y$  supports some contact structure [TW75]. Given a closed  $Y$ , a foundational theorem of Giroux [Gir02] establishes a correspondence between contact structures on  $Y$  (up to contact isotopy) and open books of  $Y$  (up to *positive stabilisation*). This enables us to consider questions of contact and symplectic geometry through a powerful lens of surface mapping class groups.

Another theorem of Giroux [Gir02] along with work of Akbulut and Özbağcı [AÖ01], Loi and Piergallini [LP01] and Plamenevskaya [Pla04] drew a further connection between the worlds of surface diffeomorphisms and symplectic manifolds, establishing that a contact manifold is Stein-fillable if and only if the monodromy of *some* supporting open book is positive. However, to show that a contact manifold is not Stein-fillable by using this fact requires demonstrating that *all* monodromies of supporting open books are non-positive: a task generally out of reach of currently existing methods.

One could speculate that *every* open book  $(\Sigma, \varphi)$  supporting a Stein-fillable contact structure  $\xi$  on a 3-manifold  $Y$  factorises positively. In fact, Wendl has shown that if the genus  $g(\Sigma) = 0$ , then Stein fillings of  $(Y, \xi)$  correspond bijectively to positive factorisations of  $\varphi$  [Wen10]. However, Baker, Etnyre and Van Horn-Morris [BEVHM10] and Wand [Wan15] have exhibited examples of non-positive open books of all genera  $g(\Sigma) \geq 2$  supporting Stein-fillable contact structures. The remaining case of  $g(\Sigma) = 1$  was studied by Lisca [Lis14] who has shown that the correspondence holds if  $Y$  is a Heegaard Floer  $L$ -space; however, our main result in Chapter 7 demonstrates that it fails for an infinite number of genus one open book decompositions.

**Theorem 4.** Let  $n \geq 0$  and let  $\tau_\sigma$  denote a positive Dehn twist about a simple closed curve  $\sigma$ . Then  $(\Sigma_{1,2}, \varphi_n)$  with  $\varphi_n = \tau_\alpha \tau_\beta \tau_\gamma^{-1} \tau_{\delta_1} \tau_{\delta_2}^{4+n}$ , as illustrated in Figure 1.1, is an open book that supports a Stein-fillable contact manifold, but  $\varphi_n$  does not admit a positive factorisation.

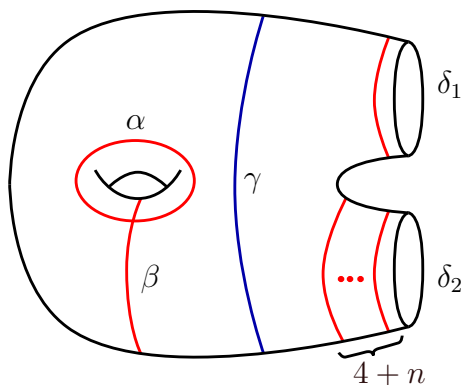


Figure 1.1: An open book  $(\Sigma_{1,2}, \tau_\alpha \tau_\beta \tau_\gamma^{-1} \tau_{\delta_1} \tau_{\delta_2}^{4+n})$  with  $n \geq 0$ .

Moreover, by adding 1-handles to  $\Sigma_{1,2}$  and extending the monodromy by the identity on the handles, we can exhibit non-positive open books supporting Stein-fillable contact manifolds with pages  $\Sigma_{g,n}$  for any non-planar surface with boundary other than the one-holed torus  $\Sigma_{1,1}$ .

# Part I

## On slice alternating 3-braid closures

# Preliminaries

---

The purpose of this chapter is to establish some fundamental concepts about links and braids, focussing specifically on links which are closures of alternating 3-braids. In Section 2.1, we give basic definitions pertaining to knots, links and braids, as well as introduce a way of describing alternating 3-braid closures via associated strings. Section 2.2 contains a discussion of Seifert surfaces, the slice–ribbon conjecture, and a generalisation of the notion of sliceness to links with an arbitrary number of components, called  $\chi$ -sliceness. In Section 2.3, we define black and white surfaces, Goeritz matrices and Tait graphs of links, fixing our conventions for alternating 3-braid closures. Concluding this chapter, Section 2.4 describes an obstruction to  $\chi$ -sliceness coming from an application of Donaldson’s theorem and formulated in terms of lattices associated to chessboard colourings of alternating link diagrams.

## § 2.1 | Alternating links and 3-braids

Throughout, a *knot*  $K$  is a smooth embedding  $K : S^1 \hookrightarrow S^3$ , and an  $n$ -component *link*  $L$  is a smooth embedding  $L : \sqcup_n S^1 \hookrightarrow S^3$  for  $n \geq 1$ . As usual, we confuse such embeddings with their images in  $S^3$  unless ambiguity occurs, considering knots and links up to ambient isotopy. We shall use the term ‘link’ in statements that apply to links with an arbitrary number of components, and the term ‘knot’ to stress that a statement only applies to, or is only known to hold for, one-component links. A *link diagram* is a four-valent planar graph obtained by projecting a link onto  $S^2$  such that the vertices, called *crossings*, correspond to transverse double points of the projection and indicate which strand is running over the other by standard pictorial conventions.

Fix  $n$  points  $x_1, \dots, x_n$  in the interior of  $D^2$  such that their  $y$ -coordinates strictly decrease with increasing index. An  $n$ -braid is an embedding  $\beta : \sqcup_n I \hookrightarrow D^2 \times I$  of  $n$  copies of  $I = [0, 1]$ , taken up to isotopy rel boundary, that is transversal to each disc  $D^2 \times \{t\}$  for  $t \in I$  and satisfying that  $\beta(\sqcup_n \{0\}) = \{x_1, \dots, x_n\} \times \{0\}$  and  $\beta(\sqcup_n \{1\}) = \{x_1, \dots, x_n\} \times \{1\}$ . A braid may be projected onto the plane such that the projection consists of strands running left to right along parallel lines which are numbered 1 to  $n$  from the top, except for when a strand crosses its immediately adjacent strand; we confuse such projections with braids themselves. Denote the braid whose projection

has precisely one crossing arising from the strand running along the line  $k$  going over (respectively, under) the strand running along the line  $k + 1$  by  $\sigma_k$  (respectively,  $\sigma_k^{-1}$ ) for  $k = 1, \dots, n - 1$ . The set of  $n$ -braids  $B_n$  is made into a group via composition, where we compose  $n$ -braids  $\beta_1$  and  $\beta_2$  by reparameterising  $\beta_1$  and  $\beta_2$  to lie in  $D^2 \times [0, \frac{1}{2}]$  and  $D^2 \times [\frac{1}{2}, 1]$ , respectively, and concatenate them to obtain  $\beta_1\beta_2 \in D^2 \times I$ . The group  $B_n$  has the following convenient presentation due to Artin [Art25]:

$$\left\langle \sigma_1, \dots, \sigma_{n-1} \left| \begin{array}{ll} \sigma_i\sigma_j = \sigma_j\sigma_i & \text{if } |i - j| > 1, \\ \sigma_i\sigma_{i+1}\sigma_i = \sigma_{i+1}\sigma_i\sigma_{i+1} & \text{for } i = 1, \dots, n - 2 \end{array} \right. \right\rangle.$$

Given an  $n$ -braid  $\beta$  in  $D^2 \times I$ , consider its image in  $D^2 \times S^1$  obtained by gluing  $D^2 \times \{0\}$  to  $D^2 \times \{1\}$  via the identity map. Identifying this  $D^2 \times S^1$  with a tubular neighbourhood of the unknot in  $S^3$  by taking the product framing to the zero framing of the unknot yields a link in  $S^3$  called the *closure* of  $\beta$  and denoted  $\widehat{\beta}$ . A diagram of  $\widehat{\beta}$  is obtained from a projection of  $\beta$  by joining the projections of points  $(x_i, 0)$  and  $(x_i, 1)$  for  $i = 1, \dots, n$  without introducing any new crossings. We may *stabilise* an  $n$ -braid  $\beta$  by adding the  $(n + 1)^{\text{th}}$  strand and composing  $\beta$  with  $\sigma_n^{\pm 1}$ . The inverse operation is called *destabilisation*; neither of these two operations changes the isotopy class of  $\widehat{\beta}$ . Clearly, if two  $n$ -braids  $\beta_1$  and  $\beta_2$  are conjugate in  $B_n$ , then their closures are isotopic. In fact, Markov's theorem states that  $\widehat{\beta}_1$  and  $\widehat{\beta}_2$  are isotopic if and only if  $\beta_1$  is related to  $\beta_2$  by a sequence of conjugations, stabilisations and destabilisations [Mar36]. Another classic theorem of Alexander states that every link  $L$  can be obtained as a closure of some braid [Ale23]. The minimal number of strands in a braid whose closure is isotopic to  $L$  is called the *braid index* of  $L$ .

Say that a braid or a link is *alternating* if it admits a diagram such that, when traversing along any component, over- and undercrossings alternate. Let us now focus on 3-braids. By work of Murasugi [Mur74], any alternating 3-braid is conjugate to exactly one of the following:

- a 3-braid of the form

$$\sigma_1^{a_1} \sigma_2^{-b_1} \sigma_1^{a_2} \sigma_2^{-b_2} \dots \sigma_1^{a_n} \sigma_2^{-b_n} \quad (\star)$$

with  $n \geq 1$  and  $a_i, b_i \geq 1$  for all  $i = 1, \dots, n$ ;

- a 3-braid  $\sigma_1^k$  or  $\sigma_2^{-k}$  for  $k \geq 1$ ;
- or, the trivial 3-braid with no crossings.

Recall that a link  $L$  is *split* if there exists an  $S^2$  embedded in  $S^3 \setminus L$  that separates one or more components of  $L$  from the others. In the first case, taking the closure yields a link that may have one, two or three components; in the second, the split union of a  $(2, \pm k)$ -torus link and an unknot; in the third, the 3-component unlink. Crowell [Cro55] and Aumann [Aum56] have shown that an alternating link is non-split if and only if its alternating diagram is connected, hence only non-split closures of alternating 3-braids

are closures of 3-braids of the form  $(\star)$ . We remark that Stoimenow has classified all alternating links with braid index 3 in [Sto03]. Also note that not every alternating link can be obtained as a closure of an alternating braid: one such counterexample with braid index 3 is the knot  $5_2$  [Cro89].

Every 3-braid  $\beta$  of the form  $(\star)$  can be described by its *associated string*

$$\mathbf{a}(\beta) = (2^{[a_1-1]}, b_1 + 2, \dots, 2^{[a_n-1]}, b_n + 2),$$

where  $2^{[a_i-1]}$  represents the substring consisting of the number 2 repeated  $a_i - 1$  times. The usefulness of associated strings lies in that they are more compact to write down, while also encoding valencies of the vertices of the associated Tait graph, as we shall see in Section 2.3. Call every maximal substring of  $\mathbf{a}(\beta)$  of the form  $(2^{[x]})$  or  $(3 + x)$  for  $x \geq 0$  an *entry* of  $\mathbf{a}(\beta)$ . Given a 3-braid  $\beta$  of the form  $(\star)$ , we can recover its closure from any cyclic permutation and/or reflection of  $\mathbf{a}(\beta)$ ; hence, we consider associated strings as equivalent up to those two operations. Now let us define two important operations on strings that we shall be performing later.

**Definition 2.1.1.** Let  $\mathbf{a}$  be a string of integers that can be written in the form

$$\mathbf{a} = (2^{[m_1]}, 3 + n_1, \dots, 2^{[m_l]}, 3 + n_l)$$

for  $l \geq 1$  and  $m_i, n_i \geq 0$  for all  $i$ . The *cyclic dual*  $\text{cd}(\mathbf{a})$  of  $\mathbf{a}$  is given by

$$\text{cd}(\mathbf{a}) = (3 + m_1, 2^{[n_1]}, \dots, 3 + m_l, 2^{[n_l]}).$$

Observe that if  $\mathbf{a} = \mathbf{a}(\beta)$  for some 3-braid  $\beta$  of type  $(\star)$ , then  $\text{cd}(\mathbf{a}) = \mathbf{a}(\beta^*)$ , where

$$\beta^* = \sigma_1^{b_n} \sigma_2^{-a_n} \sigma_1^{b_{n-1}} \sigma_2^{-a_{n-1}} \dots \sigma_1^{b_1} \sigma_2^{-a_1}$$

is the *dual braid* of  $\beta$  possessing the property that  $\widehat{\beta}^*$  is isotopic to the mirror image of  $\widehat{\beta}$ . If  $\mathbf{a}(\beta)$  is equivalent to  $\mathbf{a}(\beta^*)$ , say that  $\beta$  is *self-dual*.

**Definition 2.1.2.** Let  $\mathbf{b} = (b_1, \dots, b_k)$  be a string of integers with all  $b_i \geq 2$ . The *linear dual*  $\text{ld}(\mathbf{b})$  of  $\mathbf{b}$  is defined as follows:

- if  $b_j \geq 3$  for some  $j$ , write  $\mathbf{b}$  in the form

$$\mathbf{b} = (2^{[m_1]}, 3 + n_1, 2^{[m_2]}, 3 + n_2, \dots, 2^{[m_l]}, 2 + n_l)$$

with  $m_i, n_i \geq 0$  for all  $i = 1, \dots, l$ ; then

$$\text{ld}(\mathbf{b}) = (2 + m_1, 2^{[n_1]}, 3 + m_2, 2^{[n_2]}, 3 + m_3, \dots, 3 + m_l, 2^{[n_l]});$$

- if  $\mathbf{b} = (2^{[l]})$  for  $l \geq 1$ , then  $\text{ld}(\mathbf{b}) = (l + 1)$ .

By convention, if  $\mathbf{b} = (1)$ , then  $\text{ld}(\mathbf{b})$  is the empty string.

**Example 2.1.3.** Let  $\mathbf{a} = (2^{[2]}, 3, 5, 2, 4)$ . Then we can write  $\mathbf{a} = (2^{[2]}, 3 + 0, 2^{[0]}, 3 + 2, 2^{[1]}, 3 + 1)$  and conclude that

$$\text{cd}(\mathbf{a}) = (3 + 2, 2^{[0]}, 3 + 0, 2^{[2]}, 3 + 1, 2^{[1]}) = (5, 3, 2^{[2]}, 4, 2).$$

Up to reflection and cyclic permutation,  $\mathbf{a} = \text{cd}(\mathbf{a})$ . Setting  $\beta = \sigma_1^3 \sigma_2^{-1} \sigma_1 \sigma_2^{-3} \sigma_1^2 \sigma_2^{-2}$ , we have  $\mathbf{a} = \mathbf{a}(\beta)$ , so we conclude that  $\beta$  is self-dual. To take the linear dual, we write  $\mathbf{a} = (2^{[2]}, 3 + 0, 2^{[0]}, 3 + 2, 2^{[1]}, 2 + 2)$ . Then

$$\text{ld}(\mathbf{a}) = (2 + 2, 2^{[0]}, 3 + 0, 2^{[2]}, 3 + 1, 2^{[2]}) = (4, 3, 2^{[2]}, 4, 2^{[2]}).$$

**Remark 2.1.4.** Linear and cyclic duals can be thought of in the following useful way. Given a string  $\mathbf{a} = (a_1, \dots, a_n)$  with  $a_i \geq 2$  for all  $i$ , one can draw the wheel graph  $\Gamma_c$  with valencies of the rim vertices given cyclically by  $a_1, \dots, a_n$ ; then  $\text{cd}(\mathbf{a})$  is given, up to reflection and cyclic permutation, by the valencies of the rim vertices of the planar dual  $\Gamma_c^*$  of  $\Gamma_c$  (which is also a wheel graph). To get  $\text{ld}(\mathbf{a})$ , draw a horizontal linear graph  $\Gamma_l$  with  $n$  vertices  $v_1, \dots, v_n$  in  $\mathbb{R}^2 \cup \{\infty\}$  and add edges going upwards and meeting at infinity so that the valency of  $v_i$  is given by  $a_i$ ; then  $\text{ld}(\mathbf{a})$  is given by the valencies of the vertices of the planar dual  $\Gamma_l^*$  of  $\Gamma_l$ , read left to right.

## § 2.2 | Surfaces bounded by links

In the rest of this chapter, we work exclusively in the smooth category. Every link  $L$  bounds a connected orientable surface in  $S^3$ , called a *Seifert surface*, that can be algorithmically constructed from any diagram  $D$  of  $L$  [Sei35]. Recall that the *genus* of  $L$ , denoted  $g(L)$ , is the minimal genus of all Seifert surfaces of  $L$ . The only knot of genus zero is the unknot: no other knot bounds an embedded disc in  $S^3$ . However, many knots bound embedded discs in  $D^4$ : we say that a knot  $K \subset S^3$  is *slice* if there exists a properly embedded disc  $\Delta \subset D^4$  with  $K = \partial\Delta$ . If, moreover,  $\Delta$  can be arranged in  $D^4$  such that it only has index 0 and 1 critical points with respect to the radial distance function  $D^4 \rightarrow [0, 1]$ , then we say  $K$  is *ribbon*. The six-decade-old *slice–ribbon conjecture* of Fox [Fox62] asks if slice knots are precisely ribbon knots, ultimately motivating the contents of the first part of this thesis.

The notion of sliceness is natural and useful: for instance, we say that two knots  $K$  and  $K'$  are *concordant* if the connected sum  $K \# K'$  is slice; the set of all knots modulo concordance is a group with many interesting properties. The terminology comes from the fact that a slice knot is a cross-cut of a knotted  $S^2$  in  $S^4$  (to see this, glue two 4-balls  $D_1^4$  and  $D_2^4$  with a slice knot  $K$  in the boundary of each  $D_i^4$  such that the knots coincide; the slice discs glued together give a knotted sphere). Thus, the slice–ribbon conjecture concerns our basic understanding of knotting of surfaces in 4-manifolds: in particular, it asks if for any cross-cut of a knotted sphere we can find a ‘simple’ knotted sphere possessing the same cross-cut.

There are several reasonable extensions of the concepts of ‘slice’ and ‘ribbon’ to

links: for instance, we say that if a link  $L$  bounds a disjoint union of properly embedded discs in  $D^4$ , then  $L$  is *strongly slice*. However, for reasons that will be clarified in Section 2.4, we shall use an extension due to Donald and Owens.

**Definition 2.2.1** ([DO12]). Say that a link  $L \subset S^3$  is  $\chi$ -*slice* if it bounds a properly embedded surface  $S \subset D^4$  of Euler characteristic one ( $\chi(S) = 1$ ) with no closed components; we call such  $S$  a *slice surface* for  $L$ . If, moreover,  $S$  can be chosen such that it only has index 0 and 1 critical points with respect to the radial distance function  $D^4 \rightarrow [0, 1]$ , then we say that  $L$  is  $\chi$ -*ribbon* and  $S$  is a *ribbon surface* for  $L$ .

Note that we do not require that  $S$  be connected or orientable. The definitions of ‘ $\chi$ -slice’ and ‘ $\chi$ -ribbon’ are equivalent to the definitions of ‘slice’ and ‘ribbon’ in the case of knots. We will refer to the assertion that every  $\chi$ -slice link is  $\chi$ -ribbon as the  *$\chi$ -slice–ribbon conjecture*, or simply as the *slice–ribbon conjecture* when it is clear that we are working with links. There are no known counterexamples to this stronger form of Fox’s conjecture, and we shall establish in this thesis that it holds for several infinite families of alternating 3-braid closures.

In the following, we will be interested in explicitly exhibiting ribbon surfaces for links. In order to do so, we need the notion of a *band move*.

**Definition 2.2.2.** Given a link  $L$ , performing a *band move* on  $L$  means choosing an embedding  $\varphi : D^1 \times D^1 \hookrightarrow S^3$  of a *band*  $D^1 \times D^1$  so that the image of  $\varphi$  is disjoint from  $L$  except for  $\varphi(\partial D^1 \times D^1)$  coincident with two segments of  $L$ , removing those segments, joining corresponding ends of  $L$  along  $\varphi(D^1 \times \partial D^1)$ , and smoothing the corners.

A band move amounts to removing a 1-handle in a putative ribbon surface  $S$  for  $L$ . If after  $n$  band moves, the resulting link is isotopic to the  $(n + 1)$ -component unlink, one has indeed obtained a ribbon surface  $S$  of Euler characteristic one bounded by  $L$ , since each component of the unlink bounds a 0-handle of  $S$  (so  $\chi(S) = \# 0\text{-handles} - \# 1\text{-handles} + \# 2\text{-handles} = (n + 1) - n + 0 = 1$ ). Each band may be represented on a link diagram by an arc with endpoints on the strands of the diagram, representing the core  $D^1 \times \{\frac{1}{2}\}$  of the band, that elsewhere crosses the strands transversely, has no self-crossings, and is annotated by the number of half-twists in the band relative to the blackboard framing [OS21]. An example of a band move producing a ribbon surface for the square knot is shown in Figure 2.1.

## § 2.3 | Goeritz matrices and Tait graphs

Given a diagram  $D$  for a link  $L$ , we can construct two surfaces in  $S^3$  bounded by  $L$  in the following way: choose a *chessboard colouring* of the regions of the plane defined by  $D$  (that is, a black and white colouring where regions of the same colour only meet diagonally at every crossing)<sup>1</sup>, then take a disc in  $S^3$  for every white (respectively,

---

<sup>1</sup>To see that this is always possible, resolve all crossings of  $D$  arbitrarily to obtain a collection of closed curves in the plane. By the Jordan curve theorem, it admits a chessboard colouring; now put the crossings back in.

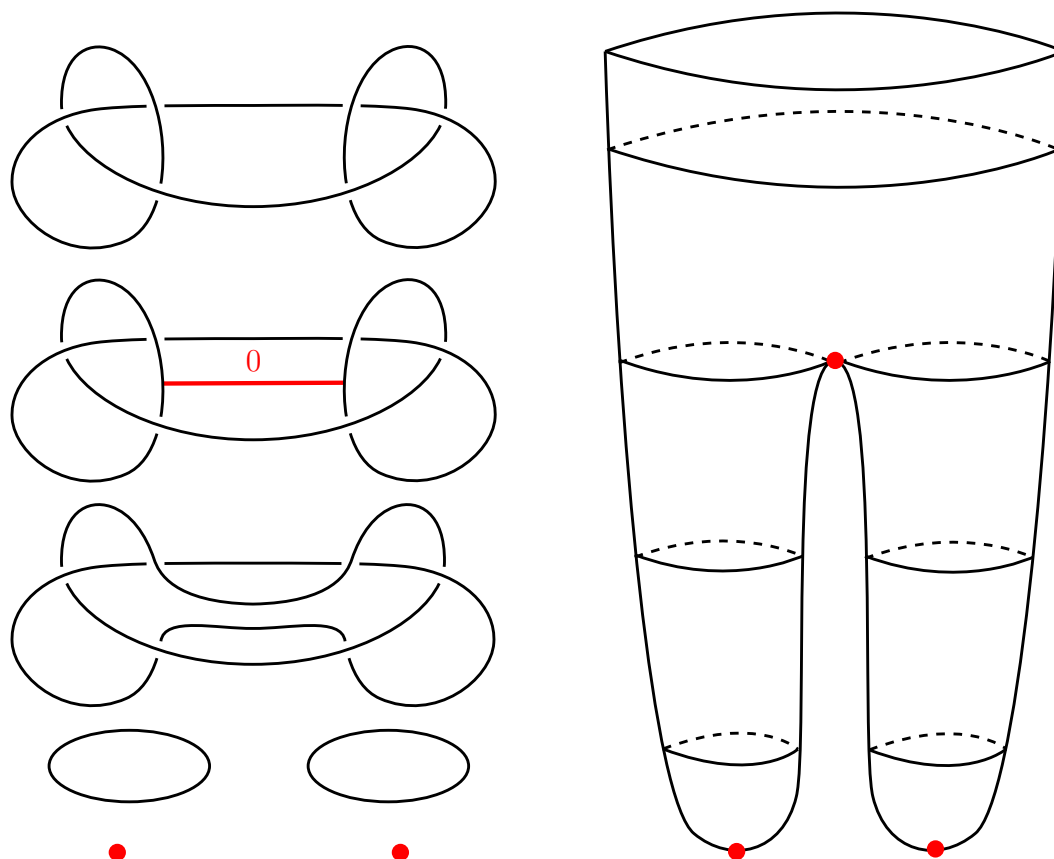


Figure 2.1: On the left: a band move that exhibits a ribbon surface for the square knot. On the right: the corresponding ribbon surface in  $D^4$ , with index 0 and 1 critical points marked; the radial distance function  $D^4 \rightarrow [0, 1]$  increases upwards.

black) region<sup>2</sup> and join the discs by half-twisted bands at every crossing. This yields a *white* (respectively, *black*) *surface* bounded by  $L$ , which we denote  $F_w$  (respectively,  $F_b$ ). Clearly, choosing the other possible colouring produces the same two surfaces with the names interchanged. For a choice of colouring, we can assign an incidence number  $\mu(c) \in \{\pm 1\}$  to each crossing  $c$  of  $D$  according to the convention in Figure 2.2. If  $D$  is a connected alternating diagram, we will be choosing the colouring such that  $\mu(c) = +1$  for all crossings.<sup>3</sup>

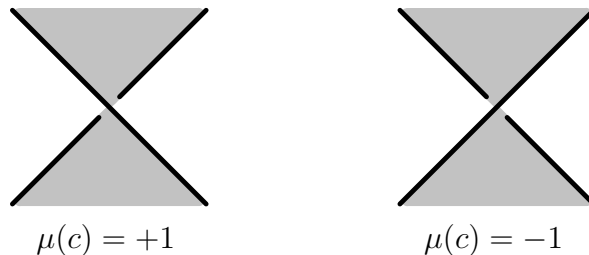


Figure 2.2: Our convention for the incidence number of a crossing.

Now, given a diagram  $D$ , fix a chessboard colouring as above, choose a distinguished white region  $X_0$  and label the rest of the white regions  $X_1, \dots, X_n$ . Then construct a planar multigraph  $\Gamma_w(D)$  with signed edges, called the *white Tait graph*, by placing a vertex  $v_i$  in each white region  $X_i$  for  $i = 0, \dots, n$  and adding an edge  $e$  between vertices for every crossing  $c$  between their respective regions, setting  $\mu(e) = \mu(c)$ . This gives rise to the *white Goeritz matrix*  $G_w(D)$ , whose entries  $g_{ij}$  are defined for  $i, j = 1, \dots, n$  by

$$G_w(D) := (g_{ij}) = \begin{cases} \sum_{e \in E(v_i, v_j)} \mu(e) & \text{if } i \neq j, \\ -\sum_{e \in E(v_i, \Gamma_w(D) \setminus v_i)} \mu(e) & \text{if } i = j. \end{cases}$$

Note that self-loops are not counted in the above definition. Carrying out an analogous construction for the black surface gives the *black Tait graph*  $\Gamma_b(D)$ , which is the planar dual of  $\Gamma_w(D)$ , and the *black Goeritz matrix*  $G_b(D)$ .

Recall that if for a diagram  $D$  there exists a circle in  $S^2$  that meets the diagram only at the crossing  $c$ , then  $c$  is a *nugatory crossing*; in particular, Reidemeister 1 (R1) moves on  $D$  remove nugatory crossings. If  $D$  is reduced (that is,  $D$  is non-split and has no nugatory crossings), then the Tait graphs  $\Gamma_w(D)$  and  $\Gamma_b(D)$  have no cut-edges or loop edges; otherwise, performing an R1 move removes a vertex of degree one from either  $\Gamma_w(D)$  or  $\Gamma_b(D)$  and a loop edge from its planar dual.

The *determinant* of  $L$  is defined as

$$\det L := |\det G_w(D)| = |\det G_b(D)|;$$

it is independent of the choice of link diagram  $D$  for  $L$  [Goe33]. Noting that for the unknot  $U$ , by convention we have  $\det U = 1$ , observe that the closure of an alternating

<sup>2</sup>The disc corresponding to the unbounded region goes through the point at infinity in  $S^3$ .

<sup>3</sup>Such choice is possible since for an alternating link, incidence numbers are the same along the boundary of any black region, and every crossing lies on the boundary of some black region.

3-braid has non-zero determinant if and only if the braid is of the form  $(\star)$  (that is, of the form  $\sigma_1^{a_1}\sigma_2^{-b_1}\dots\sigma_1^{a_n}\sigma_2^{-b_n}$  with  $n \geq 1$  and  $a_i, b_i \geq 2$  for all  $i$ ).

Given a 3-braid  $\beta$  of the form  $(\star)$ , we draw the diagram  $D$  of  $\hat{\beta}$  by drawing  $\beta$  from left to right, closing it underneath and orienting all strings clockwise, as shown in Figure 2.3.

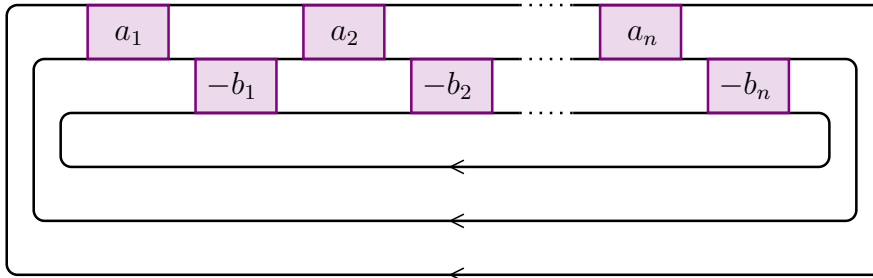


Figure 2.3: A closure of a 3-braid of the form  $(\star)$ . We denote sequences of positive (respectively, negative) crossings by blocks annotated by positive (respectively, negative) coefficients.

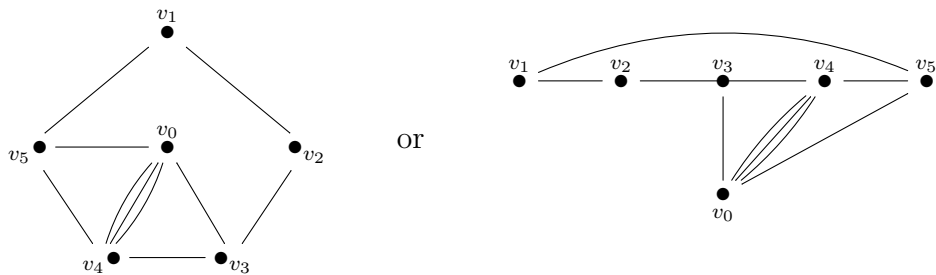
Clearly,  $D$  is alternating for any choice of positive  $a_i$  and  $b_i$  with  $i = 1, \dots, n$ . We use this form of the diagram throughout, so unless explicitly stated otherwise, we confuse  $\hat{\beta}$  with its diagram as above. Choose the chessboard colouring of  $D$  where the unbounded region is black, letting  $a = \sum_{i=1}^n a_i$  and  $b = \sum_{i=1}^n b_i$ . Then there are  $a + 1$  white regions. Label the white region that does not border the unbounded region by  $X_0$ . Now label the rest of the white regions  $X_1, \dots, X_n$  subject to the following conditions:

- $X_1$  is the first region cut out by  $D$  to the right of the crossing coming from the first  $\sigma_1$  term of  $\beta$ ;
- the number of crossings along the boundary of the region labelled by  $X_i$  is given by the  $i^{\text{th}}$  element of the associated string  $\mathbf{a}(\beta) = (2^{\lfloor a_1 - 1 \rfloor}, b_1 + 2, \dots, 2^{\lfloor a_n - 1 \rfloor}, b_n + 2)$  of  $\beta$ , counting twice those crossings that a region shares with itself;
- if  $a \geq 3$ , the region labelled by  $X_i$  for  $i = 2, \dots, a - 1$  shares one crossing with each of the regions labelled by  $X_{i-1}$  and  $X_{i+1}$ , and  $X_1$  shares a crossing with each of  $X_2$  and  $X_a$ ;
- if  $a = 2$ , then  $X_1$  shares two crossings with  $X_2$ ;
- if  $a = 1$ , then  $X_1$  shares a crossing with itself.

Notice that if  $a = 1$  or  $b = 1$ , then  $D$  is not reduced. In particular, if  $a = 1$ , then  $\Gamma_w(\hat{\beta})$  has a self-loop and  $\hat{\beta}$  is isotopic to the  $(2, -b)$ -torus link; if  $b = 1$ , then  $v_0 \in V(\Gamma_w(\hat{\beta}))$  has degree one for any  $a \geq 1$  and  $\hat{\beta}$  is isotopic to the  $(2, a)$ -torus link. If  $a = b = 1$ , then  $D$  is a two-crossing diagram of the unknot. An example illustrating the labelling of regions and the corresponding white Tait graph for  $\beta = \sigma_1^3\sigma_2^{-1}\sigma_1\sigma_2^{-3}\sigma_1\sigma_2^{-1}$  is demonstrated in Figure 2.4.







## § 2.4 | Lattice obstructions to $\chi$ -sliceness

Recall that a compact oriented 4-manifold  $X$  possesses a symmetric bilinear form

$$H_2(X; \mathbb{Z}) \times H_2(X; \mathbb{Z}) \rightarrow \mathbb{Z},$$

called the *intersection form*, that vanishes when either argument is torsion and hence descends to a bilinear form on  $H_2(X; \mathbb{Z})/\text{Tors}$ , denoted  $Q_X$ . We say  $X$  is *negative-definite* (respectively, *positive-definite*) if  $Q_X$  is negative-definite (respectively, positive-definite). Recall also that an (*integral*) *lattice*  $\Lambda$  is a finitely generated free abelian group  $\Lambda$  together with a symmetric bilinear form  $\Lambda \times \Lambda \rightarrow \mathbb{Z}$ .

For a link  $L$ , consider a chessboard colouring of its diagram  $D$  as in Section 2.3 and smoothly push the interior of the white surface  $F_w$  into  $D^4$ . Gordon and Litherland have shown [GL78] that the double cover of  $D^4$  branched over  $F_w$ , denoted  $X_b := \Sigma_2(D^4, F_w)$ , is a smooth manifold with the intersection form  $Q_{X_b}$  given by  $G_w(D)$  with respect to an appropriate basis. In particular, this defines the *black lattice*

$$\Lambda_b(D) := (H_2(X_b; \mathbb{Z})/\text{Tors}, Q_{X_b}).$$

Keeping the same colouring, by pushing in the black surface  $F_b$  one analogously obtains the *white lattice*

$$\Lambda_w(D) := (H_2(X_w; \mathbb{Z})/\text{Tors}, Q_{X_w}),$$

where  $X_w := -\Sigma_2(D^4, F_b)$  and  $Q_{X_w}$  is given by  $G_b(D)$ .<sup>4</sup> With our conventions, if  $D$  is a non-split alternating diagram and  $\mu(c) = +1$  for all crossings  $c$ , then both  $X_w$  and  $X_b$  are negative-definite [GL78].

Now let  $K$  be a slice knot with a slice disc  $\Delta \subset D^4$ . It is well-known that  $\Sigma_2(D^4, \Delta)$  is a *rational (homology) ball*, that is,

$$H_i(\Sigma_2(D^4, \Delta); \mathbb{Q}) \cong H_i(D^4; \mathbb{Q})$$

for all  $i \geq 0$  (a proof can be found in [Kau87, Lemma 17.2]). Donald and Owens have shown [DO12] that this property is shared by  $\chi$ -slice links: if  $L$  is a  $\chi$ -slice link with a slice surface  $S$  and non-zero determinant, then  $\Sigma_2(D^4, S)$  is, too, a rational ball. Note

<sup>4</sup>Notice that the *white* (respectively, *black*) Goeritz matrix determines the *black* (respectively, *white*) lattice. We apologise to the reader for this rather confusing historical convention.



# Classification of embeddable ABCs

---

In this chapter we describe our progress on classifying alternating 3-braid closures with non-zero determinant (henceforth, *ABCs*) that are potentially  $\chi$ -slice because their double branched covers are not obstructed from bounding rational balls by Donaldson’s theorem. Specifically, we classify embeddings of both black and white lattices associated to *ABCs* into the standard negative-definite integral lattice if they have the same rank, and embeddings of the higher rank lattice otherwise, provided that these embeddings satisfy the technical ‘heavy label conjecture’ (Conjecture 3.3.2) that is motivated by computational evidence. The results of this chapter, unless indicated otherwise, have been obtained independently and then largely superseded by work of Simone [Sim20] who, as part of an effort to classify torus bundles that bound rational homology circles, provided an unconditional classification of *ABCs* whose double branched covers bound rational balls. In particular, it follows from Simone’s results that lattices associated to *ABCs* whose double branched covers bound rational balls admit embeddings satisfying the aforementioned conjecture. While broadly similar, our methods have a somewhat different flavour to Simone’s in that we work with labelled Tait graphs rather than associated strings and do not rely on Lisca’s results in [Lis07]. In fact, our classification contains additional information since we keep track of all embeddings of interest for a particular *ABC*, not just their existence.

In Section 3.1, we establish a vocabulary for describing embeddings of black and white lattices via labelled Tait graphs, while in Section 3.2 we define the basic operation of *contraction* on such graphs. Section 3.3 contains Conjecture 3.3.2 and proves some of its basic implications. The most substantial and technical section of this chapter, Section 3.4, is devoted to the classification of labelled Tait graphs associated to *ABCs* into contraction classes. In the final Section 3.5, we briefly discuss how our classification is related to that of Simone.

## § 3.1 | Lattice embeddings as labelled Tait graphs

Throughout, we work with the negative-definite integral lattice  $(\mathbb{Z}^n, -I)$  which we denote simply by  $\mathbb{Z}^n$ , representing the pairing  $-I$  by a dot. By a *canonical basis* of  $\mathbb{Z}^n$  we mean a basis  $\{e_1, \dots, e_n\}$  such that  $e_i \cdot e_j = -\delta_{ij}$ . We will always endow  $\mathbb{Z}^n$  with

such canonical basis, sometimes implicitly. Given  $v \in \mathbb{Z}^n$ , we write  $|v|^2 = -v \cdot v$ .

Recall from Section 2.4 that if  $L$  is a link with a chessboard colouring of its diagram  $D$ , then there exists a smooth manifold  $X_b$  whose intersection form  $Q_{X_b}$  is given by the Goeritz matrix  $G_w(D)$ . In particular, this implies that the vertices in  $V(\Gamma_w(D)) \setminus \{v_0\}$ , where  $\Gamma_w(D)$  is the white Tait graph and  $v_0$  is the vertex coming from the distinguished white region  $X_0$ , correspond bijectively to the generators of the lattice  $\Lambda_b(D)$ . We abuse notation to denote both the elements of  $V(\Gamma_w(D)) \setminus \{v_0\}$  and the corresponding generators of  $\Lambda_b(D)$  by  $v_i$ . The pairing in  $\Lambda_b(D)$  will also be represented by a dot. This pairing between different generators of  $\Lambda_b(D)$  may be read off  $\Gamma_w(D)$  directly by counting with sign the number of edges between corresponding vertices. (Interchanging the subscripts  $w$  and  $b$  along with the words ‘white’ and ‘black’ in the preceding paragraph, we obtain an analogous statement for  $\Lambda_w(D)$ .) In the following,  $\Gamma(D)$  can stand for either of  $\Gamma_w(D)$  or  $\Gamma_b(D)$  and  $\Lambda(D)$  for either of  $\Lambda_b(D)$  or  $\Lambda_w(D)$ , of the opposite colour to  $\Gamma(D)$ . We may drop  $D$  from notation when it is understood, and, when working with an ABC  $\widehat{\beta}$ , write  $\Gamma(\beta)$  to mean  $\Gamma(D)$  for the standard diagram  $D$  of  $\widehat{\beta}$  as detailed in Section 2.3, also writing  $\Lambda(\beta)$  for the lattice corresponding to  $\Gamma(\beta)$ .

Suppose that  $D$  is a chessboard-coloured non-split alternating link diagram with  $\mu(c) = +1$  for all crossings  $c$ . Assume that  $|V(\Gamma(D))| = n + 1$  and set

$$v_0 := -v_1 - \cdots - v_n \in \Lambda(D).$$

Observe that  $v_0 \cdot v_i$  for  $i = 1, \dots, n$  is given by the number of edges in  $\Gamma(D)$  between  $v_0$  and  $v_i$ . Also, we have  $\deg(v_i) = |v_i|^2$  for  $i = 1, \dots, n$  and

$$\deg(v_0) = |v_0|^2 = -\sum_{i=1}^n \sum_{j=1}^n v_i \cdot v_j.$$

Notice that if  $D$  is unreduced, then performing an R1 move may remove either a degree one vertex or a loop edge from  $\Gamma(D)$ , amounting to the other operation on the planar dual  $\Gamma^*(D)$ . In the former case, this reduces the rank of  $\Lambda(D)$  by one.

Now consider  $D$  as above that represents a link  $L$  and cuts out  $k + 1$  white and  $l + 1$  black regions in the plane.

**Definition 3.1.1.** Let  $\{v_1, \dots, v_k\}$  and  $\{u_1, \dots, u_l\}$  be bases for  $\Lambda_b(D)$  and  $\Lambda_w(D)$  corresponding to elements of  $V(\Gamma_w(D)) \setminus \{v_0\}$  and  $V(\Gamma_b(D)) \setminus \{v_0\}$ , respectively. Say that  $L$  is *embeddable* if there exist lattice embeddings

$$\begin{aligned} \varphi : \Lambda_b(D) &\hookrightarrow \mathbb{Z}^k & \psi : \Lambda_w(D) &\hookrightarrow \mathbb{Z}^l \\ v_i &\mapsto \sum_{j=1}^k \alpha_i^j e_j & \text{and} & & u_i &\mapsto \sum_{j=1}^l \beta_i^j f_j, \end{aligned}$$

where  $\{e_1, \dots, e_k\}$  and  $\{f_1, \dots, f_l\}$  are canonical bases for  $\mathbb{Z}^k$  and  $\mathbb{Z}^l$ , respectively.

We have that

$$v_0 \mapsto \sum_{j=1}^k \alpha_0^j e_j := - \sum_{i=1}^k \sum_{j=1}^k \alpha_i^j e_j,$$

and similarly for  $u_0$ . In the following, we will be choosing canonical bases such that  $\alpha_0^j$  and  $\beta_0^j$  are non-positive for all  $j$ ; there could, of course, be many possible choices.

For an embeddable  $L$ , we can represent  $\varphi$  by *labelling* vertices of  $\Gamma_w(D)$  with the images of the corresponding generators in  $\Lambda_b(D)$  under  $\varphi$  and labelling the vertex  $v_0$  by  $\varphi(v_0)$ .<sup>1</sup> That is, to each vertex  $v_i$  for every non-zero  $\alpha_i^j$  we associate the symbol  $j$  with multiplicity  $|\alpha_i^j|$  if  $\alpha_i^j > 0$ , or the symbol  $\underline{j}$  with multiplicity  $|\alpha_i^j|$  if  $\alpha_i^j < 0$ . (Analogously, we can represent  $\psi$  by labelling  $\Gamma_b(D)$ .)

**Definition 3.1.2.** In the above setting with  $\Gamma \in \{\Gamma_w(D), \Gamma_b(D)\}$ ,

- each symbol  $j$  and  $\underline{j}$  is called a *label*;
- the multiset of labels associated to a vertex  $v \in V(\Gamma)$  is denoted  $l(v)$  and called the *labelling* of  $v$ ;
- the multiset consisting of all labels in  $l(v)$  for all  $v \in V(\Gamma)$  is denoted  $l(\Gamma)$  and called the *labelling* of  $\Gamma$ ;
- the graph  $\Gamma$  endowed with a labelling is called a *labelled graph*.

Fixing an index  $j$ ,

- the multiset of all labels  $j$  and  $\underline{j}$  in  $l(\Gamma)$  is called the *label set* of  $j$  and denoted  $[j]$ ;
- denote the multiset of non-zero values of  $\alpha_i^j$  for  $i = 0, \dots, k$  if  $\Gamma = \Gamma_w(D)$ , resp., of  $\beta_i^j$  for  $i = 0, \dots, l$  if  $\Gamma = \Gamma_b(D)$ , by

$$[[j]] := \{t_1^{(\mu_1)}, \dots, t_{n_w}^{(\mu_{n_w})}\}, \quad \text{resp.,} \quad [[\underline{j}]] := \{t_1^{(\mu_1)}, \dots, t_{n_b}^{(\mu_{n_b})}\}, \quad (3.1.1)$$

where  $t_i$  are the values and  $\mu_i$  are the multiplicities; then  $[[j]]$  is called the *magnitude set* for  $j$ ;

- given  $[[j]]$  as in Equation (3.1.1), the *weight* of  $[j]$  is denoted  $w(j)$  and defined by

$$w(j) = \sum_{s=1}^{n_w} \sum_{l=1}^{\mu_s} t_s^2, \quad \text{resp.,} \quad w(\underline{j}) = \sum_{s=1}^{n_b} \sum_{l=1}^{\mu_s} t_s^2;$$

- the multiplicity of a given label  $j$  or  $\underline{j}$  in  $l(v)$  is denoted by  $m(v, j)$  or  $m(v, \underline{j})$ , respectively;
- the multiplicity of a given label  $j$  or  $\underline{j}$  in  $l(\Gamma)$  is denoted by  $m(j)$  or  $m(\underline{j})$ , respectively.

Our convention for choosing canonical bases so that  $\alpha_0^j \leq 0$  and  $\beta_0^j \leq 0$  for all  $j$  amounts to only having underlined labels in  $l(v_0)$  and  $l(u_0)$ . For  $v \in V(\Gamma)$ , we will often write  $l(v)$  as a string of decorated non-decreasing integers, or a string of decorated

<sup>1</sup>Note that our usage of the word ‘labelling’ is different from [Lis17].

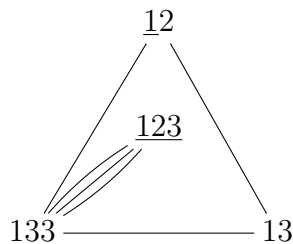
variables representing integers, some of them possibly repeating. Whenever it occurs as a result of some operation that both  $j \in l(v)$  and  $\underline{j} \in l(v)$  for some  $v$ , we remove  $\min(m(v, j), m(v, \underline{j}))$  instances of both  $j$  and  $\underline{j}$  from  $l(v)$  as that does not change the corresponding embedding. We also adopt the convention that label sets are written out with repeating elements (that is,  $[j] = \{j, \dots, j, \underline{j}, \dots, \underline{j}\}$ ) and magnitude sets are written out in condensed multiset notation as in Equation (3.1.1), for additional avoidance of confusion.

**Definition 3.1.3.** We say that a label set  $[j]$  is a *pair* if  $[[j]] = \{1^{(1)}, (-1)^{(1)}\}$  and a *quartet* if  $[[j]] = \{1^{(2)}, (-1)^{(2)}\}$ . Also say that  $[j]$  is *heavy* if there exists  $t \in [[j]]$  with  $|t| > 1$ .

**Example 3.1.4.** Let  $\beta = \sigma_1^3 \sigma_2^{-3}$  and consider the lattice  $\Lambda_b(\beta)$  coming from  $\Gamma_w(\beta)$ . Fix a canonical basis  $\{e_1, e_2, e_3\}$  of  $\mathbb{Z}^3$ . There exists an embedding  $\Lambda_b(\beta) \hookrightarrow \mathbb{Z}^3$  given by

$$v_1 \mapsto -e_1 + e_2, \quad v_2 \mapsto e_1 - e_3, \quad v_3 \mapsto e_1 + 2e_3.$$

Thus,  $v_0 \mapsto -e_1 - e_2 - e_3$ . The corresponding labelling of  $\Gamma_w(\beta)$  is shown below:



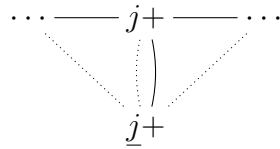
We see that  $l(v_0) = \underline{123}$ ,  $l(v_1) = \underline{12}$ ,  $l(v_2) = \underline{13}$  and  $l(v_3) = 133$ . Also,  $[1] = \{1, 1, \underline{1}, \underline{1}\}$  and  $[[1]] = \{1^{(2)}, (-1)^{(2)}\}$ ;  $[2] = \{2, \underline{2}\}$  and  $[[2]] = \{1^{(1)}, (-1)^{(1)}\}$ ;  $[3] = \{3, 3, \underline{3}, \underline{3}\}$  and  $[[3]] = \{2^{(1)}, (-1)^{(2)}\}$ . The facts that  $v_1 \cdot v_2 = v_2 \cdot v_3 = v_3 \cdot v_1 = 1$ ,  $v_0 \cdot v_1 = v_0 \cdot v_2 = 0$  and  $v_0 \cdot v_3 = 3$  could, with some practice, be easily read off from looking at all  $l(v_i)$ . Notice also that in this labelling  $[1]$  is a quartet,  $[2]$  is a pair, and  $[3]$  is heavy. Finally, observe that  $\beta$  is self-dual, so  $\Gamma_w(\beta)$  is the same as  $\Gamma_b(\beta)$ , hence an embedding  $\Lambda_w(\beta) \hookrightarrow \mathbb{Z}^3$  also exists, implying that  $\beta$  is embeddable.

We will also be dealing with *partial labellings*, that is, labellings that are incomplete. For instance, it may be possible that we fully know the labelling of a particular vertex, which in turn requires that certain labels be on adjacent vertices, but have no information beyond that. Thus, we adopt the following notation: if  $S$  is a sub-multiset of  $l(v)$ , we write  $l(v)$  as  $S+$ , where  $S$  is written out as a string of labels. Moreover, if for some sub-multiset of labels  $N$ , we also know that  $N \cap l(v) = \emptyset$ , we may write  $l(v)$  as  $S + |N$  to highlight that fact.

**Definition 3.1.5.** Say that a labelling of  $\Gamma$  is *valid* if it determines an embedding of its corresponding  $\Lambda$  into the integral lattice  $\mathbb{Z}^{\text{rk } \Lambda}$ .

In particular, a link  $L$  with a non-split alternating diagram  $D$  is embeddable if and only if there exist valid labellings of  $\Gamma_w(D)$  and  $\Gamma_b(D)$ .

**Example 3.1.6** (‘Projecting out’). An important example of a labelling that is not valid involves the closure of a braid of the form  $(\star)$  with  $a = \sum_i a_i \geq 2$ ,  $\deg(v_0) \geq 2$ , some outer  $v_i$  with  $\deg(v_i) \geq 3$  and a pair  $[j]$ . Suppose that  $j \in l(v_i)$ ,  $\underline{j} \in l(v_0)$ , and the labelling is valid, so there exists a corresponding lattice embedding  $\varphi : \Lambda_b(\beta) \hookrightarrow \mathbb{Z}^a$ . Denote by  $\mathbb{Z}_j^{a-1}$  the subspace of  $\mathbb{Z}^a$  that is orthogonal to the subspace spanned by  $e_j$ . Since  $v_0 \cdot v_i \geq 1$ , composing  $\varphi$  with the projection  $\mathbb{Z}^a \twoheadrightarrow \mathbb{Z}_j^{a-1}$  gives an embedding  $\Lambda_b(\beta') \hookrightarrow \mathbb{Z}_j^{a-1}$ , where  $\beta'$  is an ABC such that  $\Gamma_w(\beta')$  differs from  $\Gamma_w(\beta)$  by the deletion of a single inner edge between  $v_0$  and  $v_i$ . However,  $\text{rk } \Lambda_b(\beta) = \text{rk } \Lambda_b(\beta') = a$  and  $\text{rk } \mathbb{Z}_j^{a-1} = a-1$ , a contradiction. The following is a local picture of this invalid labelling:

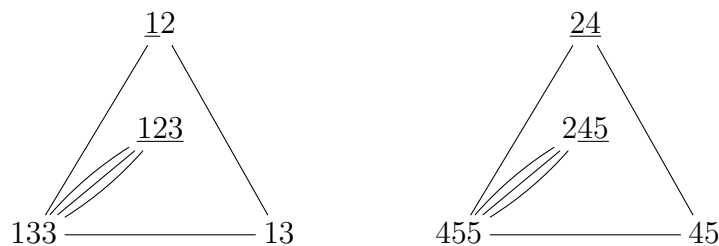


Analogously, if  $a \geq 3$  and  $[j]$  is a pair such that  $j \in l(v_i)$  and  $\underline{j} \in l(v_{i+1})$  for two adjacent outer vertices  $v_i$  and  $v_{i+1}$ , we reach a contradiction to the validity of the labelling. However, the graph obtained by removing the edge between  $v_i$  and  $v_{i+1}$  need not be a Tait graph for any ABC.

As noted before, different choices of canonical bases for the integral lattice give rise to different labellings. However, for the purposes of classification, we are only interested in embeddings up to an automorphism of the integral lattice, which motivates the following definition.

**Definition 3.1.7.** Say that two valid labellings of  $\Gamma$  are *equivalent* if they determine embeddings  $\varphi, \varphi' : \Lambda \hookrightarrow \mathbb{Z}^{\text{rk } \Lambda}$  that differ by composition with an element of  $\text{Aut } \mathbb{Z}^{\text{rk } \Lambda}$ , possibly with a re-indexing of the basis of  $\mathbb{Z}^{\text{rk } \Lambda}$ . In this case, say that one labelling can be obtained from the other by *relabelling*, and denote the relabelling that exchanges all instances of a label  $j$  with a label  $j'$  by  $j \leftrightarrow j'$ .

**Example 3.1.8.** Once again consider  $\beta = \sigma_1^3 \sigma_2^{-3}$ . Two labellings below determine embeddings  $\Lambda_b(\beta) \hookrightarrow \mathbb{Z}^3$  with canonical bases for  $\mathbb{Z}^3$  indexed  $\{e_1, e_2, e_3\}$  and  $\{e_2, e_4, e_5\}$ , respectively. These labellings are equivalent via the relabelling  $1 \leftrightarrow 4, 2 \leftrightarrow \underline{2}, 3 \leftrightarrow 5$ :



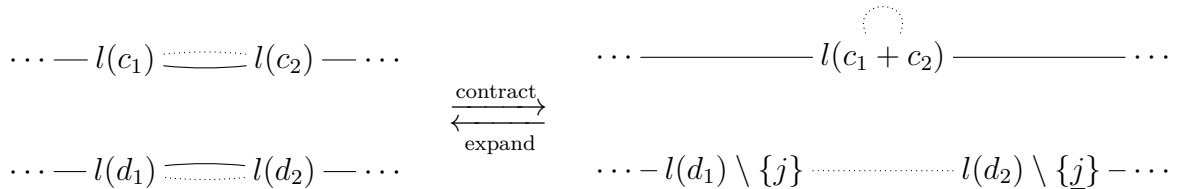
## § 3.2 | Operations on labelled Tait graphs

In this section, we define two main operations on labelled Tait graphs that we shall be using, namely *contractions* and *expansions*. We then specialise the discussion to the case of ABCs.

Suppose  $D$  is a non-split alternating diagram for a link  $L$  and  $\Gamma \in \{\Gamma_w(D), \Gamma_b(D)\}$  is a validly labelled Tait graph determining an embedding  $\varphi : \Lambda \hookrightarrow \mathbb{Z}^{\text{rk} \Lambda}$ , where  $\Lambda$  is the lattice of the opposite colour from  $\Gamma$ . To perform a *contraction* on  $\Gamma$ , suppose that, up to relabelling, for some label set  $[j]$  one of the following holds:

- (1) there exist four distinct vertices  $c_1, c_2, d_1$  and  $d_2$  of  $\Gamma$  such that  $c_1 \cdot c_2 \geq 1$  and  $d_1 \cdot d_2 \geq 1$ ,  $m(c_1, j) = m(d_1, j) = 1$ ,  $m(c_2, \underline{j}) = m(d_2, \underline{j}) = 1$  and  $j, \underline{j} \notin l(v)$  for all other  $v \in V(\Gamma)$ ;
- (2) there exist three distinct vertices  $s, c_2$  and  $d_2$  of  $\Gamma$  such that  $s \cdot c_2 \geq 1$  and  $s \cdot d_2 \geq 1$ ,  $m(s, j) = 2$ ,  $m(c_2, \underline{j}) = m(d_2, \underline{j}) = 1$  and  $j, \underline{j} \notin l(v)$  for all other  $v \in V(\Gamma)$ ;
- (3) there exist three distinct vertices  $e, c_1$  and  $d_1$  of  $\Gamma$  such that  $e \cdot c_1 \geq 1$  and  $e \cdot d_1 \geq 1$ ,  $m(e, j) = 2$ ,  $m(c_1, j) = m(d_1, j) = 1$  and  $j, \underline{j} \notin l(v)$  for all other  $v \in V(\Gamma)$ ;
- (4) there exist two distinct vertices  $s$  and  $e$  of  $\Gamma$  such that  $s \cdot e \geq 4$ ,  $m(s, j) = m(e, j) = 2$ , and  $j, \underline{j} \notin l(v)$  for all other  $v \in V(\Gamma)$ ;
- (5) there exist three distinct vertices  $s, e$  and  $v$  of  $\Gamma$  such that  $s \cdot e = 0$ ,  $s \cdot v > 0$ ,  $e \cdot v > 0$ ,  $m(s, j) = m(e, \underline{j}) = 1$  and  $j, \underline{j} \notin l(v)$  for all other  $v \in V(\Gamma)$ .

Let us focus on case (1). A *contraction on  $[j]$*  amounts to the following sequence of operations: first, contract an edge between  $c_1$  and  $c_2$ , merging them together into a new vertex  $c$  and setting  $l(c) = l(c_1 + c_2)$ , then delete an edge between  $d_1$  and  $d_2$  along with deleting  $j$  and  $\underline{j}$  from  $l(d_1)$  and  $l(d_2)$ , respectively. In the resulting labelled graph  $\Gamma'$  there are one fewer vertices, two fewer edges, and  $j, \underline{j} \notin l(\Gamma')$ . The inverse operation of passing from  $\Gamma'$  to  $\Gamma$  is called an *expansion*. An illustration is as follows:



On the level of link diagrams, contracting amounts to smoothing crossings between white regions corresponding to  $c_1, c_2, d_1$  and  $d_2$  as shown in Figure 3.1. Cases (2)–(5) are, in fact, special instances of case (1) with the following vertices coinciding, respectively:  $c_1$  and  $d_1$ ;  $c_2$  and  $d_2$ ; both  $c_1$  and  $d_1$ , and  $c_2$  and  $d_2$ ;  $c_2$  and  $d_1$ . Contractions in those cases are analogous to case (1) and result in a labelled graph with no  $j$  and  $\underline{j}$  labels. Notice that a contraction results in a creation of loop edges if  $c_1 \cdot c_2 \geq 2$ .

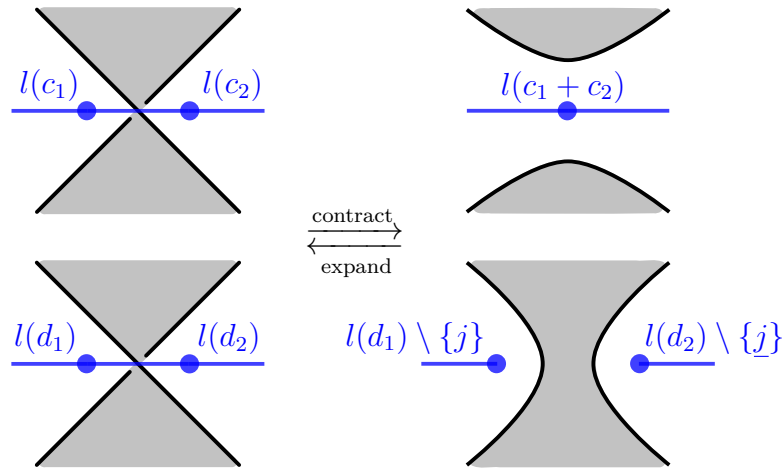
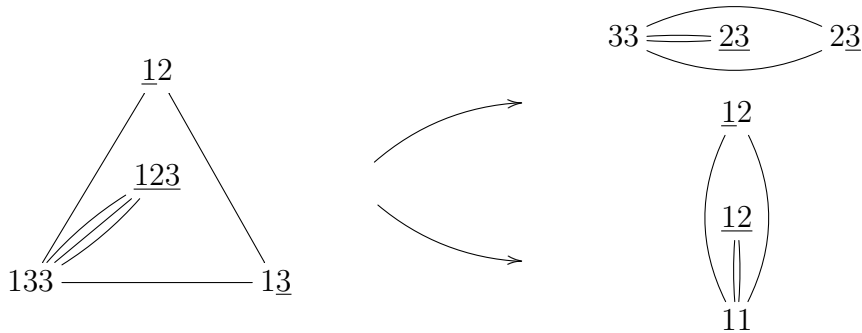


Figure 3.1: Effect of a contraction on the underlying link diagram.

When carrying out contractions on labelled graphs of ABCs, we would like the link corresponding to the contracted graph to remain an ABC; this motivates the following definition.

**Definition 3.2.1.** For an ABC  $\hat{\beta}$  with a validly labelled Tait graph  $\Gamma(\beta)$ , a *preserving contraction* of  $\Gamma(\beta)$  is a contraction in which an outer edge is contracted, an inner edge is deleted, and the resulting graph  $\Gamma'$  is a validly labelled Tait graph of the same colour for some ABC  $\hat{\beta}'$ , that is,  $\Gamma' = \Gamma(\beta')$ .

**Example 3.2.2.** Consider the validly labelled  $\Gamma_w(\sigma_1^3 \sigma_2^{-3})$  in Examples 3.1.4 and 3.1.8. It admits two preserving contractions on [1] and [3]: in both cases, delete the inner edge adjacent to  $v_3$ , and contract, respectively, the edge between  $v_1$  and  $v_2$  and the edge between  $v_2$  and  $v_3$ .



The two resulting labelled graphs are equivalent via relabelling  $1 \leftrightarrow 3$  and determine embeddings of  $\Lambda_b(\beta')$  for  $\beta' = \sigma_1^2 \sigma_2^{-2}$ .

### § 3.3 | Properties of embeddable ABCs

The goal of this section is to investigate elementary properties of embeddings of lattices associated to ABCs and establish a fundamental dichotomy between such embeddings. For the rest of this chapter, let  $\hat{\beta}$  be an embeddable ABC together with a validly labelled

Tait graph  $\Gamma(\beta)$  giving rise to a lattice  $\Lambda(\beta)$  of rank  $k$  that admits an embedding

$$\begin{aligned} \varphi : \Lambda(\beta) &\hookrightarrow \mathbb{Z}^k \\ v_i &\mapsto \sum_{j=1}^k \alpha_i^j e_j, \end{aligned}$$

where  $v_1, \dots, v_k$  are the generators of  $\Lambda(\beta)$  and  $v_0 = -v_1 - \dots - v_k$ . Out of two possible choices of  $\Gamma(\beta)$ , we make the one corresponding to the higher rank lattice (that is, if  $\text{rk } \Lambda_b(\beta) \geq \text{rk } \Lambda_w(\beta)$ , then take  $\Gamma(\beta) = \Gamma_w(\beta)$  and  $\Lambda(\beta) = \Lambda_b(\beta)$ , and make the other choice in the opposite case). The Tait graph of the colour opposite to our chosen  $\Gamma(\beta)$  is its planar dual  $\Gamma^*(\beta)$ . We also occasionally abuse notation by writing  $\text{rk } \Gamma(\beta)$  for  $\text{rk } \Lambda(\beta)$ , and denote  $\text{rk } \Gamma^*(\beta) = l$ .

**Lemma 3.3.1** (‘Dichotomy lemma’). In the above setting, either

(i) for all label sets  $[j]$  in  $l(\Gamma(\beta))$ , we have  $[[j]] = \{1^{(2)}, (-1)^{(2)}\}$ , or

(ii) there exists a label set  $[j]$  in  $l(\Gamma(\beta))$  such that  $[[j]] = \{1^{(1)}, (-1)^{(1)}\}$ .

*Proof.* Let  $\text{rk } \Gamma(\beta) = k$  and  $\text{rk } \Gamma^*(\beta) = l$ , so  $k \geq l$ . Observe that the crossing number of our standard diagram for  $\beta$  is  $\text{cr}(\beta) = k + l \leq 2k$ . Since  $|E(\Gamma(\beta))| = \text{cr}(\beta)$ , using the handshake lemma we have

$$2 \text{cr}(\beta) = \sum_{i=0}^k \deg(v_i) = \sum_{i=0}^k v_i \cdot v_i = \sum_{j=1}^k \left( \sum_{i=0}^k (\alpha_i^j)^2 \right) \leq 4k. \quad (3.3.1)$$

Hence, either  $\sum_{i=0}^k (\alpha_i^j)^2 = 4$  for all  $j$ , or there exists  $j$  such that  $\sum_{i=0}^k (\alpha_i^j)^2 < 4$ . Since  $\alpha_0^j = -\sum_{i=1}^k \alpha_i^j$  for all  $j$ , we have that  $\sum_{i=0}^k \alpha_i^j = 0$  for all  $j$ . Thus, (i) holds in the former case. In the latter case, notice that  $\sum_{i=0}^k (\alpha_i^j)^2 \neq 0$  for all  $j$ , since otherwise  $\text{rk } \Gamma(\beta) < k$ ; thus, (ii) holds.  $\square$

Notice that case (i) amounts to attaining equality in Equation (3.3.1), which implies that  $\text{rk } \Gamma(\beta) = \text{rk } \Gamma^*(\beta)$ .

The following conjecture was obtained by considering all embeddings of black and white lattices for ABCs with up to 20 crossings produced by the script in Appendix A.

**Conjecture 3.3.2** (‘Heavy label conjecture’). If case (ii) in Lemma 3.3.1 holds for  $\Gamma(\beta)$ , then there is precisely one  $[j]$  with  $w(j) > 4$ . Moreover, for such  $[j]$  we have  $[[j]] = \{(\pm 2)^{(1)}, (\mp 1)^{(2)}\}$  or  $[[j]] = \{2^{(1)}, (-2)^{(1)}\}$ .

Recall our convention that  $l(v_0)$  should only contain underlined labels. Conjecture 3.3.2 then implies that there are nine possible configurations of any label set  $[x]$  with respect to how elements of  $[x]$  are contained in  $l(\Gamma(\beta))$ : five when  $[x]$  is heavy, denoted (H1) to (H5), two when  $[x]$  is a pair, denoted (P1) and (P2), and two when  $[x]$  is a quartet, denoted (Q1) and (Q2). Note that labels on outer vertices need not



Fixing a valid labelling of  $\Gamma(\beta)$ , denote the number of label sets in configuration (Hi) by  $h_i(\Gamma(\beta))$  for  $i = 1, \dots, 5$ , and, similarly, define  $p_i(\Gamma(\beta))$  and  $q_i(\Gamma(\beta))$  for  $i = 1, 2$ ; when the graph is clear from context, we will drop it from notation.<sup>2</sup> Notice that Conjecture 3.3.2 states that  $0 \leq \sum_{i=1}^5 h_i \leq 1$ , so at most one of the  $h_i$  is non-zero.

**Definition 3.3.3.** For a validly labelled  $\Gamma(\beta)$  with  $h_i = 1$  for some  $i$ , call the vector  $\langle d; i; p_1, p_2; q_1, q_2 \rangle$  its *profile*. If  $h_i = 0$  for all  $i$ , write  $\langle d; 0; p_1, p_2; q_1, q_2 \rangle$ .

Conjecture 3.3.2 implies some restrictions on  $d(\beta)$ .

**Lemma 3.3.4.** The rank difference  $d = d(\beta)$  depends only on  $p_i = p_i(\Gamma(\beta))$  as follows:

$$d = \begin{cases} p_1 + p_2 - 2 & \text{if } h_1 = 1 \text{ or } h_5 = 1, \\ p_1 + p_2 - 1 & \text{if } h_2 = 1 \text{ or } h_3 = 1 \text{ or } h_4 = 1, \\ p_1 + p_2 & \text{if } h_i = 0 \text{ for } i = 1, \dots, 5. \end{cases}$$

*Proof.* The graph  $\Gamma(\beta)$  has  $k$  outer edges; we can write  $k$  by the handshake lemma as half the sum of degrees of outer vertices  $v_1, \dots, v_k$ , excluding the inner edges from consideration. In terms of  $\alpha_i^j$ , we have

$$k = \frac{1}{2} \left( \left( \sum_{i=1}^k \deg(v_i) \right) - \deg(v_0) \right) = \sum_{j=1}^k \frac{1}{2} \left( \left( \sum_{i=1}^k (\alpha_i^j)^2 \right) - (\alpha_0^j)^2 \right).$$

For each  $j$ , let  $k_j = \frac{1}{2} \left( \left( \sum_{i=1}^k (\alpha_i^j)^2 \right) - (\alpha_0^j)^2 \right)$ , so  $k = \sum_{j=1}^k k_j$ . Since  $\text{rk } \Gamma^*(\beta) = l$  is given by the number of inner edges of  $\Gamma(\beta)$  (that is,  $l = \sum_{j=1}^k (\alpha_0^j)^2$ ), we have

$$d = k - l = \sum_{j=1}^k \frac{1}{2} \left( \left( \sum_{i=1}^k (\alpha_i^j)^2 \right) - 3(\alpha_0^j)^2 \right).$$

For each  $j$ , set  $d_j = \frac{1}{2} \left( \left( \sum_{i=1}^k (\alpha_i^j)^2 \right) - 3(\alpha_0^j)^2 \right)$ , so  $d = \sum_{j=1}^k d_j$ . Observe that the average of  $k_j$  over all  $j = 1, \dots, k$  is equal to 1. We can calculate the contribution from a label set in given configuration to  $k$  and  $d$  in terms of  $k_j$  and  $d_j$ , respectively:

	(H1)	(H2)	(H3)	(H4)	(H5)	(P1)	(P2)	(Q1)	(Q2)
$k_j$	0	-1	2	3	4	0	1	1	2
$d_j$	-4	-5	1	3	4	-1	1	0	2

Since  $k_j = 1$  for  $[j]$  in (P2) and (Q1) configurations, we know that  $k_j$  for label sets in all other configurations must average to 1, too. We have six cases to consider, one for each  $h_i = 1$  and one if all  $h_i = 0$ :

- if  $h_1 = 1$ :  $\frac{0 + 0 \cdot p_1 + 2 \cdot q_2}{1 + p_1 + q_2} = 1 \implies q_2 = p_1 + 1$  and  $q_2 \geq 1$ ;
- if  $h_2 = 1$ : similarly,  $q_2 = p_1 + 2$  and  $q_2 \geq 2$ ;

<sup>2</sup>NB: In our notation,  $p_1$  and  $p_2$  are different from the same symbols introduced by Lisca in [Lis07].

- if  $h_3 = 1$ :  $q_2 = p_1 - 1$  and  $p_1 \geq 1$ ;
- if  $h_4 = 1$ :  $q_2 = p_1 - 2$  and  $p_1 \geq 2$ ;
- if  $h_5 = 1$ :  $q_2 = p_1 - 3$  and  $p_1 \geq 3$ ;
- if  $h_i = 0$  for  $i = 1, \dots, 5$ :  $\frac{0 \cdot p_1 + 2 \cdot q_2}{p_1 + q_2} = 1 \implies p_1 = q_2$ .

The result then follows easily by considering  $d = \sum_{j=1}^k d_j$  since labels in (Q1) configuration do not contribute to  $d$ : for example, if  $h_1 = 1$ , then

$$d = -4 - p_1 + p_2 + 2(p_1 + 1) = p_1 + p_2 - 2. \quad \square$$

### § 3.4 | Contraction classes of embeddable ABCs

For the rest of the chapter, assume that Conjecture 3.3.2 holds. With this assumption, we develop a classification of embeddings of  $\Lambda(\beta)$ , where  $\Lambda(\beta)$  can be either  $\Lambda_b(\beta)$  or  $\Lambda_b(\beta)$  if they have the same rank, or is the higher rank lattice otherwise.

In the following, we will find it necessary to directly check all embeddings of all  $\Lambda(\beta)$  up to rank at most 9 for having desired properties. We have written a SageMath script, presented in Appendix A, to generate Goeritz matrices for all non-isotopic ABCs with up to a fixed number of crossings, and determine all embeddings of corresponding lattices into the integral lattice via the algorithm of Plesken for solving the matrix equation  $XX^T = A$  for  $X$  over  $\mathbb{Z}$  [Ple95], implemented in GAP. Hence, when referring to a direct check, we mean explicitly going through the list of all embeddings generated by this script.

Let us list all braids whose closures are embeddable ABCs with  $k \leq 3$ : these are  $\sigma_1\sigma_2^{-1}$  for  $k = 1$ ,  $\sigma_1^2\sigma_2^{-2}$  for  $k = 2$ , and  $\sigma_1^3\sigma_2^{-3}$  and  $(\sigma_1\sigma_2^{-1})^3$  for  $k = 3$ . All of these braids are self-dual with  $d(\beta) = 0$ . The unique labellings of  $\Gamma(\beta)$  in these cases are shown below:

$$(3.4.1)$$

#### § 3.4.1 | Case I: $p_1 > 0$

It turns out that if a valid labelling of  $\Gamma(\beta)$  includes a label in the (P1) configuration, then  $\Gamma(\beta)$  readily admits preserving contractions.

**Proposition 3.4.1.** If  $p_1(\Gamma(\beta)) > 0$ , then  $d(\beta) \in \{0, 3\}$ . Moreover, if  $d(\beta) = 0$  or  $d(\beta) = 3$ , then  $\Gamma(\beta)$  admits a sequence of preserving contractions to the unique validly labelled graph for the closure of  $\sigma_1\sigma_2^{-1}$  or the closure of  $\sigma_1^4\sigma_2^{-1}$ , respectively.



labelling of  $\Gamma(\sigma_1^4\sigma_2^{-1})$  is unique and shown below:

$$\begin{array}{ccc}
 & \underline{zt} & \\
 & / \quad \backslash & \\
 \underline{xzw} & \text{---} \underline{x} & \underline{zw} \\
 & \backslash \quad / & \\
 & \underline{zw} & 
 \end{array} \tag{3.4.2}$$

□

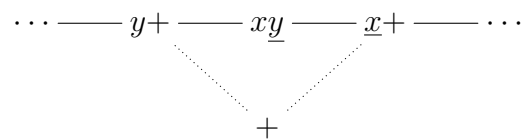
Since the profiles of the unique labellings of  $\Gamma(\sigma_1^3\sigma_2^{-3})$  and  $\Gamma(\sigma_1^4\sigma_2^{-1})$  are, respectively,  $\langle 0; 3; 1, 0; 1, 0 \rangle$  and  $\langle 3; 0; 1, 2; 0, 1 \rangle$ , we conclude that every valid labelling of  $\Gamma(\beta)$  with  $p_1 > 0$  and  $k \geq 4$  has profile  $\langle 0; 3; 1, 0; k - 2, 0 \rangle$  or  $\langle 3; 0; 1, 2; k - 4, 1 \rangle$ . This follows from the proof since we only performed preserving contractions on label sets in (Q1) configuration.

**§ 3.4.2 | Case II:  $p_1 = 0$**

We now study the case when  $p_1(\Gamma(\beta)) = 0$ , where there are more distinct profiles to consider. Let  $V_2(\Gamma(\beta))$  be the set of labelled outer vertices of  $\Gamma(\beta)$  of degree two.

**Remark 3.4.2.** Immediately observe that  $|V_2(\Gamma(\beta))|$  is an upper bound on  $d(\beta)$  by the assumption that  $k \geq l$ . Also notice that for  $k \leq 3$ , the only valid labelling of  $\Gamma(\beta)$  with  $p_1(\Gamma(\beta)) = 0$  is the one for  $\beta = (\sigma_1\sigma_2^{-1})^3$  shown in Diagram (3.4.1). This labelled graph admits a preserving contraction on any of the label sets down to the graph for  $\sigma_1^2\sigma_2^{-2}$ , and further contracts to the graph for  $\sigma_1\sigma_2^{-1}$ .

Suppose  $p_1(\Gamma(\beta)) = 0$ ,  $k \geq 4$  and  $v \in V_2(\Gamma(\beta))$ . Write  $l(v) = \underline{xy}$ . It is easy to see that neither  $[x]$  nor  $[y]$  can be in (H1) or (H2) configurations, or in (P1) configuration by assumption. Suppose both  $[x]$  and  $[y]$  are in (P2) configuration, so the local picture is the following:



Example 3.1.6 shows this is not valid labelling. Up to relabelling, this leaves us with three options: (a)  $[x]$  and  $[y]$  are both in (Q1) configuration, (b)  $[x]$  and  $[y]$  are both in (Q2) configuration, and (c)  $[x]$  is in (Q2) and  $[y]$  is in (P2) configuration.

**Definition 3.4.3.** Call  $v \in V_2(\Gamma(\beta))$  *removable* in case (a), and *essential* in cases (b) and (c). Specifically, say that  $v$  is *QQ-essential* in case (b), and *QP-essential* in case (c).

**Lemma 3.4.4.** If  $p_1(\Gamma(\beta)) = 0$ , then  $\Gamma(\beta)$  admits a sequence of preserving contractions to a validly labelled graph  $\Gamma_{\text{red}}(\beta)$ , with  $\Gamma_{\text{red}}(\beta) = \Gamma(\beta')$  for some ABC  $\hat{\beta}'$ , such that for all  $v \in V_2(\Gamma_{\text{red}}(\beta))$ , the vertex  $v$  is essential.

*Proof.* The statement holds for  $k \leq 3$  by Remark 3.4.2, so suppose  $p_1(\Gamma(\beta)) = 0$  and  $k \geq 4$ . Let  $v \in V_2(\Gamma(\beta))$  be removable. Adopting the same notation as in the proof



of  $[x]$  appear in their labellings.

Suppose (a(ii)), with  $u \cdot r_1 = 1$  and  $u \cdot l_1 = 0$ . Then  $[z] \cap l(u) = \emptyset$ , so  $w \in l(u)$  and  $w \in l(l_1)$  for some  $[w]$  so that  $u \cdot l_1 = 0$ . Thus  $\deg(l_1) \geq 3$ . Suppose  $\deg(r_1) = 2$ . The local picture is then

$$\begin{array}{ccccccc}
 \cdots & \text{---} & \underline{xzw+} & \text{---} & \underline{xy} & \text{---} & \underline{xz} & \text{---} & \underline{xyw+} & \text{---} & \cdots \\
 & & \searrow & & \searrow & & \searrow & & \searrow & & \\
 & & & & +|\underline{xyz} & & & & & & \\
 & & \swarrow & & \swarrow & & \swarrow & & \swarrow & & 
 \end{array} \tag{3.4.4}$$

Again, it follows that there are at most two vertices in  $V_2(\Gamma_{\text{red}}(\beta))$  for each  $[x]$  in (Q2) configuration. Also notice that  $[z]$  must be in the (P2) configuration in this case. (The argument in case  $u \cdot r_1 = 0$  and  $u \cdot l_1 = 1$  is analogous.)

Now suppose that (b) holds and  $v$  is QQ-essential. Observe that if  $\underline{x} \in l(l_1)$ , it is the case that  $\underline{x} \notin l(r_1)$ . To see that, suppose otherwise and consider  $u \notin \{v, l_1, r_1\}$  such that  $\underline{y} \in l(u)$  (such  $u$  exists as  $[y]$  is in (Q2) configuration): then  $\underline{x} \in l(u)$  so that  $v \cdot u = 0$ , a contradiction. Hence  $\underline{x} \in l(l_1)$  and  $\underline{y} \in l(r_1)$ , thus there are two distinct outer vertices  $t$  and  $u$  not coinciding with either of  $l_1$  or  $r_1$  such that  $xy \subset l(t)$  and  $\underline{xy} \subset l(u)$ . Then for some  $[z]$  we must have  $z \in l(t)$  and  $\underline{z} \in l(r_1)$  so that  $t \cdot r_1 \geq 0$ , and for some  $[w]$  we must have  $w \in l(u)$  and  $\underline{w} \in l(l_1)$  so that  $u \cdot l_1 \geq 0$ . Thus,  $\deg(t)$  and  $\deg(u)$  are each at least 3:

$$\begin{array}{ccccccccccc}
 \cdots & \text{---} & \underline{xyz+} & \text{---} & \cdots & \text{---} & \underline{xw+} & \text{---} & \underline{xy} & \text{---} & \underline{yz+} & \text{---} & \cdots & \text{---} & \underline{xyw+} & \text{---} & \cdots \\
 & & \searrow & & & & \searrow & & \searrow & & \searrow & & & & \searrow & & \\
 & & & & & & +|\underline{xy} & & & & & & & & & & \\
 & & \swarrow & & & & \swarrow & & \swarrow & & \swarrow & & & & \swarrow & & 
 \end{array} \tag{3.4.5}$$

Hence, for every two label sets  $[x]$  and  $[y]$  each in (Q2) configuration there are at most three essential vertices. Consequently, in both (a) and (b) cases,  $|V_2(\Gamma_{\text{red}}(\beta))| \leq 2q_2(\Gamma_{\text{red}}(\beta))$ .  $\square$

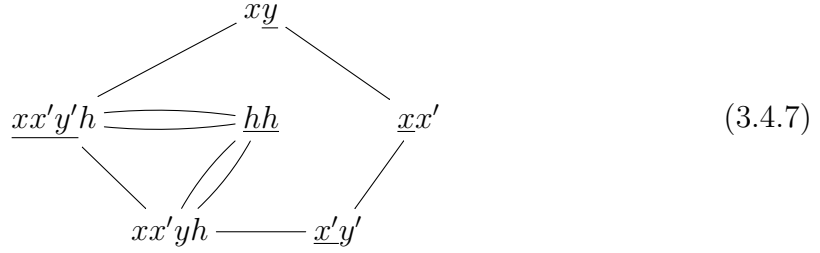
**Remark 3.4.6.** Lemma 3.4.5 does not hold if  $\text{rk } \Gamma_{\text{red}}(\beta) \leq 4$ : the sole counterexample is the following labelled  $\Gamma(\sigma_1^4 \sigma_2^{-4})$  with three essential vertices and  $q_2 = 1$ :

$$\begin{array}{ccc}
 & \underline{xy} & \\
 & / \quad \backslash & \\
 \underline{xzh} & \equiv \equiv \equiv & \underline{hz} \\
 & \backslash \quad / & \\
 & \underline{xy} & 
 \end{array} \tag{3.4.6}$$

**Definition 3.4.7.** A  $3^+$ -chain is a sequence of outer vertices  $v_1, \dots, v_n$  of  $\Gamma(\beta)$  such that  $v_i \cdot v_{i+1} = 1$  for  $i = 1, \dots, n - 1$  and  $\deg(v_i) \geq 3$  for  $i = 1, \dots, n$ .

We are now ready to describe preserving contraction classes with  $p_1(\Gamma(\beta)) = 0$ .

**Theorem 3.4.8.** If  $p_1(\Gamma(\beta)) = 0$ , then  $d(\beta) \in \{0, 1\}$ . Moreover, if  $d(\beta) = 1$ , then  $\Gamma(\beta)$  admits a sequence of preserving contractions to the labelled  $\Gamma(\sigma_1^4\sigma_2^{-2}\sigma_1\sigma_2^{-2})$



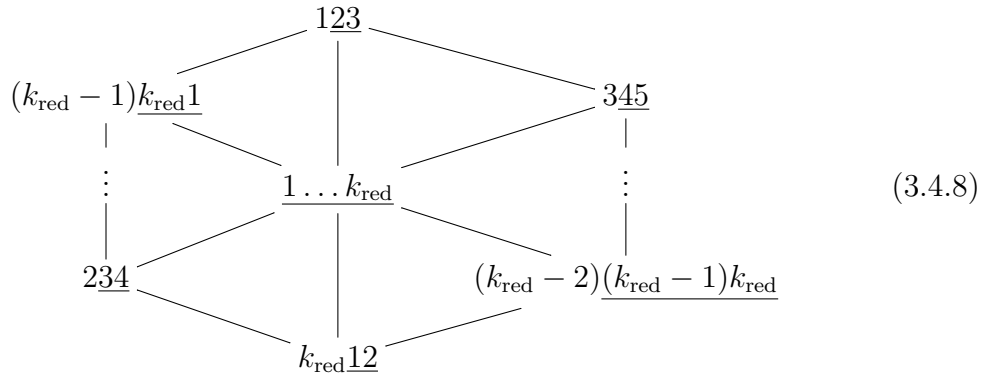
and if  $d(\beta) = 0$ , then  $\Gamma(\beta)$  admits a sequence of preserving contractions to either  $\Gamma(\sigma_1\sigma_2^{-1})$  in Diagram (3.4.1) or  $\Gamma(\sigma_1^4\sigma_2^{-4})$  in Diagram (3.4.6).

*Proof.* The case of  $k \leq 3$  has been considered in Remark 3.4.2, so suppose  $p_1(\Gamma(\beta)) = 0$  and  $k \geq 4$ . By Lemma 3.4.4, apply preserving contractions to  $\Gamma(\beta)$  to obtain  $\Gamma_{\text{red}}(\beta)$  such that all vertices in  $V_2(\Gamma_{\text{red}}(\beta))$  are essential, and the only possible difference between the profiles of  $\Gamma(\beta)$  and  $\Gamma_{\text{red}}(\beta)$  is in  $q_1$ ; in particular, we can confuse  $p_2(\Gamma(\beta))$  and  $p_2(\Gamma_{\text{red}}(\beta))$  and drop the parentheses, similarly for  $q_2$  and  $h_i$  for  $i = 1, \dots, 5$ . Let  $k_{\text{red}} = \text{rk } \Gamma_{\text{red}}(\beta)$ . Lemma 3.3.4 implies that  $h_3 = h_4 = h_5 = 0$  when  $p_1 = 0$ , otherwise  $q_2$  would need to be negative. This leaves three cases:

- (1)  $h_1 = h_2 = 0$ , hence  $q_2 = p_2 = 0$ ;
- (2)  $h_1 = 1$ , hence  $q_2 = 1$  and  $p_2 \geq 2$ ;
- (3)  $h_2 = 1$ , hence  $q_2 = 2$  and  $p_2 \geq 1$ .

(1) Suppose (1) holds. Since  $q_2 = p_2 = 0$ , there are no essential vertices, so every outer vertex of  $\Gamma_{\text{red}}(\beta)$  has degree at least 3. Since  $0 \leq d(\beta) \leq |V_2(\Gamma_{\text{red}}(\beta))| = 0$ , there is an equal number of outer vertices and inner edges, hence every outer vertex has degree exactly 3 and  $\Gamma_{\text{red}}(\beta) = \Gamma((\sigma_1\sigma_2^{-1})^{k_{\text{red}}})$ . We could prove the following claim with our methods, however, we appeal to [Lis17, Proposition 3.21], restated in more familiar terms in [Sim20, Lemma 7.3], in the interests of brevity.

**Claim 3.4.9** ([Lis17, Proposition 3.21]). In case (1),  $k_{\text{red}}$  is odd, and the unique valid labelling of  $\Gamma(\beta)$  is given by

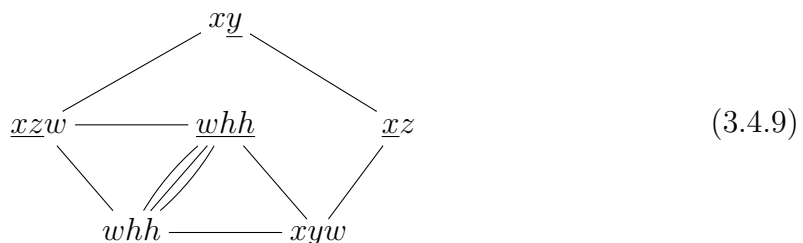


The profile of  $\Gamma_{\text{red}}(\beta)$  is thus  $\langle 0; 0; 0, 0; k_{\text{red}}, 0 \rangle$ , and one arrives at the labelled  $\Gamma(\sigma_1\sigma_2^{-1})$  by performing contractions on  $[1], [k_{\text{red}}], [2], [k_{\text{red}} - 1], \dots$  in order. This concludes case (1).

Since  $q_2 \neq 0$  in cases (2) and (3), we may assume that  $|V_2(\Gamma_{\text{red}}(\beta))| \geq 1$  now (if  $|V_2(\Gamma_{\text{red}}(\beta))| = 0$ , we are in case (1)). Moreover, by Remark 3.4.6, in the following we can assume that  $k_{\text{red}} \geq 5$ .

**(2)** Suppose (2) holds, so  $q_2 = 1$  and by Lemma 3.4.5,  $|V_2(\Gamma_{\text{red}}(\beta))| \leq 2$ . Suppose that  $|V_2(\Gamma_{\text{red}}(\beta))| = 2$ , in which case the (Q2) label  $[x]$  must appear as in Diagram (3.4.4) (since the case of Diagram (3.4.3) requires  $q_2 \geq 2$ ). From left to right, call the outer vertices visible in the Diagram (3.4.4)  $l_1 = r_{k_{\text{red}}-1}, v, r_1$  and  $r_2$ , and call the rest of the vertices, consecutively,  $r_3, \dots, r_{k_{\text{red}}-2}$ . Thus,  $r_2, \dots, r_{k_{\text{red}}-1}$  is a  $3^+$ -chain  $R$ .

The heavy label set  $[h]$  appears in (H1) configuration, so for any two adjacent vertices  $r_i$  and  $r_{i+1}$  in  $R$ , there is a label set  $[s]$  in (Q1) configuration with  $s \in l(r_i)$  and  $\underline{s} \in l(r_{i+1})$ , or vice versa (if  $[s]$  were in (P2) configuration, we could project it out as in Example 3.1.6, leading to a contradiction). Since  $s \in l(r_j)$  for some  $j \notin \{1, i, i+1\}$  and  $\underline{s} \in l(v_0)$ , we can contract on  $[s]$ , reducing  $q_1$  by one and keeping the rest of the profile unchanged. After performing enough such contractions (possibly also contracting away removable vertices of degree two if they appear during intermediate steps), we arrive at the following labelled graph for the closure of  $\sigma_1^3\sigma_2^{-1}\sigma_1\sigma_2^{-3}\sigma_1\sigma_2^{-1}$ :



It further contracts on  $[w]$  to the labelled graph in Diagram (3.4.6). Notice that we have not changed  $p_2$  and  $q_2$  along the way, so the profile for  $\Gamma(\beta)$  is  $\langle 0; 1; 0, 2; k - 4, 1 \rangle$ .

Now if  $|V_2(\Gamma_{\text{red}}(\beta))| = 1$  in case (2), there is a  $3^+$ -chain  $r_1, \dots, r_{k_{\text{red}}-1}$  with  $x \in l(r_j)$  for some  $j$ . Using the same reasoning as above, we can contract this chain until it has length 3 by only reducing  $q_1$  of the labelled graph. However are no valid labellings for graphs with rank 4 and the corresponding profile. Thus, we are done with case (2).

**(3)** Finally, suppose (3) holds, so  $q_2 = 2$  and  $|V_2(\Gamma_{\text{red}}(\beta))| \leq 4$ . Let us first consider Diagram (3.4.5) in more detail in this case. Recall that we denote the outer vertices visible in the diagram, in order from left to right, by  $t, l_1, v, r_1$  and  $u$ . If  $\deg(l_1) = \deg(r_1) = 2$ , then  $l_1 \cdot t = r_1 \cdot u = 1$  and both  $[z]$  and  $[w]$  are in (P2) configurations. Moreover,  $t$  and  $u$  are connected by a  $3^+$ -chain that we can contract as before until  $t \cdot u = 1$ . Then, the only possible labelled graph is the one for the closure of  $\sigma_1^4\sigma_2^{-2}\sigma_1\sigma_2^{-2}$  in Diagram (3.4.7). However, further considering Diagram (3.4.7) we observe that it

admits no expansions which preserve  $\deg(l_1) = \deg(r_1) = 2$ , hence  $\beta$  must have been  $\sigma_1^4\sigma_2^{-2}\sigma_1\sigma_2^{-2}$  all along. Thus, unless  $\Gamma(\beta)$  is the labelled graph in Diagram (3.4.7), the configuration in Diagram (3.4.5) contributes at most two essential vertices. Now, there are four subcases to consider:

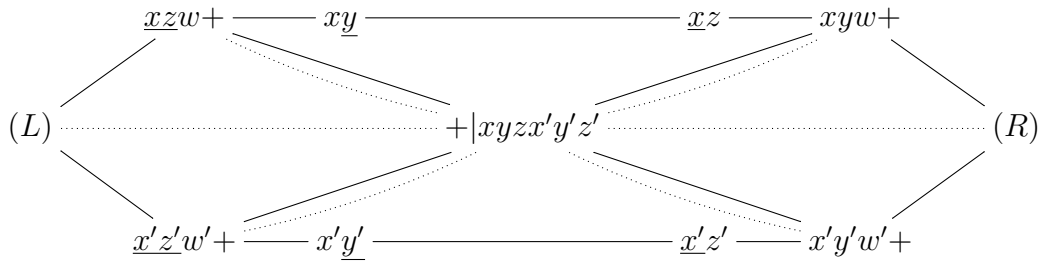
(3(i))  $|V_2(\Gamma_{\text{red}}(\beta))| = 4$ ;

(3(ii))  $|V_2(\Gamma_{\text{red}}(\beta))| = 3$ ;

(3(iii))  $|V_2(\Gamma_{\text{red}}(\beta))| = 2$ ;

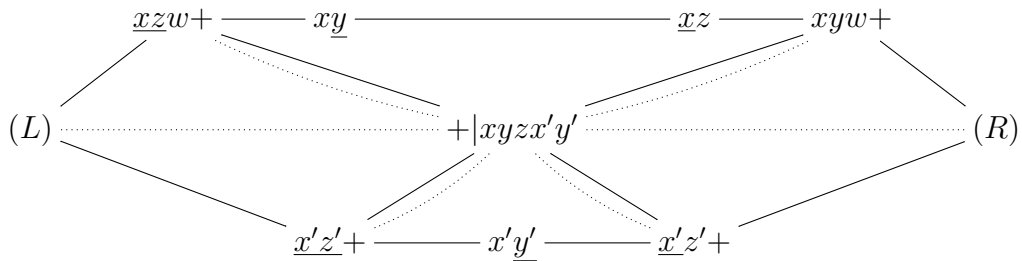
(3(iv))  $|V_2(\Gamma_{\text{red}}(\beta))| = 1$ .

**3(i)** Suppose that  $|V_2(\Gamma_{\text{red}}(\beta))| = 4$ . When  $k_{\text{red}} \leq 8$ , no such labellings exist, so assume  $k_{\text{red}} \geq 9$ . Hence, the labelled  $\Gamma_{\text{red}}(\beta)$  contains two copies of Diagram (3.4.4) joined to each other by  $3^+$ -chains  $L$  and  $R$  as shown below, with the length of at least one of  $L$  or  $R$  being non-zero. The configuration is as follows:



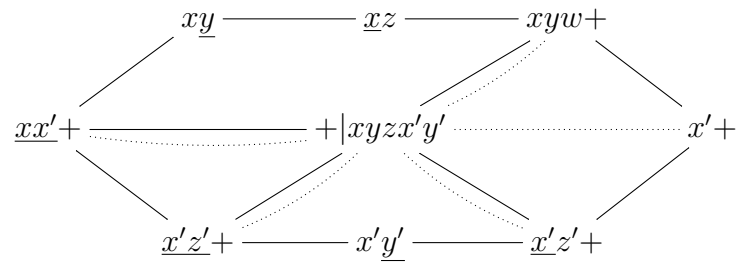
But then we can contract the  $3^+$ -chains, reducing the lengths of  $L$  and  $R$ , until there are eight outer vertices. This yields a contradiction.

**3(ii)** Suppose  $|V_2(\Gamma_{\text{red}}(\beta))| = 3$ . Then two cases are possible: either (a)  $\Gamma_{\text{red}}(\beta)$  contains a copy of Diagram (3.4.4) joined by  $3^+$ -chains  $L$  and  $R$  to an essential vertex labelled with an element of the (Q2) label set  $[x']$ , as shown,



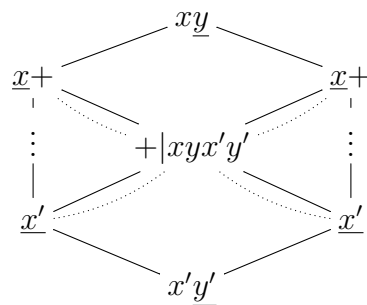
or, (b) the essential vertices are all adjacent, which is indeed the case of the closure of  $\sigma_1^4\sigma_2^{-2}\sigma_1\sigma_2^{-2}$  analysed previously. In case (a), check directly that no valid labellings exist if  $k_{\text{red}} \leq 8$ , so assume  $k_{\text{red}} \geq 9$  and the length of at least one of  $L$  and  $R$  is positive. Note that  $x' \in l(u)$  for some  $u \in \{L, R\}$  with  $\deg(u) \geq 3$ , so we know that by applying contractions we can remove all vertices in the chains except  $u$ . For example,

if  $u \in R$ , then the result would be

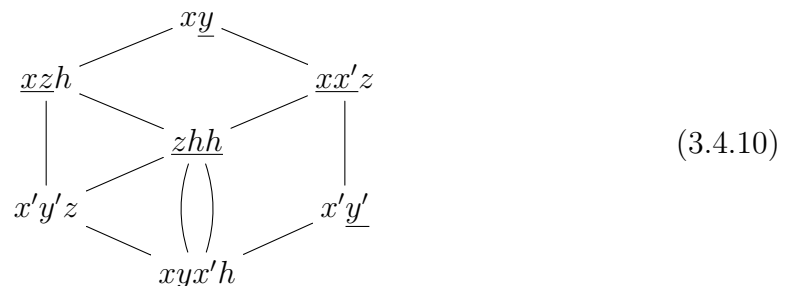


However, one verifies that such labellings do not exist for graphs of rank eight.

**3(iii)** Suppose  $|V_2(\Gamma_{\text{red}}(\beta))| = 2$ . Then there are four options: (a) the essential vertices are adjacent as in Diagram (3.4.3),  $[x]$  and  $[z]$  are (Q2) label sets, and  $\deg(r_2) \geq 3$ ; (b) the essential vertices are adjacent as in Diagram (3.4.4),  $[x]$  is a (Q2) label set,  $[y]$  and  $[z]$  are (P2) label sets, and the other (Q2) label set  $[x']$  appears only on outer vertices with degree at least 3; (c) the essential vertices are adjacent as in Diagram (3.4.5) with either  $\deg(l_1) = 2$  or  $\deg(r_1) = 2$ , and with  $[x]$  and  $[y]$  being (Q2) label sets; or (d) both essential vertices are joined by  $3^+$ -chains as shown:



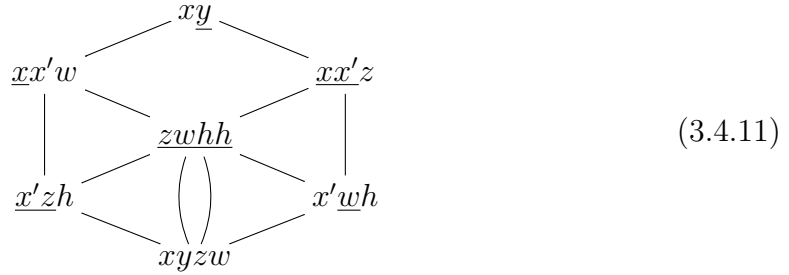
Apply the approach from (3(i)) and (3(ii)) to see that cases (a), (b) and (c) yield no validly labelled graphs, while in case (d) we can contract the  $3^+$ -chains until there are six outer vertices in total, when only  $\Gamma(\sigma_1^2\sigma_2^{-2}\sigma_1\sigma_2^{-1}\sigma_1\sigma_2^{-1}\sigma_1^2\sigma_2^{-1})$  admits the following unique valid labelling:



It has the profile  $\langle 1; 2; 0, 2; 1, 2 \rangle$  and further contracts to the labelled graph in Diagram (3.4.7).

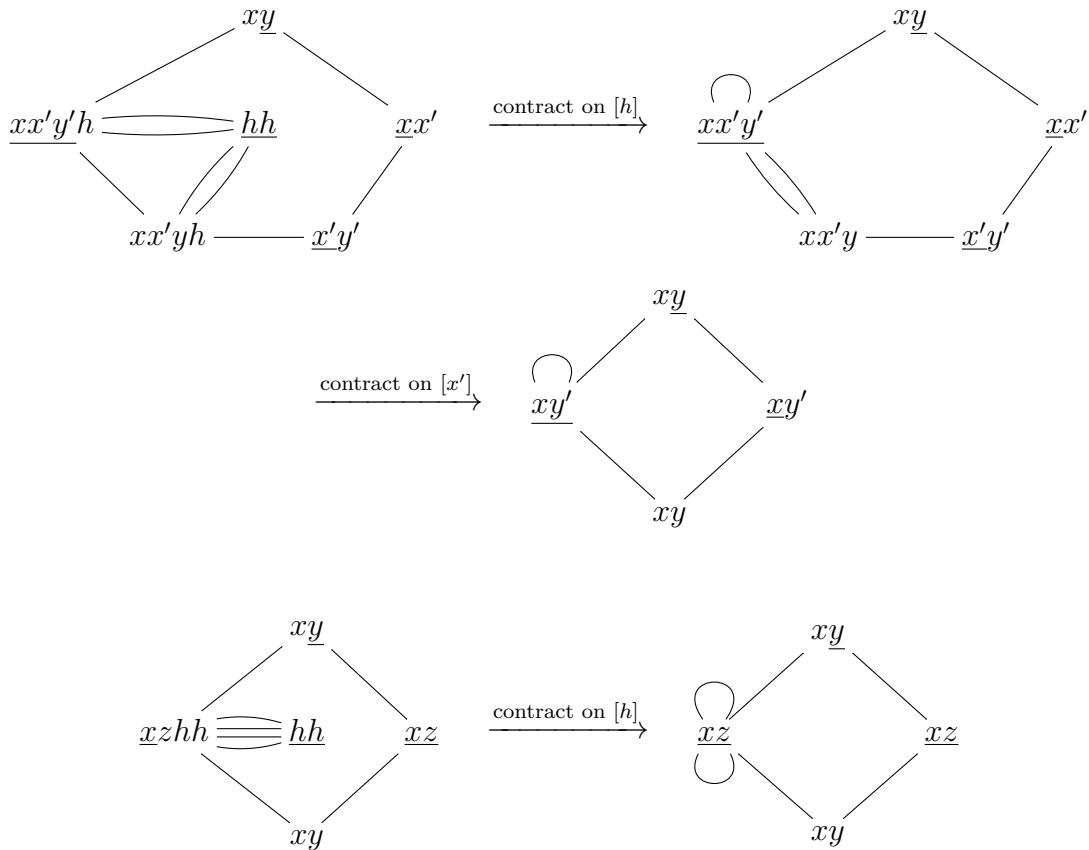
**3(iv)** The last case to consider is when  $|V_2(\Gamma_{\text{red}}(\beta))| = 1$ , that is, there is a unique QP-essential vertex  $v$  with  $[x]$  in (Q2) configuration and some  $[x']$  in (Q2) configuration

such that for any  $v'$  with  $x' \in l(v')$  or  $\underline{x}' \in l(v')$ , we have  $\deg(v') \geq 3$ . Contract the  $3^+$ -chains until there are eight outer vertices, in which case either the labelling of every vertex contains some label in  $[x]$  or  $[x']$ , or the graph admits further contractions on a label set in (Q1) configuration. The only two possible outcomes then are labelled  $\Gamma(\sigma_1^3 \sigma_2^{-2} \sigma_1 \sigma_2^{-1} \sigma_1 \sigma_2^{-3} \sigma_1^2 \sigma_2^{-1} \sigma_1 \sigma_2^{-1})$  and  $\Gamma(\sigma_1^2 \sigma_2^{-2} \sigma_1^2 \sigma_2^{-1} \sigma_1 \sigma_2^{-2} \sigma_1^2 \sigma_2^{-2} \sigma_1 \sigma_2^{-1})$  which both admit preserving contractions to the following labelled  $\Gamma(\sigma_1^2 \sigma_2^{-1} \sigma_1 \sigma_2^{-1} \sigma_1 \sigma_2^{-2} \sigma_1 \sigma_2^{-1} \sigma_1 \sigma_2^{-1})$ :



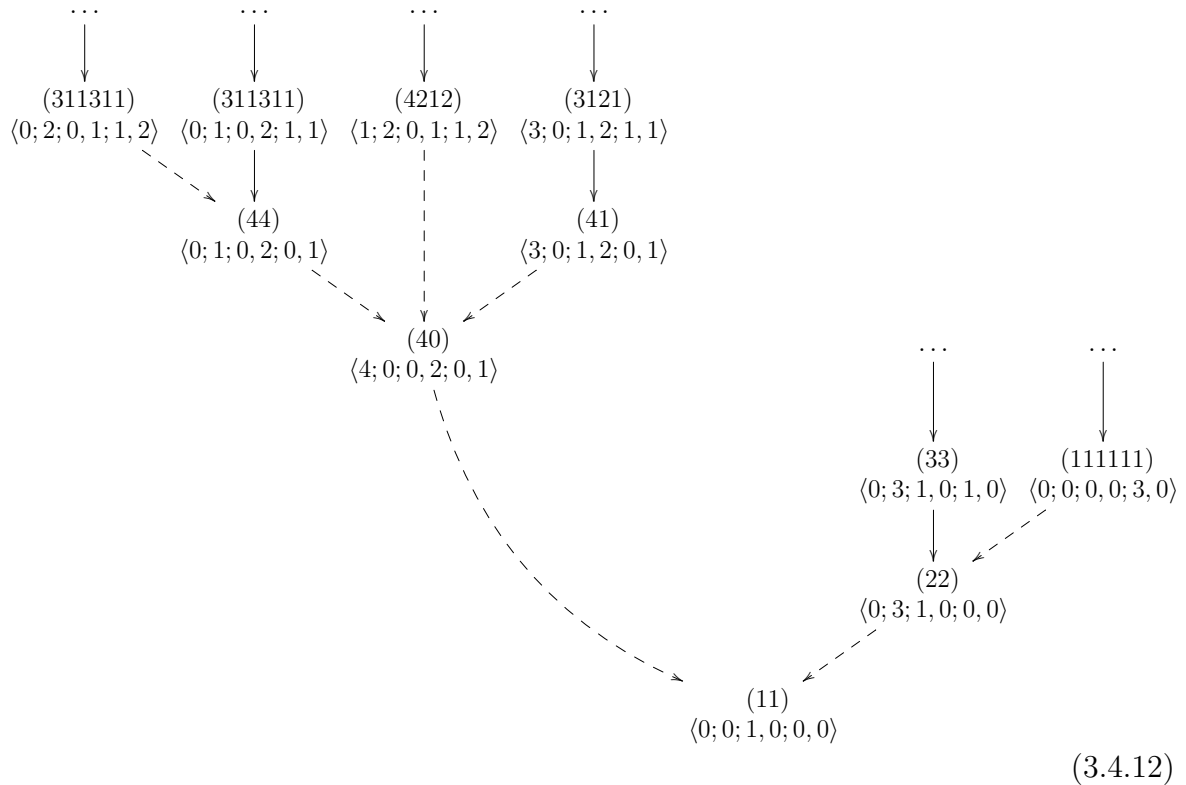
It has profile  $\langle 0; 2; 0, 1; 2, 2 \rangle$  and further contracts to the labelled  $\Gamma(\sigma_1^3 \sigma_2^{-1} \sigma_1 \sigma_2^{-3} \sigma_1 \sigma_2^{-1})$  with profile  $\langle 0; 2; 0, 1; 1, 2 \rangle$  that, in turn, contracts to the labelled graph in Diagram (3.4.6). This concludes the proof.  $\square$

Before we summarise the above, let us make an observation that the labelled graphs  $\Gamma(\sigma_1^4 \sigma_2^{-2} \sigma_1 \sigma_2^{-2})$  in Diagram (3.4.7) and  $\Gamma(\sigma_1^4 \sigma_2^{-4})$  in Diagram (3.4.6) admit the following *non-preserving* contractions:



Performing R1 moves on the underlying links to remove loop edges yields the labelled 4-cycle, which in turn admits two contractions to  $\Gamma(\sigma_1 \sigma_2^{-1})$  with the loop edge also

removed. Now, in the following diagram numbers in parentheses represent the sequence of exponents  $(a_1 b_1 a_2 b_2 \dots)$  of  $\beta$  in the form  $(\star)$ , solid arrows correspond to preserving contractions on (Q1) labels that only change  $q_1$  in the profile of  $\Gamma(\beta)$ , and dashed arrows correspond to the following: non-preserving contractions, contractions that change  $p_1, p_2, q_2$  or the heavy label set, and performing R1 moves on the underlying link diagram. For notational convenience, we denote the ‘sequence of exponents’ for the 4-cycle by (40).



Thus, all validly labelled  $\Gamma(\beta)$  with  $k \geq 5$  whose labellings satisfy Conjecture 3.3.2 may be divided into six families according to which one of the following six profiles they have:

- $\langle 0; 0; 0, 0; k, 0 \rangle;$
- $\langle 0; 1; 0, 2; k - 4, 1 \rangle;$
- $\langle 0; 2; 0, 1; k - 4, 2 \rangle;$
- $\langle 0; 3; 1, 0; k - 2, 0 \rangle;$
- $\langle 1; 2; 0, 1; k - 4, 2 \rangle;$
- $\langle 3; 0; 1, 2; k - 4, 1 \rangle.$

This implies that, given an embedding of the higher rank lattice corresponding to an ABC  $\widehat{\beta}$  that satisfies Conjecture 3.3.2, we can tell immediately what contraction class it belongs to by looking at its profile.

The following theorem concludes the section, summarising the contents of Lemma 3.3.1, Conjecture 3.3.2 and Diagram (3.4.12).

**Theorem 3.4.10.** Suppose that  $\Gamma(\beta)$  is a validly labelled graph for an ABC  $\widehat{\beta}$  such that  $\Lambda(\beta)$  of the opposite colour is the higher rank lattice corresponding to  $\widehat{\beta}$ . Then  $l(\Gamma(\beta))$  satisfies that either (i)  $[[j]] = \{1^{(2)}, (-1)^{(2)}\}$  for all  $[j] \subset l(\Gamma(\beta))$ , or (ii) there exists a label set  $[j] \subset l(\Gamma(\beta))$  such that  $[[j]] = \{1^{(1)}, (-1)^{(1)}\}$ . If (ii) holds, suppose that there is

precisely one  $[h] \subset l(\Gamma(\beta))$  with  $w(h) > 4$ , and that, moreover,  $[[h]] = \{(\pm 2)^{(1)}, (\mp 1)^{(2)}\}$  or  $[[h]] = \{2^{(1)}, (-2)^{(1)}\}$ . If  $\text{rk } \Lambda(\beta) \geq 5$ , then  $\Gamma(\beta)$  admits a sequence of preserving contractions to precisely one of the base cases in Diagram (1.1.1). Moreover,  $\Gamma(\beta)$  admits a sequence of (not necessarily preserving) contractions to the labelled graph for the unknot, represented as the closure of  $\sigma_1 \sigma_2^{-1}$ .

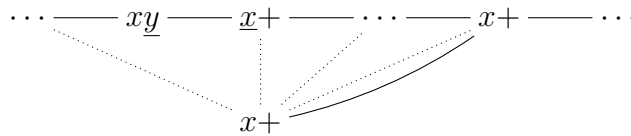
### § 3.5 | Relation to Simone's classification

In this section, we briefly explain how the classification derived in the previous section is related to the one in [Sim20]. In [Sim20, Corollary 1.10], Simone has divided into the following five families the associated strings of all ABCs  $\hat{\beta}$  such that  $\Sigma_2(S^3, \hat{\beta})$  bounds a rational ball:

- $\mathcal{S}_{2a} = \{(b_1 + 3, b_2, \dots, b_k, 2, c_l, \dots, c_1)\}$ ;
- $\mathcal{S}_{2b} = \{(3 + x, b_1, \dots, b_{k-1}, b_k + 1, 2^{[x]}, c_l + 1, c_{l-1}, \dots, c_1) \mid x \geq 0 \text{ and } k + l \geq 2\}$ ;
- $\mathcal{S}_{2c} = \{(3 + x_1, 2^{[x_2]}, 3 + x_3, 2^{[x_4]}, \dots, 3 + x_{2k+1}, 2^{[x_1]}, 3 + x_2, 2^{[x_3]}, \dots, 3 + x_{2k}, 2^{[x_{2k+1}]}) \mid k \geq 0 \text{ and } x_i \geq 0 \text{ for all } i\}$ ;
- $\mathcal{S}_{2d} = \{(2, 2 + x, 2, 3, 2^{[x-1]}, 3, 4) \mid x \geq 1\} \cup \{(2, 2, 2, 4, 4)\}$ ;
- $\mathcal{S}_{2e} = \{(2, b_1 + 1, b_2, \dots, b_k, 2, c_l, \dots, c_2, c_1 + 1, 2) \mid k + l \geq 3\} \cup \{(2, 2, 2, 3)\}$ .

In the above,  $(c_1, \dots, c_l) = \text{ld}(b_1, \dots, b_k)$  in each case, and  $k$  and  $l$  no longer denote the ranks of  $\Gamma(\beta)$  and  $\Gamma^*(\beta)$ . Write  $\mathcal{S}_2 = \mathcal{S}_{2a} \cup \mathcal{S}_{2b} \cup \mathcal{S}_{2c} \cup \mathcal{S}_{2d} \cup \mathcal{S}_{2e}$ . Notice that  $\mathcal{S}_{2a}$ ,  $\mathcal{S}_{2b}$  and  $\mathcal{S}_{2c}$  are not mutually disjoint; implications of this fact, as well as examples, will be discussed in Section 4.2. In the proof, Simone used the following more restrictive notion of contraction that we reformulate from [Sim20, Definition 5.13].

**Definition 3.5.1.** Let  $v_s, v_{s'}$  and  $v_t$  be distinct outer vertices of  $\Gamma(\beta)$  with  $v_s \cdot v_{s'} = 1$ ,  $|v_{s'}| = 2$  and  $|v_t|^2 \geq 3$ , let  $[x]$  be a label set in (Q1) configuration such that  $l(v_{s'}) = \underline{xy}$  for some  $[y]$ , and suppose  $\underline{x} \in l(v_s)$  and  $x \in l(v_t)$ :



A contraction on  $[x]$  where the edge between  $v_s$  and  $v_{s'}$  is contracted and the edge between  $v_t$  and  $v_0$  is deleted is said to be *centred at  $v_t$*  if  $v_s \cdot v_t = 0$ , and *centred at  $v_s$*  if  $v_s \cdot v_t = 1$ ; in the latter case, call  $v_s$  the *centre* of  $\Gamma(\beta)$  relative to  $[x]$ . If  $v_c$  is the vertex formed by the merging of  $v_s$  and  $v_{s'}$  as a result of a centred contraction, say that the inverse operation is an expansion *centred at  $v_c$* .

Given a labelled graph, there may be several different expansions centred at a given vertex. Notice also that centred contractions are preserving.

A crucial component of the classification is the following lemma.

**Lemma 3.5.2** ([Sim20, Lemma 5.14]). Let  $\Gamma(\beta')$  be obtained from a validly labelled  $\Gamma(\beta)$  by a contraction centred at  $v$  with  $|v|^2 = a$ . Then  $\beta$  has the associated string  $(b_1, \dots, b_k, a, c_1, \dots, c_l)$  with  $(c_1, \dots, c_l) = \text{ld}(b_1, \dots, b_k)$  if and only if  $\beta'$  has the associated string of  $(b'_1, \dots, b'_{k'}, a, c'_1, \dots, c'_l)$  with  $(c'_1, \dots, c'_l) = \text{ld}(b_1, \dots, b'_{k'})$ .

Simone's classification is established by showing that if  $\widehat{\beta}$  is embeddable, then some validly labelled  $\Gamma(\beta)$  with  $\text{rk } \Gamma(\beta) \geq \text{rk } \Gamma^*(\beta)$  admits a sequence of centred contractions down to a list of base cases. Coupled with Lemma 3.5.2, this allows him to give a description, formulated in terms of linearly dual substrings, of families into which associated strings  $\mathbf{a}(\beta)$  may be classified. Simone then explicitly constructs rational balls bounded by  $\Sigma_2(S^3, \widehat{\beta})$  for all families, concluding the classification. We now list those base cases, contained in [Sim20, Sections 6–7]:

- Labelled  $\Gamma(\sigma_1^4 \sigma_2^{-4})$  shown below<sup>3</sup>:

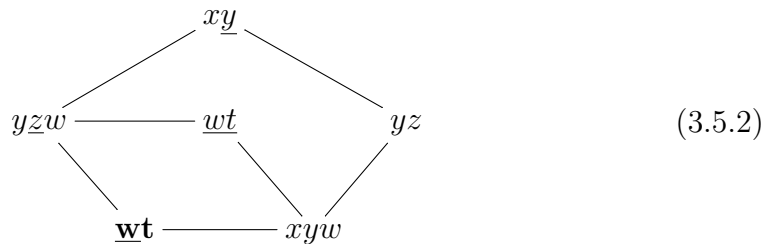
$$\begin{array}{ccc}
 & xz & \\
 & \diagdown \quad \diagup & \\
 yzw & \equiv \equiv \equiv \underline{xyzw} & zw \\
 & \diagup \quad \diagdown & \\
 & \mathbf{yw} & 
 \end{array} \tag{3.5.1}$$

This graph admits a further contraction on  $[w]$ , centred on the bolded vertex, to  $\Gamma(\sigma_1^3 \sigma_2^{-3})$  in Diagram (3.4.1), which in turn contracts to  $\Gamma(\sigma_1^2 \sigma_2^{-2})$  in the same diagram. We can write  $\mathbf{a}(\sigma_1^4 \sigma_2^{-4})$  as  $(6, 2, 2, 2)$ , which has the form  $(b_1 + 3, b_2, \dots, b_k, 2, c_1, \dots, c_l)$  for  $(b_1, \dots, b_k) = (3)$  and  $(c_1, \dots, c_l) = (2, 2)$ ;  $\mathbf{a}(\sigma_1^3 \sigma_2^{-3}) = (5, 2, 2)$  and  $\mathbf{a}(\sigma_1^2 \sigma_2^{-2}) = (4, 2)$  are also in this form. Performing expansions centred on the bolded vertex  $v_c$ , then making  $v_s$ , resp.,  $v_t$ , the new bolded vertex if  $v_s \cdot v_t = 0$ , resp.,  $v_s \cdot v_t = 1$ , and repeating, yields  $\Gamma(\beta)$  with  $\mathbf{a}(\beta) \in \mathcal{S}_{2a}$ .

- Labelled  $\Gamma(\sigma_1^3 \sigma_2^{-1} \sigma_1 \sigma_2^{-3} \sigma_1 \sigma_2^{-1})$  in Diagram (3.4.9). The string  $(5, 3, 2, 2, 3)$  has the form  $(3 + x, b_1, \dots, b_{k-1}, b_k + 1, 2^{[x]}, c_l + 1, c_{l-1}, \dots, c_1)$  with  $(b_1, \dots, b_k) = (c_1, \dots, c_l) = (2)$  and  $x = 2$ . Expansions centred on the vertex of degree 5 give labelled  $\Gamma(\beta)$  with  $\mathbf{a}(\beta)$  of this form for  $x \geq 3$ , while a contraction centred on the same vertex gives labelled  $\Gamma(\sigma_1^4 \sigma_2^{-4})$  in Diagram (3.4.6) (the case  $x = 1$ ). Since  $\Sigma_2(S^3, \widehat{\beta})$  bounds a rational ball for  $\beta = (\sigma_1 \sigma_2^{-1})^3$  and  $\mathbf{a}((\sigma_1 \sigma_2^{-1})^3) = (3, 3, 3)$  (the case  $x = 0$ ), this gives the  $\mathcal{S}_{2b}$  family.
- Labelled  $\Gamma((\sigma_1 \sigma_2^{-1})^n)$  for odd  $n \geq 3$  in Diagram (3.4.8). If  $\mathbf{a}(\beta) \in \mathcal{S}_{2c}$ , then either  $\beta = (\sigma_1 \sigma_2^{-1})^n$  or some validly labelled  $\Gamma(\beta)$  admits a sequence of centred contractions to this set of base cases.

<sup>3</sup>Notice this is different from the labelled  $\Gamma(\sigma_1^4 \sigma_2^{-4})$  in Diagram (3.4.6).

- Labelled  $\Gamma(\sigma_1^2\sigma_2^{-2}\sigma_1\sigma_2^{-1}\sigma_1\sigma_2^{-1}\sigma_1^2\sigma_2^{-1})$  in Diagram (3.4.10). It gives, via expansions centred on  $v$  with  $l(v) = \underline{xx'z}$ , labelled graphs  $\Gamma(\beta)$  with  $\mathbf{a}(\beta) = (2, 2 + x, 2, 3, 2^{[x-1]}, 3, 4)$  for  $x \geq 1$ . The graph in Diagram (3.4.10) admits a further preserving contraction to  $\Gamma(\sigma_1^4\sigma_2^{-2}\sigma_1\sigma_2^{-2})$  in Diagram (3.4.7). Since  $\mathbf{a}(\sigma_1^4\sigma_2^{-2}\sigma_1\sigma_2^{-2}) = (2, 2, 2, 4, 4)$ , we obtain  $\mathcal{S}_{2d}$ .
- Labelled  $\Gamma(\sigma_1^3\sigma_2^{-1}\sigma_1^2\sigma_2^{-1})$  shown below:



We have  $\mathbf{a}(\sigma_1^3\sigma_2^{-1}\sigma_1^2\sigma_2^{-1}) = (2, 3, 2, 3, 2)$  of the form  $(2, b_1 + 1, b_2, \dots, b_k, 2, c_1, \dots, c_2, c_1 + 1, 2)$  with  $(b_1, \dots, b_k) = (c_1, \dots, c_l) = (2)$ . Also, this labelled graph admits a contraction on  $[w]$  to  $\Gamma(\sigma_1^4\sigma_2^{-1})$  in Diagram (3.4.2). Like in the  $\mathcal{S}_{2a}$  case, performing expansions centred on the bolded vertex gives the rest of the  $\mathcal{S}_{2e}$  family.

Importantly, Simone was only interested in classifying associated strings (and, hence, alternating 3-braids), rather than embeddings of lattices that they give rise to. This means that if  $\mathbf{a}(\beta)$  lies, for instance, in  $\mathcal{S}_{2a} \cap \mathcal{S}_{2b}$ , there exist different labelled  $\Gamma(\beta)$  such that they contract to (at least) two different base cases above. Our classification makes this distinction at the expense of being more complicated. However, tracing through the proofs of Proposition 3.4.1 and Theorem 3.4.8, we discover that for a given validly labelled  $\Gamma(\beta)$  we have, or may have, used only centred contractions to arrive at base cases for the  $\mathcal{S}_{2a}$ ,  $\mathcal{S}_{2b}$ ,  $\mathcal{S}_{2d}$  and  $\mathcal{S}_{2e}$  families<sup>4</sup>; these base cases have profiles, respectively,  $\langle 0; 3; 1, 0; 2, 0 \rangle$ ,  $\langle 0; 1; 0, 2; 1, 1 \rangle$ ,  $\langle 3; 0; 1, 2; 1, 1 \rangle$  and  $\langle 1; 2; 0, 1; 1, 2 \rangle$ . Recall from the proof of Theorem 3.4.8 that any validly labelled  $\Gamma(\sigma_1\sigma_2^{-1})^n$  for odd  $n \geq 3$  admits a sequence of preserving contractions to  $\Gamma((\sigma_1\sigma_2^{-1})^3)$  in Diagram (3.4.1) (q.v. Claim 3.4.9). Thus, every ABC  $\hat{\beta}$  with  $\mathbf{a}(\beta) \in \mathcal{S}_2$  has a valid labelling of  $\Gamma(\beta)$  that is accounted for by our classification. This implies that  $\Lambda(\beta)$  for any embeddable  $\hat{\beta}$  has an embedding satisfying Conjecture 3.3.2.

We also note that our classification has the extra base case  $\Gamma(\sigma_1^3\sigma_2^{-1}\sigma_1\sigma_2^{-3}\sigma_1\sigma_2^{-1})$  with profile  $\langle 0; 2; 0, 1; 1, 2 \rangle$  obtained by a preserving contraction of the graph in Diagram (3.4.11). Thus, even though any labelled  $\Gamma(\beta)$  that contracts down to this graph is not explicitly considered by Simone (cf. [Sim20, Remark 6.4]), we still have  $\mathbf{a}(\beta) \in \mathcal{S}_2$ .

---

<sup>4</sup>Rather than first contracting away removable vertices and then working with  $\Gamma_{\text{red}}(\beta)$ , we could have viewed them as belonging to  $3^+$ -chains; chain contraction arguments would still be analogous.

# Ribbon surfaces for ABCs

---

In this chapter we attempt the second step in resolving the slice–ribbon conjecture for alternating 3-braid closures with non-zero determinant (ABCs), namely carrying out explicit constructions of ribbon surfaces for those ABCs whose double branched covers are unobstructed from bounding rational balls and hence can be  $\chi$ -slice. For the reader’s convenience, this chapter is designed to be independent from the technical Chapter 3. As a starting point, we use Simone’s classification of said 3-braid closures from [Sim20], consisting of five non-disjoint families  $\mathcal{S}_{2a}$  to  $\mathcal{S}_{2e}$ , and construct ribbon surfaces for all of these families but  $\mathcal{S}_{2c}$ . Then, we focus on  $\mathcal{S}_{2c}$  in greater detail, giving an alternative description of the complement  $\mathcal{S}_{2c}^\dagger = \mathcal{S}_{2c} \setminus (\mathcal{S}_{2a} \cup \mathcal{S}_{2b} \cup \mathcal{S}_{2d} \cup \mathcal{S}_{2e})$ . While  $\mathcal{S}_{2c}^\dagger$  is known to include non-slice knots, we exhibit infinitely many  $\chi$ -slice links also contained in  $\mathcal{S}_{2c}^\dagger$ . We then investigate more potentially non- $\chi$ -slice links in  $\mathcal{S}_{2c}^\dagger$  and single out three candidate knots to which Chapter 5 is devoted. The contents of the following two chapters are based on the author’s work [Bre20].

## § 4.1 | Ribbon surfaces for $\mathcal{S}_{2a} \cup \mathcal{S}_{2b} \cup \mathcal{S}_{2d} \cup \mathcal{S}_{2e}$

Recall that an alternating 3-braid  $\beta = \sigma_1^{a_1} \sigma_2^{-b_1} \dots \sigma_1^{a_n} \sigma_2^{-b_n}$  with  $n \geq 1$  and  $a_i, b_i \geq 1$  for all  $i = 1, \dots, n$  is equivalently described by its associated string  $\mathbf{a}(\beta) = (2^{[a_1-1]}, b_1 + 2, \dots, 2^{[a_n-1]}, b_n + 2)$ . In [Sim20, Corollary 1.10], Simone has classified associated strings of all alternating 3-braids  $\beta$  such that  $\Sigma_2(S^3, \widehat{\beta})$ , the double cover of  $S^3$  branched over the braid closure  $\widehat{\beta}$ , bounds a rational ball, into the following five families:

- $\mathcal{S}_{2a} = \{(b_1 + 3, b_2, \dots, b_k, 2, c_l, \dots, c_1)\}$ ;
- $\mathcal{S}_{2b} = \{(3 + x, b_1, \dots, b_{k-1}, b_k + 1, 2^{[x]}, c_l + 1, c_{l-1}, \dots, c_1) \mid x \geq 0 \text{ and } k + l \geq 2\}$ ;
- $\mathcal{S}_{2c} = \{(3 + x_1, 2^{[x_2]}, 3 + x_3, 2^{[x_4]}, \dots, 3 + x_{2k+1}, 2^{[x_1]}, 3 + x_2, 2^{[x_3]}, \dots, 3 + x_{2k}, 2^{[x_{2k+1}]}) \mid k \geq 0 \text{ and } x_i \geq 0 \text{ for all } i\}$ ;
- $\mathcal{S}_{2d} = \{(2, 2 + x, 2, 3, 2^{[x-1]}, 3, 4) \mid x \geq 1\} \cup \{(2, 2, 2, 4, 4)\}$ ;
- $\mathcal{S}_{2e} = \{(2, b_1 + 1, b_2, \dots, b_k, 2, c_l, \dots, c_2, c_1 + 1, 2) \mid k + l \geq 3\} \cup \{(2, 2, 2, 3)\}$ .

Here,  $(c_1, \dots, c_l)$  is the linear dual of  $(b_1, \dots, b_k)$  in each case.

We have explained in Section 2.2 how one may construct a ribbon surface for a link by performing band moves. They are depicted on a link diagram by arcs with endpoints on the link itself, representing the cores of the bands; the arcs are annotated by coefficients that denote the number of half-twists in the bands. We shall now present such band moves for the closures of 3-braids with associated strings in four of the above families.

**Theorem 4.1.1.** Let  $\beta$  be an alternating 3-braid of the form  $(\star)$ . If  $\mathbf{a}(\beta) \in \mathcal{S}_{2a} \cup \mathcal{S}_{2d} \cup \mathcal{S}_{2e}$ , then  $\widehat{\beta}$  bounds a ribbon surface with a single 1-handle. If  $\mathbf{a}(\beta) \in \mathcal{S}_{2b}$ , then  $\widehat{\beta}$  bounds a ribbon surface with at most two 1-handles.

Before proceeding with the following paragraph, the reader is invited to refresh in their memory our convention for numbering plane regions bounded by the standard diagram of  $\widehat{\beta}$  described in Section 2.3. Our main observation, previously used by Lisca [Lis07] and Lecuona [Lec12], is that if  $\mathbf{a}(\beta)$  contains two disjoint linearly dual substrings (possibly perturbed on the ends), then the link diagram of  $\widehat{\beta}$  contains sub-braids that, if placed on the two ends of a half-twist  $(\sigma_2\sigma_1\sigma_2)^{-1}$ , may be cancelled out via successive isotopies. More precisely, suppose that  $(b_1, \dots, b_k) = \text{ld}(c_1, \dots, c_l)$ . Let  $\mathbf{b}' = (b_1 + x_l, b_2, \dots, b_{k-1}, b_k + x_r)$  and  $\mathbf{c}' = (c_l + y_l, c_{l-1}, \dots, c_2, c_1 + y_r)$  with  $x_i, y_i \geq 0$  for  $i \in \{l, r\}$  and suppose that  $\mathbf{a}(\beta)$  is the concatenated string  $\mathbf{b}'\mathbf{t}\mathbf{c}'\mathbf{s}$ , where  $\mathbf{t}$  and  $\mathbf{s}$  are arbitrary strings and length of  $\mathbf{t}$  is  $t \geq 0$ . Consider the sub-braid  $B$  in the link diagram of  $\widehat{\beta}$  that exactly contains all crossings along the boundary of white regions  $X_2, \dots, X_{k-1}$ , all but  $x_l + 1$  leftmost crossings along the boundary of the region  $X_1$ , and all but  $x_r + 1$  rightmost crossings along the boundary of the region  $X_k$ . Consider also the sub-braid  $C$  that exactly contains all crossings along the boundary of regions  $X_{k+t+2}, \dots, X_{k+t+l-1}$ , all but  $y_l + 1$  leftmost crossings along the boundary of the region  $X_{k+t+1}$ , and all but  $y_r + 1$  rightmost crossings along the boundary of region  $X_{k+t+l}$ . Then  $B(\sigma_2\sigma_1\sigma_2)^{-1}C = (\sigma_2\sigma_1\sigma_2)^{-1}$ . Hence, if after applying a band move to  $\widehat{\beta}$  away from  $B$  and  $C$ , they are connected by a half-twist of the three strands, one may remove all crossings in  $B$  and  $C$  via isotopies illustrated in Figure 4.1. We call  $B$  and  $C$  *dual sub-braids* and enclose them in all following figures in blue and chartreuse rectangles, respectively.

*Proof of Theorem 4.1.1.* See Figures 4.3 to 4.6. □

We remark that we do not know if one always requires at least two 1-handles in the  $\mathcal{S}_{2b}$  case, but techniques from [AGL18] could be used to investigate this question.

In searching for the band moves in Figures 4.3 to 4.6, we have used the algorithm of Owens and Swenton implemented in KLO software [OS21]. The band moves we exhibit for these four families of ABCs are *algorithmic* in the sense of [OS21].

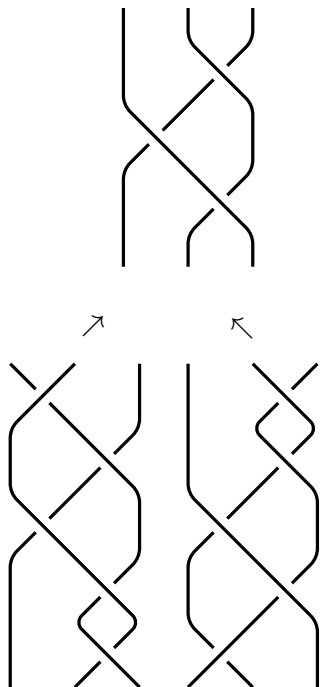


Figure 4.1: Undoing flyped tongues [Tsu09] to cancel dual sub-braids.

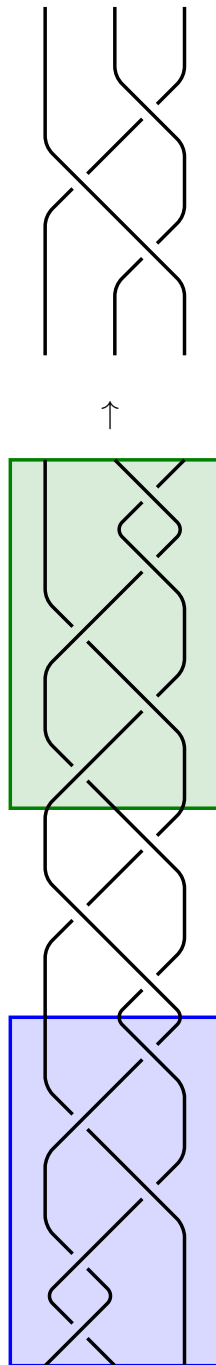


Figure 4.2: Cancellation of dual sub-braids for  $(b_1, \dots, b_k) = (2, 2, 3, 3)$  and  $(c_l, \dots, c_1) = (2, 3, 4)$  with  $x_l = x_r = y_l = y_r = 0$ . Fixing the ends on the braid shown, one may remove all crossings in  $B$  and  $C$  via moves illustrated in Figure 4.1.

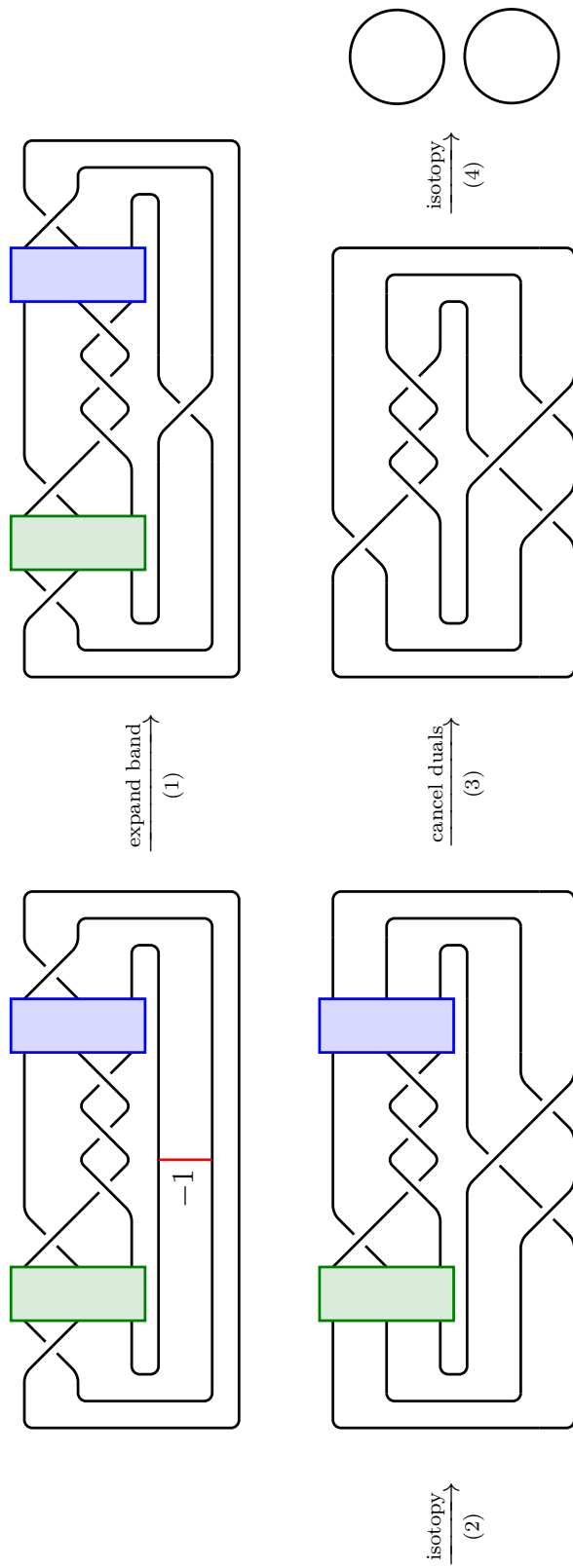


Figure 4.3: Band move for the  $\mathcal{S}_{2a}$  case.

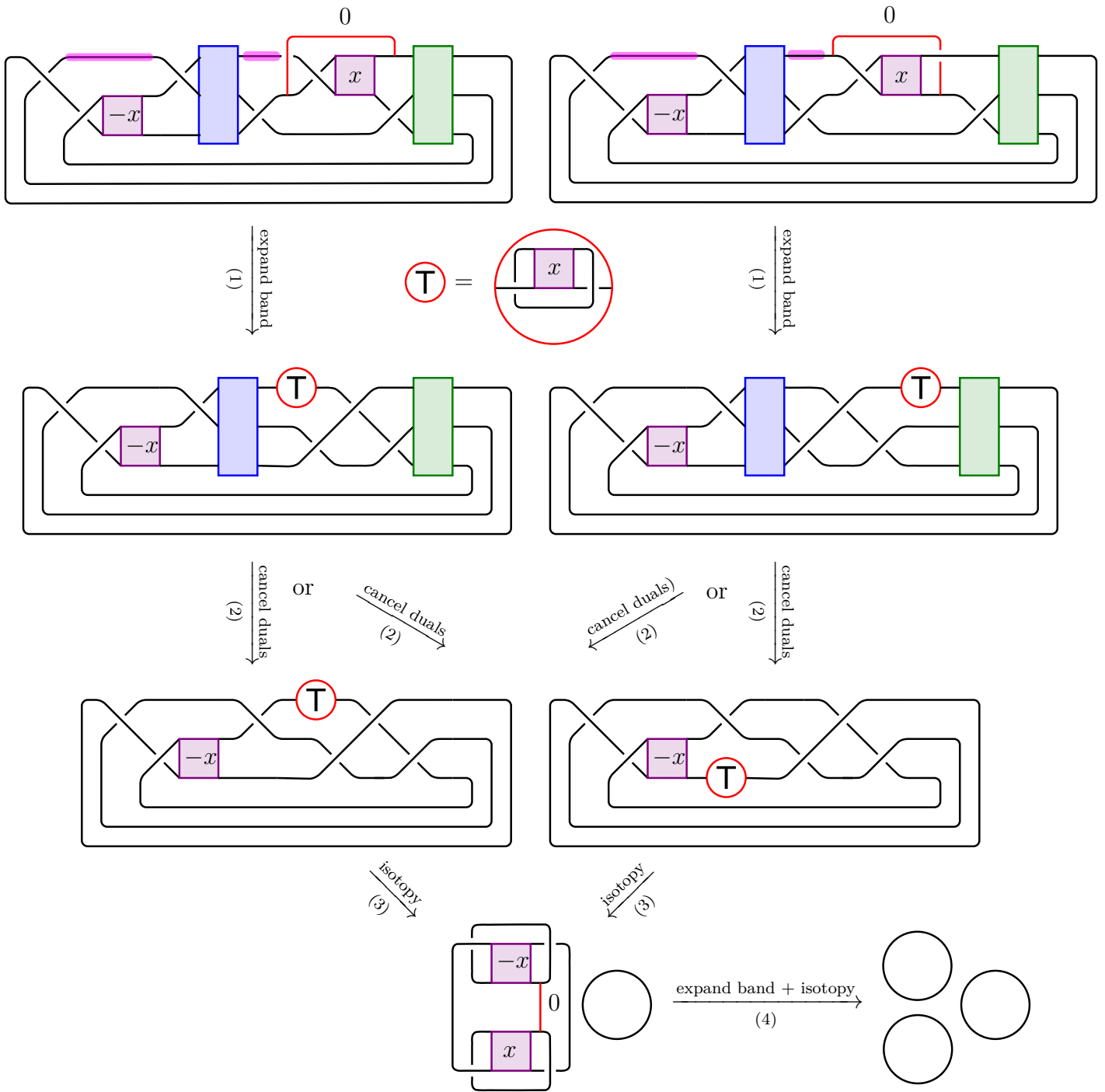


Figure 4.4: Band moves for the  $\mathcal{S}_{2b}$  case. Start with the top left diagram if the two segments highlighted in purple do not lie on the same strand, otherwise start with the top right; this ensures that after step (2), the tangle  $T$  does not lie on the otherwise unknotted split component. The nontrivial component of the link obtained after step (3) is the connected sum  $T(2, x + 2) \# T(2, -(x + 2))$  of two torus links.

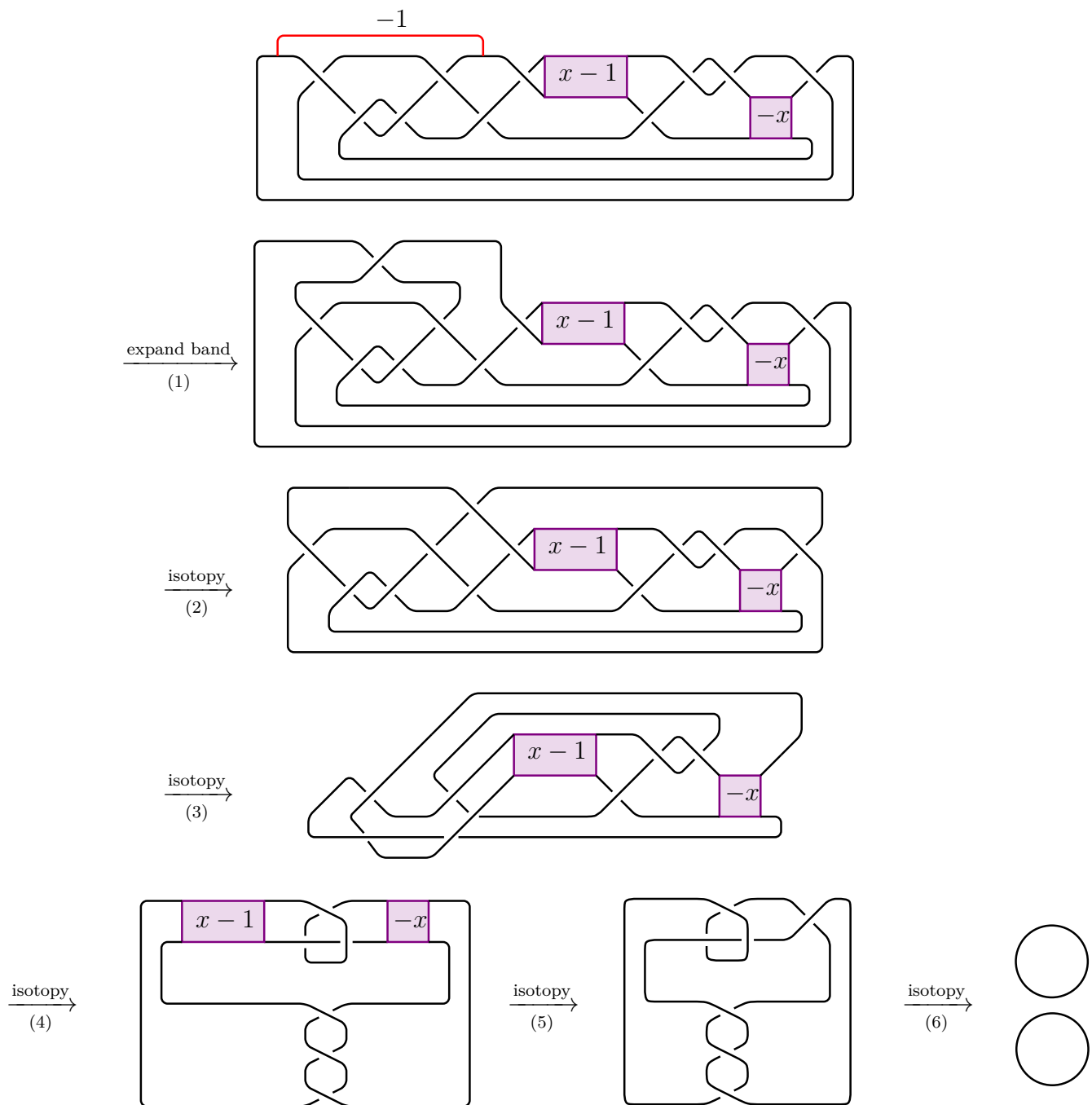


Figure 4.5: Band moves for the  $\mathcal{S}_{2d}$  case with  $x \geq 1$ . In step (5), we undo  $x-1$  crossings in both blocks by flying the tangle on the bottom of the diagram and performing Reidemeister II moves. A similar band gives the two-component unlink for  $\hat{\beta}$  if  $\mathbf{a}(\beta) = (2, 2, 2, 4, 4)$ .

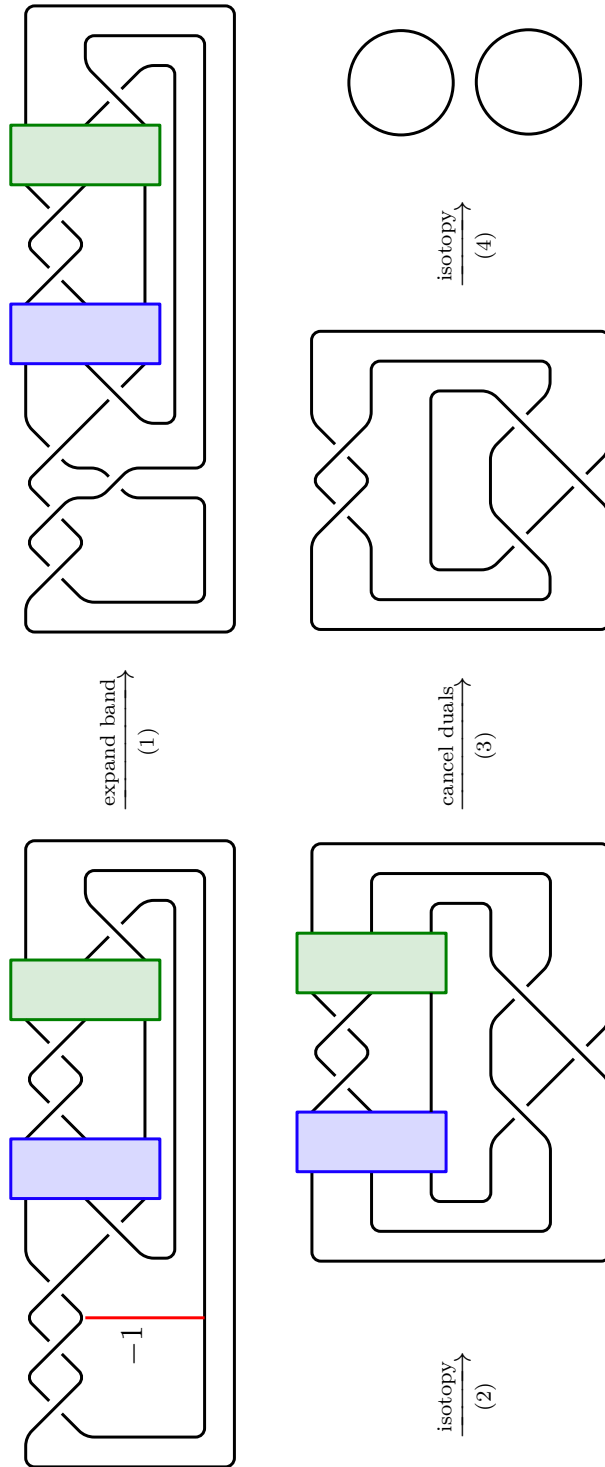


Figure 4.6: Band move for the  $\mathcal{S}_{2e}$  case. A similar band move gives the two-component unlink for  $\hat{\beta}$  if  $\mathbf{a}(\beta) = (2, 2, 2, 3)$ .

## § 4.2 | The case of $\mathcal{S}_{2c} \setminus (\mathcal{S}_{2a} \cup \mathcal{S}_{2b} \cup \mathcal{S}_{2d} \cup \mathcal{S}_{2e})$

The remaining  $\mathcal{S}_{2c}$  family is of special interest because it contains strings associated to known braids whose closures are not slice; these are Turk's head knots  $K_7$  [Sar10],  $K_{11}$ ,  $K_{17}$  and  $K_{23}$  [AMMMPS20].<sup>1</sup> Thus, we should not expect to find a set of band moves for all 3-braid closures with associated strings in  $\mathcal{S}_{2c}$ . We also note that knots of finite concordance order belonging to Family (3) in [Lis17] have associated strings in  $\mathcal{S}_{2c}$ .

We have that  $\mathcal{S}_{2c} \cap \mathcal{S}_{2d} = \mathcal{S}_{2c} \cap \mathcal{S}_{2e} = \emptyset$ : this can be seen by computing the  $I(\mathbf{a}) = \sum_{a \in \mathbf{a}} 3 - a$  invariant [Lis07] which is 0 for strings in  $\mathcal{S}_{2c}$ , but 1 or 3 for strings in  $\mathcal{S}_{2d}$  or  $\mathcal{S}_{2e}$ , respectively.<sup>2</sup> However,  $\mathcal{S}_{2c}$  has nonzero intersection with  $\mathcal{S}_{2a}$  and  $\mathcal{S}_{2b}$ : if one defines a *palindrome* to be a string  $(a_1, \dots, a_n)$  such that  $a_i = a_{n-(i-1)}$  for all  $i = 1, \dots, n$ , then the following lemma holds.

**Lemma 4.2.1** ([Sim20, Lemma 3.6]). Suppose  $(b_1, \dots, b_k) = \text{ld}(c_1, \dots, c_l)$  and let  $\mathbf{a} = (b_1 + 3, b_2, \dots, b_k, 2, c_l, \dots, c_1) \in \mathcal{S}_{2a}$  and  $\mathbf{b} = (3 + x, b_1, \dots, b_{k-1}, b_k + 1, 2^{[x]}, c_l + 1, c_{l-1}, \dots, c_1) \in \mathcal{S}_{2b}$ . Then  $\mathbf{a} \in \mathcal{S}_{2c}$  if and only if  $(b_1 + 1, b_2, \dots, b_k)$  is a palindrome, and  $\mathbf{b} \in \mathcal{S}_{2c}$  if and only if  $(b_1 \dots, b_k)$  is a palindrome.

We seek to study the complement  $\mathcal{S}_{2c}^\dagger := \mathcal{S}_{2c} \setminus (\mathcal{S}_{2a} \cup \mathcal{S}_{2b} \cup \mathcal{S}_{2d} \cup \mathcal{S}_{2e})$ . Let

$$\begin{aligned} \mathbf{c} = & (3 + x_1, 2^{[x_2]}, 3 + x_3, 2^{[x_4]}, \dots, 3 + x_{2k+1}, \\ & 2^{[x_1]}, 3 + x_2, 2^{[x_3]}, \dots, 3 + x_{2k}, 2^{[x_{2k+1}]}) \in \mathcal{S}_{2c}, \end{aligned} \quad (*)$$

where  $k \geq 0$  and  $x_i \geq 0$  for all  $i$ . One can more compactly describe  $\mathbf{c}$  by its  $\mathbf{x}$ -string  $\mathbf{x}(\mathbf{c}) = [x_1, \dots, x_{2k+1}]$ ; we use square brackets to denote  $\mathbf{x}$ -strings and, as with associated strings, consider them up to cyclic rotations and reversals. For example, the  $\mathbf{x}$ -string of the string  $(3^{[i]}) \in \mathcal{S}_{2c}$  is  $[0^{[i]}]$ . Also, when writing  $\mathbf{c}$  in the form  $(*)$  with the first element being at least 3, recall that every maximal substring of the form  $(2^{[x]})$  or  $(3 + x)$  for  $x \geq 0$  is called an *entry*; the total number of entries  $e(\mathbf{c})$  in  $\mathbf{c}$  is congruent to 2 mod 4.

**Lemma 4.2.2.** Let  $\mathbf{a} = (b_1 + 3, b_2, \dots, b_k, 2, c_l, \dots, c_1) \in \mathcal{S}_{2a} \cap \mathcal{S}_{2c}$  and  $\mathbf{b} = (3 + y, b_1, \dots, b_{k-1}, b_k + 1, 2^{[y]}, c_l + 1, c_{l-1}, \dots, c_1) \in \mathcal{S}_{2b} \cap \mathcal{S}_{2c}$ . Then

- $\mathbf{x}(\mathbf{a}) = [z_1]$  with  $z_1 \geq 1$  or  $\mathbf{x}(\mathbf{a}) = [z_1, \dots, z_{\lfloor \frac{n}{2} \rfloor}, z_{\lfloor \frac{n}{2} \rfloor + 1}, z_{\lfloor \frac{n}{2} \rfloor}, \dots, z_2, z_1 - 2]$  with  $z_1 \geq 2$  and  $n \geq 3$  odd;
- $\mathbf{x}(\mathbf{b}) = [y, 0, z_2]$  or  $\mathbf{x}(\mathbf{b}) = [y, 0, z_2, z_3, \dots, z_{\frac{n}{2}}, z_{\frac{n}{2}+1}, z_{\frac{n}{2}}, \dots, z_3, z_2 + 1]$  with  $n \geq 4$  even.

<sup>1</sup>Recall that the Turk's head knot  $K_i$  is given as the closure of  $(\sigma_1 \sigma_2^{-1})^i$  for  $i$  odd, with the associated string  $(3^{[i]})$ .

<sup>2</sup>Observe that if  $\mathbf{b} = (b_1, \dots, b_k)$  and  $\mathbf{c} = (c_1, \dots, c_l)$  are linearly dual to each other and  $k + l \geq 2$ , then  $I(\mathbf{bc}) = 2$ .

*Proof.* Consider  $\mathbf{a}$  and define  $\mathbf{a}_{\mathbf{c}} = (2, c_l, \dots, c_1)$ . Notice that  $\mathbf{a}_{\mathbf{c}} = \text{ld}(\mathbf{a}_{\mathbf{c}}^*)$  for

$$\mathbf{a}_{\mathbf{c}}^* = (b_k + 1, b_{k-1}, \dots, b_1),$$

which by Lemma 4.2.1 must be a palindrome, and that  $\mathbf{a}$  is the concatenation of  $(b_1 + 3, b_2, \dots, b_k)$  and  $\mathbf{a}_{\mathbf{c}}$ . If  $(b_1, \dots, b_k)$  is the empty string, then  $\mathbf{a} = (2, 1) \notin \mathcal{S}_{2c}$ . Otherwise, write

$$\mathbf{a}_{\mathbf{c}} = (2^{[z_1]}, 3 + z_2, \dots, 2^{[z_n]})$$

for  $n \geq 1$  odd and  $z_1 \geq 1$ . If  $n = 1$ , then  $\mathbf{a}_{\mathbf{c}} = (2^{[z_1]})$  and  $\mathbf{a} = (3 + z_1, 2^{[z_1]})$ , so  $\mathbf{x}(\mathbf{a}) = [z_1]$ . If  $n > 1$ , then

$$\mathbf{a}_{\mathbf{c}}^* = (2 + z_1, 2^{[z_2]}, 3 + z_3, \dots, 2^{[z_{n-1}]}, 2 + z_n). \quad (**)$$

Thus,

$$\mathbf{a} = (3 + (z_n + 2), 2^{[z_{n-1}]}, \dots, 2^{[z_2]}, 1 + z_1, 2^{[z_1]}, 3 + z_2, \dots, 2^{[z_n]}).$$

If  $z_1 = 1$ , then

$$\mathbf{a} = (3 + (z_n + 2), 2^{[z_{n-1}]}, \dots, 3 + z_3, 2^{[z_1+z_2+1]}, 3 + z_2, \dots, 2^{[z_n]})$$

does not belong to  $\mathcal{S}_{2c}$  because  $e(\mathbf{a}) \equiv 0 \pmod{4}$ . If  $z_1 > 1$ , then

$$\mathbf{a} = (3 + (z_n + 2), 2^{[z_{n-1}]}, \dots, 2^{[z_2]}, 3 + (z_1 - 2), 2^{[z_1]}, 3 + z_2, \dots, 2^{[z_n]}).$$

Now, by considering  $(**)$  we see that  $\mathbf{a}_{\mathbf{c}}^*$  is a palindrome if and only if

$$z_1 = z_n + 2, \quad z_2 = z_{n-1}, \quad \dots, \quad z_{\lfloor \frac{n}{2} \rfloor} = z_{\lfloor \frac{n}{2} \rfloor + 2}$$

so we conclude that  $\mathbf{a} \in \mathcal{S}_{2a} \cap \mathcal{S}_{2c}$  if and only if  $\mathbf{x}(\mathbf{a}) = [z_1]$  for  $z_1 \geq 1$  or

$$\mathbf{x}(\mathbf{a}) = [z_1, z_2, \dots, z_{\lfloor \frac{n}{2} \rfloor}, z_{\lfloor \frac{n}{2} \rfloor + 1}, z_{\lfloor \frac{n}{2} \rfloor}, \dots, z_2, z_1 - 2]$$

for  $z_1 \geq 2$  and  $n \geq 3$  odd.

Similarly, if  $(b_1, \dots, b_k)$  is empty, then  $\mathbf{b} = (3 + y, 2^{[y]}, 2) = (3 + y, 2^{[y+1]}) \notin \mathcal{S}_{2c}$ . Since  $\text{ld}(b_1) = (2^{[b_1-1]})$  for  $b_1 \geq 2$ , in the case  $k = 1$  we have that

$$\begin{aligned} \mathbf{b} &= (3 + y, 2^{[0]}, b_1 + 1, 2^{[y]}, 3 + 0, 2^{[b_1-2]}) \\ &= (3 + y, 2^{[0]}, 3 + (b_1 - 2), 2^{[y]}, 3 + 0, 2^{[b_1-2]}) \end{aligned}$$

is indeed in  $\mathcal{S}_{2c}$  with  $\mathbf{x}(\mathbf{b}) = [y, 0, b_1 - 2]$ . If  $k > 1$ , write

$$(b_1, \dots, b_k) = (2^{[z_1]}, 3 + z_2, \dots, 2^{[z_{n-1}]}, 2 + z_n)$$

for  $n \geq 2$  even and  $z_n \geq 1$ ; then  $\text{ld}(b_1, \dots, b_k)$  is given by

$$(c_1, \dots, c_l) = (2 + z_1, 2^{[z_2]}, 3 + z_3, \dots, 2^{[z_{n-2}]}, 3 + z_{n-1}, 2^{[z_n]}).$$

When  $n = 2$ , we recover the  $k = 1$  case above, so suppose  $n > 2$ . Then we have

$$\mathbf{b} = (3 + y, 2^{[z_1]}, \dots, 2^{[z_{n-1}]}, 3 + z_n, \\ 2^{[y]}, 3 + 0, 2^{[z_{n-1}]}, 3 + z_{n-1}, 2^{[z_{n-2}]}, \dots, 3 + z_3, 2^{[z_2+1]}).$$

By comparing this with  $(*)$ , we see that  $z_1$  (which corresponds to  $x_2$ ) must be zero, and

$$(b_1, \dots, b_k) = (3 + z_2, 2^{[z_3]}, \dots, 2^{[z_{n-1}]}, 3 + (z_n - 1)).$$

The string  $(b_1, \dots, b_k)$  is thus a palindrome precisely when

$$z_2 = z_n - 1, \quad z_3 = z_{n-1}, \quad \dots, \quad z_{\frac{n}{2}} = z_{\frac{n}{2}+2},$$

i.e.,  $\mathbf{x}(\mathbf{b}) = [y, 0, z_2, z_3, \dots, z_{\frac{n}{2}}, z_{\frac{n}{2}+1}, z_{\frac{n}{2}}, \dots, z_3, z_2 + 1]$ . □

In particular, we can draw an easy conclusion that if  $\mathbf{x}(\mathbf{c})$  contains neither two adjacent elements differing by 2 nor a 0, then  $\mathbf{c} \in \mathcal{S}_{2c}^\dagger$ . We now show that for infinitely many braids with associated strings in  $\mathcal{S}_{2c}^\dagger$ , their closures are  $\chi$ -ribbon.

**Lemma 4.2.3.** Let  $\hat{\beta}$  be the closure of  $\beta = \sigma_1^{m+1}(\sigma_2^{-1}\sigma_1)^2\sigma_2^{-(m+1)}(\sigma_1\sigma_2^{-1})^2$  with the associated string  $\mathbf{a}(\beta) = (3 + m, 3, 3, 2^{[m]}, 3, 3)$  and  $m \geq 3$ . Then  $\mathbf{a}(\beta) \in \mathcal{S}_{2c}^\dagger$  and  $\hat{\beta}$  admits a ribbon surface with a single 1-handle.

*Proof.* We have  $\mathbf{x}(\mathbf{a}(\beta)) = [m, 0, 0, 0, 0]$ , hence Lemma 4.2.2 implies that  $\mathbf{a}(\beta) \in \mathcal{S}_{2c}^\dagger$ . For the band move, see Figure 4.7. □

Using KLO software, we have found that 22 out of 33 closures of alternating 3-braids with up to 20 crossings whose associated strings belong to  $\mathcal{S}_{2c}^\dagger$  are algorithmically ribbon, in each instance via at most two band moves. It is known that the Turk's head knot  $K_7$ , the closure of  $(\sigma_1\sigma_2^{-1})^7$  with  $\mathbf{a}((\sigma_1\sigma_2^{-1})^7) \in \mathcal{S}_{2c}^\dagger$  and 14 crossings, is not slice [Sar10]. The remaining 10 examples for which we were unable to find the desired band moves are listed in Table 4.1. By a straightforward application of the Gordon–Litherland signature formula [GL78, Theorems 6 and 6''], the signature of the closure of a braid  $\beta = \sigma_1^{a_1}\sigma_2^{-b_1} \dots \sigma_1^{a_n}\sigma_2^{-b_n}$  with  $\sum_i a_i, \sum_i b_i > 1$  is

$$\sigma(\hat{\beta}) = \sum_{i=1}^n b_i - a_i.$$

Thus, for the closures of all braids with associated strings in  $\mathcal{S}_{2a} \cup \mathcal{S}_{2b} \cup \mathcal{S}_{2c}$  satisfying this condition (in particular, for those in Table 4.1), the signature vanishes. This means that if said closures are knots, so do the Ozsváth and Szabó's  $\tau$  and Rasmussen's  $s$  invariants [OS03; Ras10] without giving us any sliceness obstructions; Tristram–Levine signatures for knots in Table 4.1 are also zero. Moreover, by comparing their hyperbolic volumes, we have verified that none of the entries in Table 4.1 belong to the list of ‘escapee’  $\chi$ -ribbon links described in [OS21]: this further advances them as candidates for more careful study. In Chapter 5 we will show that the three knots  $K_1$ ,  $K_2$  and  $K_3$

in Table 4.1 are not slice, which lets us conclude that every knot which is a closure of an alternating 3-braid with up to 20 crossings, has non-zero determinant, and whose double branched cover bounds a rational ball, is slice, except for  $K_1$ ,  $K_2$ ,  $K_3$  and  $K_7$ .

# of crossings	Associated string	$\mathbf{x}$ -string	# of components
18	$(3^{[9]})$	$[0^{[9]}]$	3
18	$(2, 4, 2, 4, 4, 2, 4, 2, 3)$	$[1, 1, 1, 1, 0]$	1
18	$(2, 2, 4, 3, 2, 5, 2, 3, 4)$	$[2, 1, 0, 0, 1]$	1
18	$(2, 3, 4, 3, 4, 3, 2, 3, 3)$	$[1, 0, 0, 0, 1, 0, 0]$	1
20	$(2, 2, 2, 3, 3, 3, 6, 3, 3, 3)$	$[3, 0^{[6]}]$	3
20	$(2, 4, 2, 4, 2, 4, 2, 4, 2, 4)$	$[1^{[5]}]$	3
20	$(2, 4, 2, 3, 3, 4, 2, 4, 3, 3)$	$[1, 1, 1, 0, 0, 0, 0]$	3
20	$(2, 4, 3, 2, 3, 4, 2, 3, 4, 3)$	$[1, 1, 0, 0, 1, 0, 0]$	3
20	$(2, 3, 2, 3, 2, 3, 4, 4, 4, 3)$	$[1, 0, 1, 0, 1, 0, 0]$	3
20	$(2, 2, 2, 4, 3, 2, 6, 2, 3, 4)$	$[3, 1, 0, 0, 1]$	3

Table 4.1: Braids with up to 20 crossings and associated strings in  $\mathcal{S}_{2c}^{\dagger}$  whose closures are potentially non- $\chi$ -slice. The three one-component links in the table are  $K_1$ ,  $K_2$  and  $K_3$ .

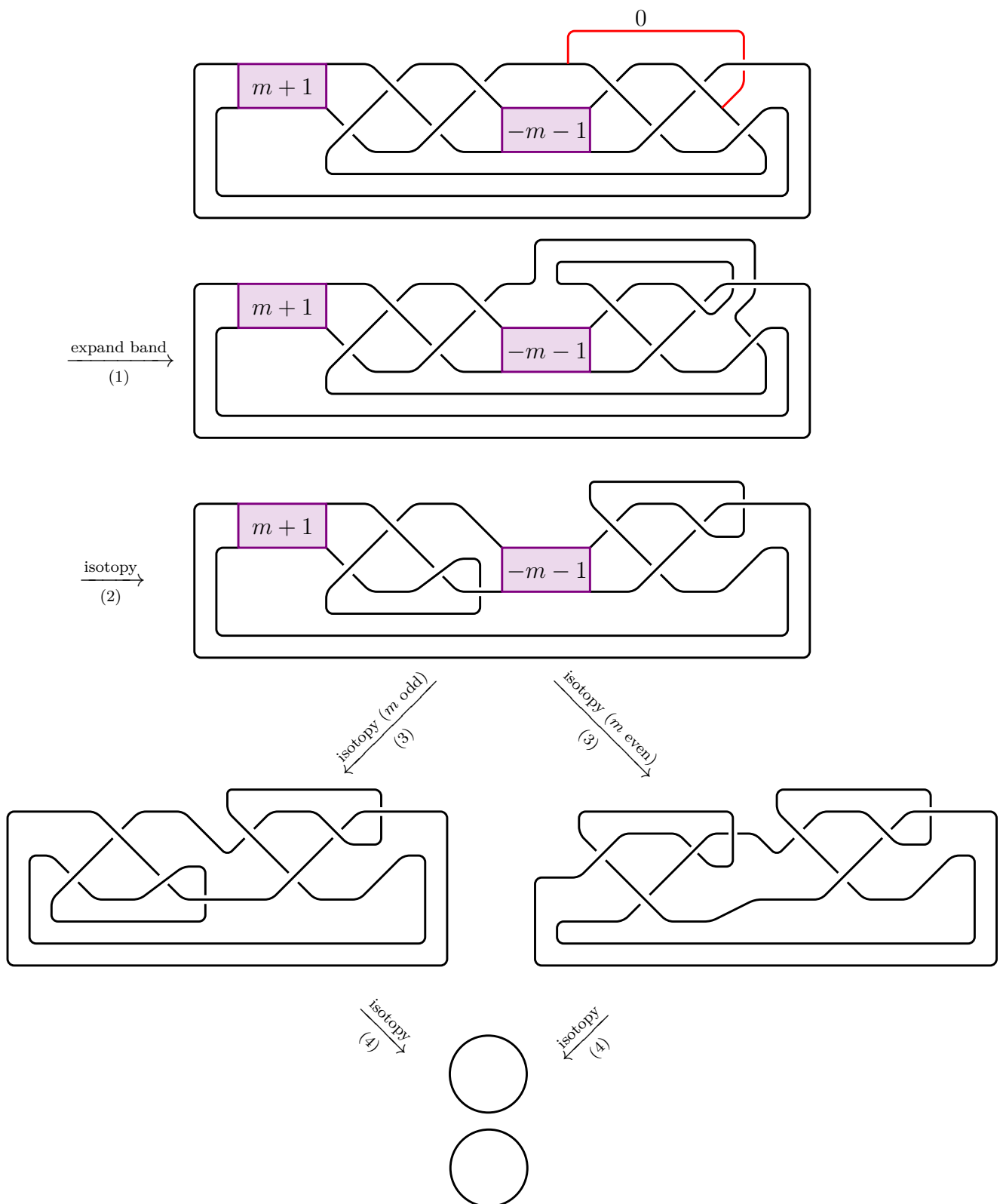


Figure 4.7: Band moves for the closure of an alternating 3-braid with  $\mathbf{x}$ -string  $[m, 0, 0, 0, 0]$  and  $m \geq 3$ . In step (3), we perform  $m + 1$  flypes of the tangle between two blocks with  $m$  crossings followed by R2 moves.

# TAPs of some ABC knots

---

In this chapter we restrict our attention to the three knots in Table 4.1. Let

$$\begin{aligned}\beta_1 &= \sigma_1^2 \sigma_2^{-2} \sigma_1^2 \sigma_2^{-2} \sigma_1 \sigma_2^{-2} \sigma_1^2 \sigma_2^{-2} \sigma_1^2 \sigma_2^{-1}, \\ \beta_2 &= \sigma_1^3 \sigma_2^{-2} \sigma_1 \sigma_2^{-1} \sigma_1^2 \sigma_2^{-3} \sigma_1^2 \sigma_2^{-1} \sigma_1 \sigma_2^{-2}, \\ \beta_3 &= \sigma_1^2 \sigma_2^{-1} \sigma_1 \sigma_2^{-2} \sigma_1 \sigma_2^{-1} \sigma_1 \sigma_2^{-2} \sigma_1 \sigma_2^{-1} \sigma_1^2 \sigma_2^{-1} \sigma_1 \sigma_2^{-1},\end{aligned}$$

and define  $K_i = \widehat{\beta}_i$  for  $i = 1, 2, 3$ . The purpose of this chapter is to show that the knots  $K_i$  are not slice and thus establish the assertion at the end of the previous chapter, namely that, along with the Turk's head knot  $K_7$ , they are the only non-slice knots which are closures of alternating 3-braids with up to 20 crossings. As noted before, various common knot invariants do not obstruct sliceness of any of the  $K_i$  for  $i = 1, 2, 3$ , so instead we seek to apply sensitive yet delicate *twisted Alexander polynomials* (TAPs). Our approach is largely based on that of Aceto et al. [AMMMPS20], which in turn builds on the work of Herald, Kirk and Livingston [HKL10].

In Section 5.1, we give an overview of the theory of twisted Alexander polynomials, focussing on the main definitions as well as the desired sliceness obstruction due to Kirk and Livingston [KL99]. Then, in Section 5.2, we explain our computations of TAPs for  $K_1$ ,  $K_2$  and  $K_3$  in more detail.

## § 5.1 | Main definitions and the sliceness obstruction

Our exposition is based on [KL99] and [HKL10], borrowing from [AMMMPS20] and the survey [FV11] on occasion. Recall that the *order* of a cyclic module over a PID is the generator of its annihilator ideal, up to multiplication by units; the order of a direct sum of cyclic modules is the product of the orders of individual summands. Recall also that for a knot  $K$ , the classical Alexander polynomial  $\Delta_K(t) \in \mathbb{Z}[t^{\pm 1}]$  is defined to be the order of the  $\mathbb{Z}[t^{\pm 1}]$ -module  $\mathcal{A}(K) := H_1(X_K^\infty; \mathbb{Z})$ , called the *Alexander module*, where  $X_K^\infty$  is the infinite cyclic cover of the knot complement  $X_K = S^3 \setminus K$  and  $t$  acts by deck transformations. One may go further and consider the homology of  $X_K^\infty$  with twisted coefficients. More specifically, if  $M$  is a right  $\mathbb{Z}[\pi_1(X_K)]$ -module and  $\pi_1(X_K)$  acts on the chain complex  $C_*(X_K^\infty)$  on the left, one defines the twisted chain complex  $C_*(X; M) := M \otimes_{\mathbb{Z}[\pi_1(X_K)]} C_*(X_K^\infty)$  yielding twisted homology groups

$H_i(X_K; M) := H_i(C_*(X; M))$ . If  $M$  is a  $(S, \mathbb{Z}[\pi_1(X_K)])$ -bimodule for some ring  $S$ , then  $H_i(X_K; M)$  inherits a left  $S$ -module structure.

Let  $\mathbb{F}$  be a field and suppose that  $M$  is a  $(\mathbb{F}[t^{\pm 1}], \mathbb{Z}[\pi_1(X_K)])$ -bimodule. Then  $\mathcal{A}^M(K) := H_1(X_K; M)$  is called the *twisted Alexander module associated to  $K$  and  $M$* . The *twisted Alexander polynomial (TAP) associated to  $K$  and  $M$*  is the order of  $\mathcal{A}^M(K)$  as a left  $\mathbb{F}[t^{\pm 1}]$ -module, written  $\Delta_K^M$  and living in  $\mathbb{F}[t^{\pm 1}]$ . For a fixed  $M$ , such  $\Delta_K^M$  is a knot invariant well-defined up to multiplication by  $at^k$  for  $a \in \mathbb{F}^\times$  and  $k \in \mathbb{Z}$ . The right  $\mathbb{Z}[\pi_1(X_K)]$ -module structure on  $M$  may be defined by a map  $\varphi : \pi_1(X_K) \rightarrow \text{Aut}(M)$ , in which case we write  $\mathcal{A}^\varphi(K)$  for the twisted Alexander module and  $\Delta_K^\varphi$  for the TAP.

Fix distinct primes  $p$  and  $q$ , let  $\zeta_q$  be a primitive  $q^{\text{th}}$  root of unity so that  $\mathbb{F} = \mathbb{Q}(\zeta_q)$  is the cyclotomic field of order  $q$ , and suppose  $M = (\mathbb{Q}(\zeta_q)[t^{\pm 1}])^p$  with the  $\mathbb{Z}[\pi_1(X_K)]$ -action given by  $\varphi : \pi_1(X_K) \rightarrow \text{GL}(p, \mathbb{Q}(\zeta_q)[t^{\pm 1}])$ . In the following, by a twisted Alexander module we mean precisely the  $\mathbb{Q}(\zeta_q)[t^{\pm 1}]$ -module  $\mathcal{A}^\varphi(K)$  and by a TAP, its order up to multiplication by units in  $\mathbb{Q}(\zeta_q)[t^{\pm 1}]$ . Note that if one relaxes the assumption that  $p$  and  $q$  are prime, takes  $p = q = 1$  and lets  $\varphi_0$  be the trivial representation, then  $\Delta_K^{\varphi_0}(t) = \Delta_K(t)$ , recovering the classical Alexander polynomial.

One may further restrict to the following class of representations. From now on, let us write  $\mathbb{Z}_n$  for the abelian group  $\mathbb{Z}/n\mathbb{Z}$  and  $\Sigma_p(K)$  for the  $p$ -fold cover of  $S^3$  branched over a knot  $K$ . Choose a (possibly trivial) *character* (an alternative term for a homomorphism)  $\chi : H_1(\Sigma_p(K); \mathbb{Z}) \rightarrow \mathbb{Z}_q$ . In [HKL10], it is demonstrated that  $\chi$  together with a choice of a based meridian in  $X_K$  determines a map  $\pi_1(X_K) \rightarrow \mathbb{Z} \ltimes H_1(\Sigma_p(K); \mathbb{Z})$ , where the semidirect product is endowed with the group structure explained in Subsection 5.2.6. This, in turn, yields a representation  $\varphi_\chi : \pi_1(X_K) \rightarrow \text{GL}(p, \mathbb{Q}(\zeta_q)[t^{\pm 1}])$  and, consequently, the TAP  $\Delta_K^{\varphi_\chi}(t)$ , which we write simply as  $\Delta_K^\chi(t)$ . Define the *reduced twisted Alexander polynomial*  $\tilde{\Delta}_K^\chi(t) := \Delta_K^\chi(t)/(1-t)^e$  with  $e = 1$  if  $\chi$  is non-trivial, and  $e = 0$  otherwise.

Now, recall that  $H_1(\Sigma_p(K); \mathbb{Z})$  for  $p$  prime is torsion, let  $[x], [y] \in H_1(\Sigma_p(K); \mathbb{Z})$  and suppose  $ly = dc$  for some 2-chain  $c$  with  $x$  transverse to  $c$  and  $l \in \mathbb{Z}$ . The *linking form* is the non-singular form

$$\lambda : H_1(\Sigma_p(K); \mathbb{Z}) \times H_1(\Sigma_p(K); \mathbb{Z}) \rightarrow \mathbb{Q}/\mathbb{Z}$$

defined by  $\lambda([x], [y]) = \frac{1}{l}(x \cdot c)$ , where  $\cdot$  means the algebraic intersection number. The *Blanchfield form* can be thought of as a generalisation of the linking form to the Alexander module: specifically, if  $[x], [y] \in \mathcal{A}(K)$  and  $c$  is a 2-chain transverse to  $x$  such that  $\Delta y = dc$  for some  $\Delta \in \mathbb{Z}[t^{\pm 1}]$ , then the Blanchfield form is the sesquilinear pairing given by

$$\begin{aligned} \text{Bl} : \mathcal{A}(K) \times \mathcal{A}(K) &\rightarrow \mathbb{Q}(t)/\mathbb{Z}[t^{\pm 1}] \\ ([x], [y]) &\mapsto \frac{1}{\Delta} \sum_i (t^i x \cdot c) t^{-i}, \end{aligned}$$

where  $\mathbb{Q}(t)$  is the field of rational functions with coefficients in  $\mathbb{Q}$ . Both linking and Blanchfield forms are well-defined for all homology classes in their domain and are computable from a Seifert matrix of  $K$ , as we shall see in Subsection 5.2.3. An (*invariant*) *metaboliser*  $N$  of  $K$  is a  $\mathbb{Z}[t^{\pm 1}]$ -submodule of  $H_1(\Sigma_p(K); \mathbb{Z})$  that is preserved by the action of covering transformations and satisfies  $N = N^\perp$ , where  $N^\perp$  is the orthogonal complement of  $N$  with respect to the linking form. The rank of any metaboliser is half the rank of  $H_1(\Sigma_p(K); \mathbb{Z})$ ; if  $H_1(\Sigma_p(K); \mathbb{Z})$  is finite, then  $|N|^2 = |H_1(\Sigma_p(K); \mathbb{Z})|$ .

Recall that the *Fox–Milnor condition* states that if a knot  $K$  is slice, then the Alexander polynomial  $\Delta_K(t)$  can be written as  $\Delta_K(t) = f(t)f(t^{-1})$  for some  $f \in \mathbb{Z}[t^{\pm 1}]$  [FM66]. The following sliceness obstruction due to Kirk and Livingston, which is closely related to the theory of Casson–Gordon invariants, can be thought of as a generalisation of the Fox–Milnor condition to TAPs.

**Theorem 5.1.1** ([KL99, Proposition 6.1]). Let  $K \subset S^3$  be a slice knot and fix distinct primes  $p$  and  $q$ . Then there exists an invariant metaboliser  $N \subset H_1(\Sigma_p(K); \mathbb{Z})$  such that the following condition holds: for every character  $\chi : H_1(\Sigma_p(K); \mathbb{Z}) \rightarrow \mathbb{Z}_q$  that vanishes on  $N$ , the associated reduced twisted Alexander polynomial  $\tilde{\Delta}_K^\chi(t) \in \mathbb{Q}(\zeta_q)[t^{\pm 1}]$  is a *norm*, that is,  $\tilde{\Delta}_K^\chi(t)$  can be written as

$$\tilde{\Delta}_K^\chi(t) = at^k f(t) \overline{f(t)}$$

for some  $a \in \mathbb{Q}(\zeta_q)$ ,  $k \in \mathbb{Z}$  and  $\overline{f(t)}$  obtained from  $f(t) \in \mathbb{Q}(\zeta_q)[t^{\pm 1}]$  by the involution  $t \mapsto t^{-1}$ ,  $\zeta_q \mapsto \zeta_q^{-1}$ .

This result allowed Herald, Kirk and Livingston to show that 16 out of 18 alternating knots with up to 12 crossings and hitherto unknown sliceness status are non-slice [HKL10]; the two remaining knots  $12a_{990}$  and  $12a_{631}$  have been found to be slice via an explicit construction of ribbon surfaces, the former by the same authors and the latter by Seeliger [See14]. Moreover, one does not necessarily need to explicitly work out all metabolisers of  $H_1(\Sigma_p(K); \mathbb{Z})$  to apply the obstruction, for the following reason. Since  $H_1(\Sigma_p(K); \mathbb{Z}_q)$  is naturally a  $\mathbb{Z}_q[\mathbb{Z}_p]$ -module, the structure theorem for such modules implies that

$$H_1(\Sigma_p(K); \mathbb{Z}_q) \cong R_{f_1}^{d_1} \oplus \cdots \oplus R_{f_l}^{d_l},$$

where  $R_{f_i}$  is the quotient of  $\mathbb{Z}_q[\mathbb{Z}_p]$  by the principal ideal generated by  $f_i \in \mathbb{Z}_q[\mathbb{Z}_p]$ ; we can think of  $f_i$  as a polynomial in  $t$  with  $\mathbb{Z}_q$ -coefficients that divides  $t^p - 1$ . If  $N$  is a metaboliser of  $H_1(\Sigma_p(K); \mathbb{Z})$ , one may instead look at every submodule  $\overline{N}$  of  $H_1(\Sigma_p(K); \mathbb{Z}_q)$  that can be a projection of  $N$  and obstruct the factorisation of the TAP coming from a character vanishing on  $\overline{N}$ . If  $H_1(\Sigma_p(K); \mathbb{Z}_q)$  has a convenient direct sum decomposition (for example,  $H_1(\Sigma_p(K); \mathbb{Z}_q) \cong R_{f_1}$  or  $H_1(\Sigma_p(K); \mathbb{Z}_q) \cong R_{f_1} \oplus R_{f_2}$  with  $f_1 \neq f_2$ , which is the case for many knots considered in [HKL10]), then one only needs to obstruct one or two TAPs from factoring as norms.

A recent implementation of the obstruction from Theorem 5.1.1 in SnapPy [CDGW] by Dunfield and Gong requires that  $H_1(\Sigma_p(K); \mathbb{Z}_q)$  decomposes into direct summands of multiplicity at most one. However, no pair of distinct primes  $(p, q)$  with  $p$  and  $q$  smaller than 500 yields the desired sliceness obstruction for  $K_1$ ,  $K_2$  and  $K_3$ , as well as for  $K_7$  (which all satisfy the Fox–Milnor condition). To exhibit  $K_7$  as non-slice, Sartori analysed the case  $(p, q) = (7, 13)$ , when  $H_1(\Sigma_p(K); \mathbb{Z}_q) \cong R_{f_1} \oplus R_{f_1}$  for  $f_1 = t^2 + 6t + 1$  and there are  $q^{\deg f_1} + 1 = 170$  candidate  $\bar{N}$ , hence 170 TAPs to obstruct from factoring as norms [Sar10]. Since applying the same approach for  $K_1$ ,  $K_2$  and  $K_3$  would be even more tedious and computationally demanding, we opted for the general approach of Aceto et al. [AMMMPS20]: this way, we need to understand the metabolisers (that is, the square-root order submodules on which the linking form vanishes) of  $H_1(\Sigma_p(K); \mathbb{Z}_q)$  explicitly, but it turns out that computing a total of 11 TAPs is sufficient to rule out all three knots in question from being slice.

## § 5.2 | Computing TAPs for $K_1$ , $K_2$ and $K_3$

In this section, we carry out the computation of TAPs associated to characters vanishing on the metabolisers of  $K_i$  for  $i = 1, 2, 3$ . As previously, let  $p$  and  $q$  be distinct primes and let  $\zeta_q$  be a primitive  $q^{\text{th}}$  root of unity. The section is structured according to the following general outline of the algorithm applied in [AMMMPS20]:

1. Construct the Seifert matrix  $S_i$  for  $K_i$  coming from the standard Seifert surface  $F_i$  associated to  $K_i$  viewed as a 3-braid closure.
2. By considering the presentation matrix  $P_i = tS_i - S_i^T \in \text{Mat}(\mathbb{Z}[t^{\pm 1}])$  of the Alexander module  $\mathcal{A}(K_i)$ , determine the structure of  $H_1(\Sigma_p(K_i))$  as well as a basis of  $H_1(\Sigma_p(K_i))$  in terms lifts of curves in  $S^3 \setminus \nu(F)$ .
3. Calculate the Blanchfield pairings  $\text{Bl}_i : \mathcal{A}(K_i) \times \mathcal{A}(K_i) \rightarrow \mathbb{Q}(t)/\mathbb{Z}[t^{\pm 1}]$  and deduce the linking pairings  $\lambda_i : H_1(\Sigma_p(K_i)) \times H_1(\Sigma_p(K_i)) \rightarrow \mathbb{Q}/\mathbb{Z}$ .
4. Enumerate all  $\mathbb{Z}[t^{\pm 1}]$ -submodules  $N$  of  $H_1(\Sigma_p(K_i))$  with  $|N|^2 = |H_1(\Sigma_p(K_i))|$  and thus find all metabolisers of  $H_1(\Sigma_p(K_i))$ , that is, those  $N$  on which  $\lambda_i$  vanishes.
5. Construct nontrivial characters  $\chi : H_1(\Sigma_p(K_i)) \rightarrow \mathbb{Z}_q$  that vanish on the metabolisers.
6. Using a Wirtinger presentation of  $\pi_1(X_i)$ , where  $X_i$  is the knot complement of  $K_i$ , for each  $\chi$  in (5) construct a homomorphism  $\pi_1(X_i) \rightarrow \mathbb{Z} \ltimes H_1(\Sigma_p(K_i))$  that induces a representation  $\varphi_\chi : \pi_1(X_i) \rightarrow \text{GL}(p, \mathbb{Q}(\zeta_q)[t^{\pm 1}])$ .
7. Use the Fox matrix for a Wirtinger presentation of  $\pi_1(X_i)$  to obtain a matrix  $\Phi_\chi$  for each  $\chi$  in (5), whose determinant  $\det \Phi_\chi$  is the reduced twisted Alexander polynomial  $\tilde{\Delta}_{K_i}^\chi(t)$ .
8. Verify that none of the  $\tilde{\Delta}_{K_i}^\chi(t)$  factor as norms, hence providing an obstruction to sliceness of all  $K_i$ .

The computations were performed in SageMath notebooks presented in Appendix B.

### § 5.2.1 | Seifert matrices

Let  $\beta$  be a 3-braid. A Seifert surface  $F$  for  $\widehat{\beta}$  can be constructed by joining three discs  $D_1$ ,  $D_2$  and  $D_3$  by half-twisted bands, where each band between  $D_1$  and  $D_2$  comes from a  $\sigma_1$  term in  $\beta$ , and each band between  $D_2$  and  $D_3$  from a  $\sigma_2$  term; identify every band with its corresponding  $\sigma_i$ . Let  $g$  be the genus of  $F$ . We can choose the generators of  $H_1(F)$  to be the loops running once through consecutive  $\sigma_1$ 's and  $\sigma_2$ 's, except for the loop between the first and last  $\sigma_1$  and the first and last  $\sigma_2$ . We order these generators  $s_1, \dots, s_{2g}$  by when the first  $\sigma_i$  through which  $s_j$  runs appears in  $\beta$ . With this setup, the Seifert matrix  $S$  can be obtained using the algorithm of Collins [Col16]. Such  $F$  with  $s_1, \dots, s_{2g}$  for  $K_1$  is shown in Figure 5.1. Also, for  $\nu(F)$  an open tubular neighbourhood of  $F$ , let  $\{\widehat{s}_1, \dots, \widehat{s}_{2g}\}$  be a basis for  $S^3 \setminus \nu(F)$  that is *Alexander dual* to  $\{s_1, \dots, s_{2g}\}$ ; this means that each  $\widehat{s}_i$  is a simple closed curve satisfying  $\text{lk}(\widehat{s}_i, s_j) = \delta_{ij}$  for all  $j$ .

### § 5.2.2 | Structure of $H_1(\Sigma_3(K_i))$

The following two subsections are applications of the following theorem, which is a combination of [FP17, Theorem 1.3] and [FP17, Theorem 1.4], summarised in the present context in [AMMMPS20]. Specifically, we seek to understand bases for  $H_1(\Sigma_3(K_i))$  in terms of lifts of curves in  $S^3 \setminus \nu(F_i)$ , and to calculate Blanchfield pairings on those bases.

**Theorem 5.2.1** ([AMMMPS20, Theorem 3.6]). Let  $K$  be a knot with a Seifert surface  $F$ . Suppose a basis for  $H_1(F; \mathbb{Z})$  is given by simple closed curves  $s_1, \dots, s_{2g}$  in  $F$  and  $S$  is the corresponding Seifert matrix. Suppose also that  $\{\widehat{s}_1, \dots, \widehat{s}_{2g}\}$  is a basis for  $S^3 \setminus \nu(F)$  in which every curve is Alexander dual to  $\{s_1, \dots, s_{2g}\}$ . Consider the decomposition of the infinite cyclic cover  $X_K^\infty$  of  $X_K$  associated to  $F$ , given by

$$X_K^\infty = \bigcup_{i=-\infty}^{\infty} (S^3 \setminus \nu(F))_i$$

and denote by  $\widetilde{s}_i$  the homology class of the unique lift of  $\widehat{s}_i$  to  $(S^3 \setminus \nu(F))_0$ . Then the map  $p : (\mathbb{Z}[t^{\pm 1}])^{2g} \rightarrow \mathcal{A}(K)$  defined by

$$p(x_1, \dots, x_{2g}) = \sum_{i=1}^{2g} x_i \widetilde{s}_i$$

is surjective and its kernel is given by  $(tS - S^T)(\mathbb{Z}[t^{\pm 1}])^{2g}$ . Moreover, the Blanchfield pairing is given as follows: for  $x, y \in (\mathbb{Z}[t^{\pm 1}])^{2g}$  we have

$$\text{Bl}(p(x), p(y)) = (t - 1)x^T (S - tS^T)^{-1} \bar{y} \in \mathbb{Q}(t)/\mathbb{Z}[t^{\pm 1}],$$

where  $\bar{y}$  is obtained from  $y$  by the involution  $t^i \mapsto t^{-i}$ .

We are able to perform column operations on the matrices  $tS_i - S_i^T$  to put them in lower triangular forms  $L_i$ ; since column operations preserve images,  $(tS_i - S_i^T)(\mathbb{Z}[t^{\pm 1}])^{2g} = L_i(\mathbb{Z}[t^{\pm 1}])^{2g}$ . If the  $j^{\text{th}}$  diagonal entry  $d_j(t) \in \mathbb{Z}[t^{\pm 1}]$  of  $L_i$  is not a unit, then  $\mathcal{A}(K_i)$

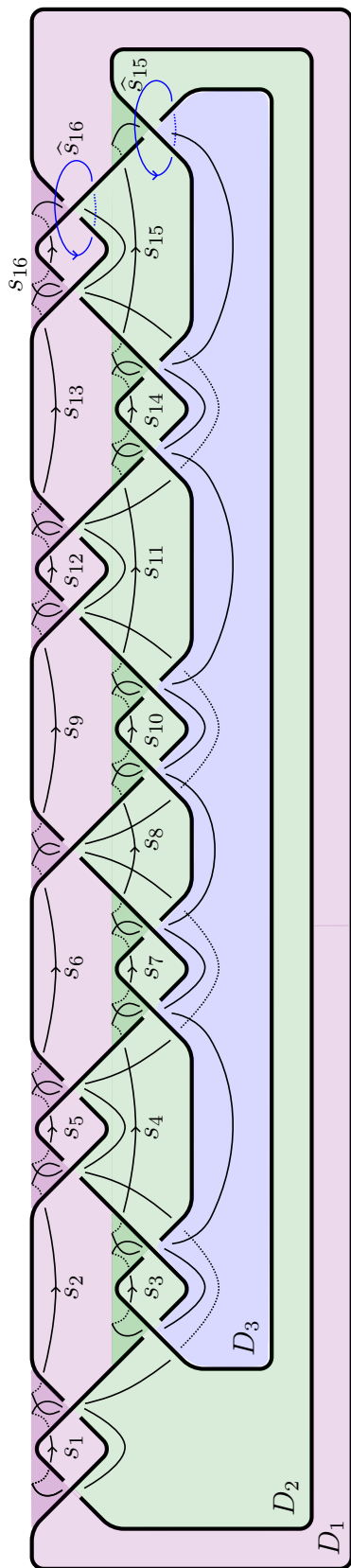


Figure 5.1: Our choice of a Seifert surface  $F_1$  for  $K_1$ . Lifts of Alexander dual curves  $\hat{s}_{15}$  and  $\hat{s}_{16}$  will turn out to generate  $H_1(\Sigma_3(K_1))$ .

contains a direct summand  $\mathbb{Z}[t^{\pm 1}]/\langle d_j(t) \rangle$  generated by  $\tilde{s}_j$ . Carrying this operation out, we obtain

$$L_1 = \left( \begin{array}{c|cc} I & & 0 \\ \hline & p_1(t) & 0 \\ * & 0 & p_1(t) \end{array} \right), \quad L_2 = \left( \begin{array}{c|ccc} I & & & 0 \\ \hline & p_2(t) & 0 & 0 \\ * & 0 & 1 & 0 \\ & 0 & * & p_2(t) \end{array} \right), \quad L_3 = \left( \begin{array}{c|cc} I & & 0 \\ \hline & p_3(t) & 0 \\ * & 0 & p_3(t) \end{array} \right)$$

where each  $p_i(t)$  is the square root of the untwisted Alexander polynomial  $\Delta_{K_i}(t)$ ,  $I$  is the identity matrix and  $*$  represents other entries. Specifically,

$$\begin{aligned} p_1(t) &= 1 - 3t + 7t^2 - 10t^3 + 11t^4 - 10t^5 + 7t^6 - 3t^7 + t^8, \\ p_2(t) &= 1 - 3t + 6t^2 - 9t^3 + 11t^4 - 9t^5 + 6t^6 - 3t^7 + t^8, \\ p_3(t) &= 1 - 4t + 8t^2 - 11t^3 + 13t^4 - 11t^5 + 8t^6 - 4t^7 + t^8. \end{aligned}$$

It follows that

$$\mathcal{A}(K_i) \cong \mathbb{Z}[t^{\pm 1}]/\langle p_i(t) \rangle \oplus \mathbb{Z}[t^{\pm 1}]/\langle p_i(t) \rangle,$$

where  $\mathcal{A}(K_i)$  for  $i \in \{1, 3\}$  is generated by  $\tilde{s}_{15}$  and  $\tilde{s}_{16}$ , while  $\mathcal{A}(K_2)$  is generated by  $\tilde{s}_{14}$  and  $\tilde{s}_{16}$ ; in each case, call these generators  $a$  and  $b$ , respectively. Choose  $p = 3$ . By, for example, [FL19, Section 6.1], we have

$$\begin{aligned} H_1(\Sigma_3(K_i)) &\cong \mathcal{A}(K_i)/\langle t^2 + t + 1 \rangle \\ &\cong \mathbb{Z}[t^{\pm 1}]/\langle p_i(t), t^2 + t + 1 \rangle \oplus \mathbb{Z}[t^{\pm 1}]/\langle p_i(t), t^2 + t + 1 \rangle \\ &\cong \mathbb{Z}[t^{\pm 1}]/\langle 7t, t^2 + t + 1 \rangle \oplus \mathbb{Z}[t^{\pm 1}]/\langle 7t, t^2 + t + 1 \rangle \\ &\cong \mathbb{Z}_7[t^{\pm 1}]/\langle t^2 + t + 1 \rangle \oplus \mathbb{Z}_7[t^{\pm 1}]/\langle t^2 + t + 1 \rangle \end{aligned}$$

in each of the three cases, since all of  $p_i(t)$  are congruent to  $7t$  modulo  $t^2 + t + 1$ . Hence, we fix  $q = 7$ . The generators of  $\mathcal{A}(K_i)$  descend to  $H_1(\Sigma_3(K_i))$ , so by abuse of notation we also denote their images in  $H_1(\Sigma_3(K_i))$  by  $a$  and  $b$ . As groups,  $H_1(\Sigma_3(K_i)) \cong \mathbb{Z}_7^4$ , and we may treat them as  $\mathbb{Z}_7$ -modules generated by  $a, ta, b$  and  $tb$ .

### § 5.2.3 | Blanchfield and linking forms

Let  $e_j \in (\mathbb{Z}[t^{\pm 1}])^{2g}$  be the vector with 1 in the  $j^{\text{th}}$  position and zeros elsewhere. We have  $p(e_{16}) = b$  for all  $i$ ,  $p(e_{15}) = a$  for  $i \in \{1, 3\}$  and  $p(e_{14}) = a$  for  $i = 2$ . Via Theorem 5.2.1, we can read off the Blanchfield pairings on  $\mathcal{A}(K_i)$  directly. However, since we are interested in the linking forms, we present the following result first.

**Proposition 5.2.2** ([AMMMPS20, Proposition 3.7]). Let  $p$  be a prime power and suppose  $x, y \in H_1(\Sigma_p(K))$ . Take  $\tilde{x}$  and  $\tilde{y}$  which are lifts of  $x$  and  $y$ , respectively, to  $\mathcal{A}(K)$ , and write

$$\text{Bl}(\tilde{y}, \tilde{x}) = \frac{f(t)}{\Delta_K(t)} \in \mathbb{Q}(t)/\mathbb{Z}[t^{\pm 1}].$$

Then  $t^p - 1$  and  $\Delta_K(t)$  are relatively prime and one can find  $r(t) \in \mathbb{Z}[t^{\pm 1}]$  such that

$\Delta_K(t)r(t) \equiv c \pmod{t^p - 1}$ . Writing

$$f(t)r(t) \equiv \sum_{i=1}^p \alpha_i t^i \pmod{t^p - 1},$$

for  $i = 0, \dots, p - 1$ , the linking form on  $H_1(\Sigma_p(K))$  is given by

$$\lambda(x, t^i y) = \frac{\alpha_{p-i}}{c} \in \mathbb{Q}/\mathbb{Z}.$$

A computation using the script in Appendix B yields that for all  $i = 1, 2, 3$ , the Blanchfield pairings with respect to the ordered basis  $\{a, b\}$  of  $\mathcal{A}(K_i)$  are given by the matrix  $(1/p_i(t)) \cdot M$ , where  $M \in \text{Mat}_2(\mathbb{Z}[t^{\pm 1}])$ . Multiplying both the numerator and denominator of each entry by  $p_i(t)$  in each case (which we are allowed to do since Blanchfield pairings take values in  $\mathbb{Q}(t)/\mathbb{Z}[t^{\pm 1}]$ ) and recalling that  $\Delta_{K_i}(t) = p_i^2(t)$ , we get that  $\text{Bl}_i$  is alternatively given by  $(1/\Delta_{K_i}(t)) \cdot M'$ , where  $M'_{ij} = p_i(t) \cdot M_{ij} \in \mathbb{Z}[t^{\pm 1}]$ . Now, we can use SageMath to find  $r(t)$  and  $c$  in each case, and hence read off that the resulting linking pairings  $\lambda_i : H_1(\Sigma_3(K_i)) \times H_1(\Sigma_3(K_i)) \rightarrow \mathbb{Q}/\mathbb{Z}$  with respect to the ordered basis  $\{a, ta, b, tb\}$  are given by

$$\frac{1}{7} \begin{pmatrix} -4 & 2 & -2 & 4 \\ 2 & -4 & -2 & -2 \\ -2 & -2 & 1 & -4 \\ 4 & -2 & -4 & 1 \end{pmatrix}, \quad \frac{1}{7} \begin{pmatrix} 6 & -3 & 0 & -3 \\ -3 & 6 & 3 & 0 \\ 0 & 3 & -6 & 3 \\ -3 & 0 & 3 & -6 \end{pmatrix} \quad \text{and} \quad \frac{1}{7} \begin{pmatrix} 1 & -4 & -2 & -2 \\ -4 & 1 & 4 & -2 \\ -2 & 4 & -4 & 2 \\ -2 & -2 & 2 & -4 \end{pmatrix}.$$

#### § 5.2.4 | Metabolisers of $H_1(\Sigma_3(K_i))$

Write  $M = \mathbb{Z}_7[t^{\pm 1}]/\langle t^2 + t + 1 \rangle$  so that, as a  $\mathbb{Z}_7[t^{\pm 1}]$ -module,  $H_1(\Sigma_3(K_i)) \cong M \oplus M$ . Since the cardinality  $|H_1(\Sigma_3(K_i))| = 7^4$ , we seek to describe all its  $\mathbb{Z}[t^{\pm 1}]$ -submodules of cardinality  $7^2 = 49$ . Since  $t^2 + t + 1$  has irreducible factors  $(t - 2), (t + 3) \in \mathbb{Z}_7[t^{\pm 1}]$ , the set  $\{\langle 0 \rangle, \langle 1 \rangle, \langle t - 2 \rangle, \langle t + 3 \rangle\}$  contains precisely the  $\mathbb{Z}_7[t^{\pm 1}]$ -submodules of  $M$ ; because the  $\mathbb{Z}[t^{\pm 1}]$ -action on  $M$  factors through  $\mathbb{Z}_7[t^{\pm 1}]$ , these are also precisely the  $\mathbb{Z}[t^{\pm 1}]$ -submodules of  $M$ . Observe that  $|\langle 0 \rangle| = 1$ ,  $|\langle 1 \rangle| = 49$  and  $|\langle t - 2 \rangle| = |\langle t + 3 \rangle| = 7$ . Now let  $N$  be a  $\mathbb{Z}[t^{\pm 1}]$ -submodule of  $H_1(\Sigma_3(K_i))$ , and consider the commutative diagram

$$\begin{array}{ccccc} M \oplus \{0\} & \longrightarrow & M \oplus M & \xrightarrow{\pi} & \{0\} \oplus M \\ \uparrow & & \uparrow & & \uparrow \\ \ker \pi|_N & \longrightarrow & N & \xrightarrow{\pi|_N} & \text{im } \pi|_N \end{array}$$

where  $\pi(x, y) = (0, y)$  for all  $x, y \in M$ , and unlabelled arrows are inclusions;  $\ker \pi|_N$  and  $\text{im } \pi|_N$  are submodules of  $M \oplus \{0\}$  and  $\{0\} \oplus M$ , respectively. Since  $|N| = |\ker \pi|_N| \cdot |\text{im } \pi|_N|$ , we can deduce what  $N$  could be by cardinality considerations.

- If  $|\ker \pi|_N| = 49$ , then  $|\text{im } \pi|_N| = 1$  and  $N = \ker \pi|_N = \text{span}_{\mathbb{Z}_7[t^{\pm 1}]} \{(1, 0)\}$ .
- If  $|\ker \pi|_N| = 1$ , then  $N \cong \text{im } \pi|_N = \text{span}_{\mathbb{Z}_7[t^{\pm 1}]} \{(k, 1)\}$  for some  $k \in \mathbb{Z}_7[t^{\pm 1}]$ .

Now, let  $\{\langle t-2 \rangle, \langle t+3 \rangle\} = \{\langle \alpha \rangle, \langle \beta \rangle\}$ ; we have  $\text{Ann } \alpha = \langle \beta \rangle$  and  $\text{Ann } \beta = \langle \alpha \rangle$ . There are two remaining cases to consider.

- Suppose  $\ker \pi|_N \cong \text{im } \pi|_N \cong \langle \alpha \rangle$ . Then  $N$  contains  $\{(\alpha, 0), (k, \alpha)\}$  for some  $k \in \mathbb{Z}_7[t^{\pm 1}]$ . Since  $\beta(k, \alpha) = (\beta k, 0) \in \ker \pi|_N$ , we must have  $\beta k \in \langle \alpha \rangle$ , so  $k \in \langle \alpha \rangle$ , that is,  $k = l\alpha$  for some  $l \in \mathbb{Z}_7[t^{\pm 1}]$ . Then  $-l(\alpha, 0) + (k, \alpha) = (0, \alpha) \in N$ , so  $N$  contains two linearly independent elements  $(\alpha, 0)$  and  $(0, \alpha)$  of order 7, hence is generated by them for any choice of  $k$ . This yields two submodules  $N = \text{span}_{\mathbb{Z}_7[t^{\pm 1}]} \{(t-2, 0), (0, t-2)\}$  and  $N = \text{span}_{\mathbb{Z}_7[t^{\pm 1}]} \{(t+3, 0), (0, t+3)\}$ .
- Suppose  $\ker \pi|_N = \langle \alpha \rangle$  and  $\text{im } \pi|_N \cong \langle \beta \rangle$ . We similarly observe that  $N$  contains  $\{(\alpha, 0), (k, \beta)\}$  for some  $k \in \mathbb{Z}_7[t^{\pm 1}]$ . We have  $\alpha(k, \beta) = (\alpha k, 0) \in \ker \pi|_N$ , so we can take  $k$  modulo  $\alpha$ , that is,  $k \in \mathbb{Z}_7$ . Then  $\{(\alpha, 0), (k, \beta)\}$  is a linearly independent set generating  $N$  for any choice of  $k \in \mathbb{Z}_7$ . Thus,  $N = \text{span}_{\mathbb{Z}_7[t^{\pm 1}]} \{(t-2, 0), (k, t+3)\}$  or  $N = \text{span}_{\mathbb{Z}_7[t^{\pm 1}]} \{(t+3, 0), (k, t-2)\}$  for  $k \in \mathbb{Z}_7$ .

To summarise, writing elements of  $H_1(\Sigma_3(K_i)) \cong M \oplus M$  additively with the first copy of  $M$  generated by  $a$  and the second by  $b$ , the desired submodules are

$$\begin{aligned} N_0 &= \text{span}_{\mathbb{Z}_7[t^{\pm 1}]} \{a\}; \\ N_{k_0, k_1} &= \text{span}_{\mathbb{Z}_7[t^{\pm 1}]} \{ka + b\} \text{ for } k \in \mathbb{Z}_7[t^{\pm 1}] \\ &= \text{span}_{\mathbb{Z}_7[t^{\pm 1}]} \{(k_0 + k_1 t)a + b\} \text{ for } k_0, k_1 \in \mathbb{Z}/7; \\ N_0^\alpha &= \text{span}_{\mathbb{Z}_7[t^{\pm 1}]} \{(t-2)a, (t-2)b\}; \\ N_0^\beta &= \text{span}_{\mathbb{Z}_7[t^{\pm 1}]} \{(t+3)a, (t+3)b\}; \\ N_{k_0}^{\alpha\beta} &= \text{span}_{\mathbb{Z}_7[t^{\pm 1}]} \{(t-2)a, k_0 a + (t+3)b\} \text{ for } k_0 \in \mathbb{Z}/7; \\ N_{k_0}^{\beta\alpha} &= \text{span}_{\mathbb{Z}_7[t^{\pm 1}]} \{(t+3)a, k_0 a + (t-2)b\} \text{ for } k_0 \in \mathbb{Z}/7. \end{aligned}$$

By a direct check of whether the linking pairing  $\lambda_i$  vanishes on each of the above submodules, we conclude that  $N_0^\alpha$  and  $N_0^\beta$  are metabolisers for  $K_i$  for all  $i$ ; in addition,  $K_1$  has metabolisers  $N_6^{\alpha\beta}$  and  $N_4^{\beta\alpha}$ ,  $K_2$  has metabolisers  $N_1^{\alpha\beta}$  and  $N_1^{\beta\alpha}$ , and  $K_3$  has metabolisers  $N_2^{\alpha\beta}$  and  $N_3^{\beta\alpha}$ .

### § 5.2.5 | Characters vanishing on the metabolisers

It is easy to define characters  $\chi : H_1(\Sigma_3(K_i)) \rightarrow \mathbb{Z}_7$  that vanish on the metabolisers. Let subscripts and superscripts denote corresponding metabolisers and 4-tuples in parentheses represent the values a character takes on the ordered basis  $\{a, ta, b, tb\}$ . Then we can take  $\chi_0^\alpha$  and  $\chi_0^\beta$  as defined by  $(1, 2, 1, 2)$  and  $(1, -3, 1, -3)$ , respectively. The rest of the characters are presented in Table 5.1.

### § 5.2.6 | Representations of knot groups

Let  $K \in \{K_1, K_2, K_3\}$  and  $F$  the corresponding Seifert surface as in Subsection 5.2.1. We now follow [AMMMPS20, Appendix A] and [HKL10, Chapters 5–7] to construct representations  $\varphi_\chi : \pi_1(X_K) \rightarrow \text{GL}(3, \mathbb{Q}(\zeta_7)[t^{\pm 1}])$  of the knot group of  $K$  that determine

$K_1$	$K_2$	$K_3$
$\chi_6^{\alpha\beta} : (1, 2, 1, -2)$	$\chi_1^{\alpha\beta} : (1, 2, 1, -4)$	$\chi_2^{\alpha\beta} = \chi_0^\alpha : (1, 2, 1, 2)$
$\chi_4^{\beta\alpha} : (1, -3, 1, -2)$	$\chi_1^{\beta\alpha} : (1, -3, 1, 1)$	$\chi_3^{\beta\alpha} : (1, -3, 1, 1)$

Table 5.1: Our choices of characters  $\chi : H_1(\Sigma_3(K_i)) \rightarrow \mathbb{Z}_7$  vanishing on the metabolisers of  $K_1$ ,  $K_2$  and  $K_3$ ; the characters  $\chi_0^\alpha$  and  $\chi_0^\beta$  are given for all  $K_i$  by  $(1, 2, 1, 2)$  and  $(1, -3, 1, -3)$ .

TAPs for each character in Table 5.1. Fix a basepoint  $x_0$  in  $S^3 \setminus \nu(F)$  and let  $\tilde{x}_0$  be its lift to the preferred copy of  $S^3 \setminus \nu(F)$  in  $X_K^3$ , the triple cyclic cover of the knot complement  $X_K$ . Also fix a based meridian  $\mu_0$  in  $S^3 \setminus K$  and let  $\varepsilon : \pi_1(X_K) \rightarrow \mathbb{Z}$  be the abelianisation homomorphism. Define a map  $l : \ker \varepsilon \rightarrow H_1(\Sigma_3(K))$  that takes a simple closed curve  $\gamma \subset S^3 \setminus K$  based at  $x_0$  with  $\text{lk}(K, \gamma) = 0$  to the homology class of the well-defined lift  $\tilde{\gamma}$  in  $X_K^3 \subset \Sigma_3(K)$  based at  $\tilde{x}_0$ . In particular,  $l$  has the property that for any  $\gamma \in \ker \varepsilon$ , we have

$$l(\mu_0 \gamma \mu_0^{-1}) = t \cdot l(\gamma). \quad (\ddagger)$$

Now consider the semidirect product  $\mathbb{Z} \ltimes H_1(\Sigma_3(K))$ , with  $\mathbb{Z} = \langle t \rangle$ , whose product structure is given by

$$(t^{m_1}, x_1) \cdot (t^{m_2}, x_2) = (t^{m_1+m_2}, t^{-m_2} \cdot x_1 + x_2)$$

and  $t$  acting on elements of  $H_1(\Sigma_3(K))$  by deck transformations. Fix a Wirtinger presentation of  $\pi_1(X_K) \cong \langle g_1, \dots, g_n \mid r_1, \dots, r_n \rangle$  and define a homomorphism

$$\begin{aligned} \psi : \pi_1(X_K) &\rightarrow \mathbb{Z} \ltimes H_1(\Sigma_3(K)) \\ g_i &\mapsto (t, l(\mu_0^{-1} g_i)) =: (t, v_i) \end{aligned}$$

on the generators of  $\pi_1(X_K)$ , since clearly  $\mu_0^{-1} g_i \in \ker \varepsilon$ . Observe that a relation  $g_i g_j g_i^{-1} g_k^{-1} = 1$  imposes, via the group structure on  $\mathbb{Z} \ltimes H_1(\Sigma_3(K))$ , the condition

$$(1-t)v_i + tv_j - v_k = 0. \quad (\ddagger\ddagger)$$

Finally, for a character  $\chi : H_1(\Sigma_3(K)) \rightarrow \mathbb{Z}_7$ , we obtain a representation  $\varphi_\chi : \pi_1(X_K) \rightarrow \text{GL}(3, \mathbb{Q}(\zeta_7)[t^{\pm 1}])$  by setting  $\varphi_\chi = \tau_\chi \circ \psi$ , where

$$\begin{aligned} \tau_\chi : \mathbb{Z} \ltimes H_1(\Sigma_3(K)) &\rightarrow \text{GL}(3, \mathbb{Q}(\zeta_7)[t^{\pm 1}]) \\ (t^m, v) &\mapsto \begin{pmatrix} 0 & 1 & 0 \\ 0 & 0 & 1 \\ t & 0 & 0 \end{pmatrix}^m \begin{pmatrix} \zeta_7^{\chi(v)} & 0 & 0 \\ 0 & \zeta_7^{\chi(tv)} & \\ 0 & 0 & \zeta_7^{\chi(t^2 \cdot v)} \end{pmatrix}. \end{aligned}$$

We shall apply the equation  $(\ddagger)$  to determine the form of the first few  $v_k$  for  $K$  in terms of the generators  $a$  and  $b$  of  $H_1(\Sigma_3(K))$  and then deduce the rest of  $v_k$  using  $(\ddagger\ddagger)$ , giving us the desired  $\varphi_\chi$ . We illustrate the process in detail for  $K = K_1$ , with  $K_2$  and

$K_3$  cases being analogous.

Recall that we orient  $K_1$  clockwise. Index the arcs in the diagram of  $K_1$  as shown in Figure 5.2, starting with 1 at the top left and increasing the index at every undercrossing. This yields the following Wirtinger presentation of  $\pi_1(X_1)$ , with generators being the meridians  $g_i$  about each arc  $i$  based at  $x_0$ :

$$\pi_1(X_1) = \left\langle g_1, \dots, g_{18} \left| \begin{array}{cccc} g_1 g_{13} g_1^{-1} g_{12}^{-1}, & g_{17} g_5 g_{17}^{-1} g_4^{-1}, & g_{14} g_8 g_{14}^{-1} g_9^{-1}, & \\ g_{13} g_2 g_{13}^{-1} g_1^{-1}, & g_5 g_{18} g_5^{-1} g_{17}^{-1}, & g_9 g_{15} g_9^{-1} g_{16}^{-1}, & g_{11} g_5 g_{11}^{-1} g_6^{-1}, \\ g_2 g_{15} g_2^{-1} g_{14}^{-1}, & g_{18} g_7 g_{18}^{-1} g_6^{-1}, & g_{16} g_9 g_{16}^{-1} g_{10}^{-1}, & g_6 g_{11} g_6^{-1} g_{12}^{-1}, \\ g_{15} g_3 g_{15}^{-1} g_2^{-1}, & g_7 g_1 g_7^{-1} g_{18}^{-1}, & g_{10} g_3 g_{10}^{-1} g_4^{-1}, & g_{12} g_7 g_{12}^{-1} g_8^{-1} \\ g_3 g_{17} g_3^{-1} g_{16}^{-1}, & g_8 g_{13} g_8^{-1} g_{14}^{-1}, & g_4 g_{10} g_4^{-1} g_{11}^{-1}, & \end{array} \right\rangle$$

Observe that  $\widehat{s}_{15} = g_8 g_{12}^{-1}$  and  $\widehat{s}_{16} = g_1^{-1} g_7$ . Fix  $\mu_0 = g_1$ . Then  $v_1 = l(g_1^{-1} g_1) = 0$  and  $v_7 = l(g_1^{-1} g_7) = b$ . Also, using the property (†), we have

$$\begin{aligned} a &= l(g_8 g_{12}^{-1}) = l(g_8 g_1^{-1} g_1 g_{12}^{-1}) \\ &= l(g_8 g_1^{-1}) + l(g_1 g_{12}^{-1}) \\ &= l(g_1 g_1^{-1} g_8 g_1^{-1}) - l(g_{12} g_1^{-1}) \\ &= l(g_1 g_1^{-1} g_8 g_1^{-1}) - l(g_1 g_1^{-1} g_{12} g_1^{-1}) \\ &= tv_8 - tv_{12}. \end{aligned}$$

Applying (‡) to the relation  $g_{12} g_7 g_{12}^{-1} g_8^{-1} = 1$  and recalling we are working modulo  $t^2 + t + 1$ , we get

$$\begin{aligned} (1-t)v_{12} + tv_7 - v_8 &= 0 \\ \implies (1-t)v_{12} - v_8 &= -tb \mid \cdot (-t) \\ \implies (tv_8 - tv_{12}) + t^2 v_{12} &= t^2 b \\ \implies a + t^2 v_{12} &= t^2 b \mid \cdot t \\ \implies v_{12} &= -ta + b. \end{aligned}$$

Now we can use (‡) repeatedly to obtain all  $v_i$ : for instance, we recover  $v_8$  from the relation  $g_{12} g_7 g_{12}^{-1} g_8^{-1} = 1$  since by (‡),  $(1-t)v_{12} + tv_7 = v_8$  and we already know what  $v_7$  and  $v_{12}$  are; full details of the calculation are available in the accompanying notebooks. With the same conventions and the choice  $\mu_0 = g_1$ , for  $K_2$  we have  $l(\widehat{s}_{14}) = l(g_1^{-1} g_6) = a$  and  $l(\widehat{s}_{16}) = l(g_{14} g_7^{-1}) = b$ , while for  $K_3$ ,  $l(\widehat{s}_{15}) = l(g_1^{-1} g_7) = a$  and  $l(\widehat{s}_{16}) = l(g_8 g_{13}^{-1}) = b$ . This lets us calculate the values of  $v_i$  in Table 5.2 analogously, after which it is mechanical to construct representations  $\varphi_\chi$  for the characters in Subsection 5.2.5.

### § 5.2.7 | Calculating TAPs

Again, let  $K \in \{K_1, K_2, K_3\}$  and fix the Wirtinger presentation of  $\pi_1(X_K)$  as in Subsection 5.2.6. Given a representation  $\varphi_\chi : \pi_1(X_K) \rightarrow \text{GL}(3, \mathbb{Q}(\zeta_7)[t^{\pm 1}])$ , define  $\Phi_\chi : \mathbb{Z}[\pi_1(X_K)] \rightarrow \text{Mat}_3(\mathbb{Q}(\zeta_7)[t^{\pm 1}])$  to be its natural extension to the group ring

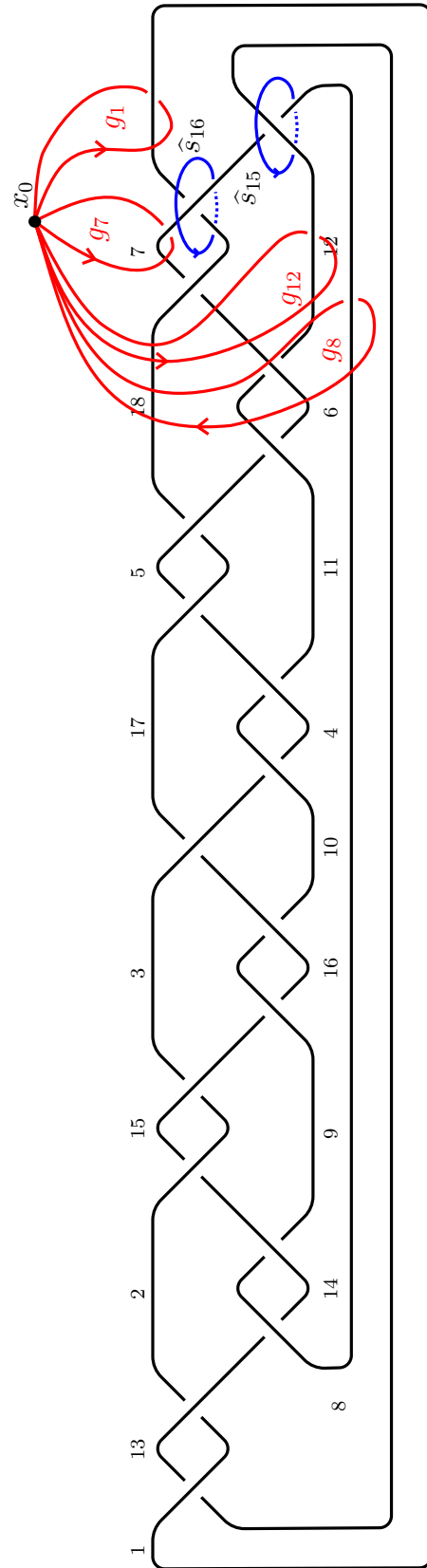


Figure 5.2: Choice of arc labels for  $K_1$  giving a Wirtinger presentation of  $\pi_1(X_1)$ .

	$\pi_1(X_1)$	$\pi_1(X_2)$	$\pi_1(X_3)$
$v_1$	0	0	0
$v_2$	$(6t + 5)a + (5t + 6)b$	$(5t + 6)a + (4t + 4)b$	$(5t + 6)a + (6t + 5)b$
$v_3$	$5ta + 5b$	$3a + (3t + 1)b$	$(4t + 3)a + (t + 1)b$
$v_4$	$(2t + 5)a + 6b$	$(2t + 6)a + 2b$	$(6t + 3)a + b$
$v_5$	$(6t + 5)a + (5t + 3)b$	$(4t + 1)a + (6t + 5)b$	$(6t + 4)a + (4t + 6)b$
$v_6$	$5tb$	$a$	$(4t + 1)a + (t + 6)b$
$v_7$	$b$	$a + (6t + 1)b$	$a$
$v_8$	$(5t + 6)a + b$	$(6t + 6)a + (6t + 5)b$	$a + (5t + 6)b$
$v_9$	$(3t + 2)a + (4t + 1)b$	$5ta + (3t + 5)b$	$(3t + 6)a + (5t + 3)b$
$v_{10}$	$(t + 2)a + (5t + 1)b$	$(2t + 3)a + (3t + 3)b$	$(4t + 6)a + (3t + 3)b$
$v_{11}$	$6a + (4t + 1)b$	$(3t + 6)a + 5b$	$(3t + 6)a + 2tb$
$v_{12}$	$6ta + b$	$(6t + 2)a + (6t + 6)b$	$(6t + 2)a + 6b$
$v_{13}$	$6a + (6t + 6)b$	$a + b$	$a + 6tb$
$v_{14}$	$(3t + 4)a + (6t + 2)b$	$a + 5tb$	$(6t + 6)a + 6b$
$v_{15}$	$3a + (2t + 4)b$	$(5t + 3)a + 6b$	$(6t + 2)a + (3t + 4)b$
$v_{16}$	$5a + (2t + 3)b$	$(5t + 5)a + (3t + 5)b$	$(t + 1)a + (2t + 6)b$
$v_{17}$	$4a + (2t + 2)b$	$ta + (5t + 3)b$	$ta + (2t + 5)b$
$v_{18}$	$(6t + 1)b$	$(6t + 1)a$	$(6t + 1)a$

 Table 5.2: Values of  $v_k = l(\mu_0^{-1}g_k) \in H_1(\Sigma_3(K))$  for  $K \in \{K_1, K_2, K_3\}$ .

$\mathbb{Z}[\pi_1(X_K)]$  taking values in the set of  $3 \times 3$  matrices with  $\mathbb{Q}(\zeta_7)[t^{\pm 1}]$  coefficients. Let

$$\Psi = \left( \frac{\partial r_i}{\partial g_j} \right)_{i,j=1,\dots,18} \in \text{Mat}_{18}(\mathbb{Z}[\pi_1(X_K)])$$

be the Fox matrix for the Wirtinger presentation of  $\pi_1(X_K)$ . Every row in  $\Psi$  corresponds to a different relation in the Wirtinger presentation, with the relation  $g_i g_j g_i^{-1} g_k^{-1}$  contributing a row with  $1 - g_k$  in the  $i^{\text{th}}$  position,  $g_i$  in the  $j^{\text{th}}$  position,  $-1$  in the  $k^{\text{th}}$  position and zeros elsewhere. Write  $r(\Psi)$  for the reduced Fox matrix obtained by dropping the first row and column from  $\Psi$  and let  $r(\Psi_\chi)$  be the  $51 \times 51$  matrix obtained by applying  $\Phi_\chi$  to  $r(\Psi)$  entrywise. By [HKL10, Section 9], the reduced twisted Alexander polynomial  $\tilde{\Delta}_K^\chi(t)$  of  $(K, \chi)$  (for non-trivial  $\chi$ ) is given by

$$\tilde{\Delta}_K^\chi(t) = \frac{\det r(\Psi_\chi)}{(t - 1) \det(\varphi_\chi(g_1) - I)}.$$

Thus we obtain the 11 reduced twisted Alexander polynomials listed in Appendix C associated with our characters of interest.

### § 5.2.8 | Obstructing sliceness

To show that  $K_1$ ,  $K_2$  and  $K_3$  are not slice, we use the generalisation of the Fox–Milnor condition from Theorem 5.1.1, recalled below.

**Theorem 5.1.1** ([KL99, Proposition 6.1]). Let  $K \subset S^3$  be a slice knot and fix distinct primes  $p$  and  $q$ . Then there exists an invariant metaboliser  $N \subset H_1(\Sigma_p(K); \mathbb{Z})$  such that the following condition holds: for every character  $\chi : H_1(\Sigma_p(K); \mathbb{Z}) \rightarrow \mathbb{Z}_q$  that vanishes

on  $N$ , the associated reduced twisted Alexander polynomial  $\tilde{\Delta}_K^\chi(t) \in \mathbb{Q}(\zeta_q)[t^{\pm 1}]$  is a *norm*, that is,  $\tilde{\Delta}_K^\chi(t)$  can be written as

$$\tilde{\Delta}_K^\chi(t) = at^k f(t) \overline{f(t)}$$

for some  $a \in \mathbb{Q}(\zeta_q)$ ,  $k \in \mathbb{Z}$  and  $\overline{f(t)}$  obtained from  $f(t) \in \mathbb{Q}(\zeta_q)[t^{\pm 1}]$  by the involution  $t \mapsto t^{-1}$ ,  $\zeta_q \mapsto \zeta_q^{-1}$ .

Using the routine implemented in **SnapPy** [CDGW] for determining whether an element of  $\mathbb{Q}(\zeta_q)[t^{\pm 1}]$  is a norm, which relies on the **SageMath** algorithm for factoring polynomials over cyclotomic fields, we conclude via a calculation in the accompanying notebooks that none of the 11 polynomials in Appendix C are norms. This implies that  $K_1$ ,  $K_2$  and  $K_3$  are not slice.

## Part II

# On Stein-fillable genus one open books

# Preliminaries

---

In the second part of this thesis, we turn our attention to open book decompositions of contact 3-manifolds and the question of their Stein fillability. Our motivation for studying this topic comes in part from the paper [Lis14] of Lisca, devoted to open books with pages given by  $\Sigma_{1,1}$ , the genus one surface with one boundary component. Since  $\Gamma_{\Sigma_{1,1}}$ , the mapping class group of  $\Sigma_{1,1}$ , is isomorphic to the 3-braid group  $B_3$ , Lisca was able to use Murasugi's classification of 3-braids up to conjugacy [Mur74] together with Donaldson's theorem to show that if a Stein-fillable contact  $L$ -space  $(Y, \xi)$  is supported by an open book  $(\Sigma_{1,1}, \varphi)$ , then the monodromy  $\varphi$  admits a factorisation into positive Dehn twists. The goal of our joint work with Andy Wand [BW21], forming the basis of the following two chapters, was to probe this implication further for Stein-fillable contact manifolds supported by open books with genus one pages. Our main result, presented in Chapter 7, is a construction of a family of such contact manifolds  $(Y_n, \xi_n)$  for  $n \geq 0$ , each supported by an open book  $(\Sigma_{1,2}, \varphi_n)$  with  $\varphi_n$  admitting no factorisations into positive Dehn twists. These are the first known genus one examples of this kind. Together with the work of Baker, Etnyre and Van Horn-Morris [BEVHM10], Wand [Wan15] and Wendl [Wen10], this construction settles the question of correspondence between Stein fillings and positive factorisations of monodromies of supporting open books in all genera.

The purpose of this chapter is to give a brief summary of relevant definitions and facts about contact topology, as well as outline the relationship between Stein fillings and positive monodromy factorisations, in order to equip the reader for Chapter 7 that contains our main results. In Section 6.1 we define two ways of representing an open book decomposition of a 3-manifold, while in Section 6.2 we consider contact structures and their tight vs. overtwisted dichotomy. The short Section 6.3 states the Giroux correspondence of open books and contact structures. Concluding the chapter, Section 6.4 is devoted to the notion of symplectic fillability and its connection to the existence of positive monodromies, with a focus on Stein fillings.

## § 6.1 | Mapping class groups and open books

This section largely follows [Etn04, Appendix] and [ÖS04, Chapter 9]. Recall that for a compact oriented surface  $\Sigma$ , possibly with non-empty boundary, the *mapping class group* of  $\Sigma$ , written  $\Gamma_\Sigma$ , consists of isotopy classes of orientation-preserving self-diffeomorphisms of  $\Sigma$  that restrict to the identity on  $\partial\Sigma$ . We will generally confuse classes in  $\Gamma_\Sigma$  with their representatives.

Fix an orientation of  $\Sigma$  and consider a simple closed curve  $\gamma \subset \Sigma$  with a tubular neighbourhood  $N$ , choosing coordinates  $(\theta, t)$  on  $N$  such that  $\theta$  is the  $S^1$ -coordinate in the identification of  $\gamma$  with  $S^1$ ,  $t$  is the  $[0, 1]$ -coordinate, and  $\{\partial/\partial\theta, \partial/\partial t\}$  is an oriented basis for a trivialisation of  $N$ . Then the (*positive*) *Dehn twist about  $\gamma$* , written  $\tau_\gamma$ , is a self-diffeomorphism of  $\Sigma$  that fixes  $\Sigma \setminus N$  and is given on  $N$  by  $(\theta, t) \mapsto (\theta + 2\pi t, t)$ , smoothed along  $\partial N$ . The *negative Dehn twist about  $\gamma$*  is given by  $\tau_\gamma^{-1} \in \Gamma_\Sigma$ . If  $\gamma$  and  $\gamma'$  are isotopic, then so are  $\tau_\gamma$  and  $\tau_{\gamma'}$ . In [Lic62], Lickorish showed that any self-diffeomorphism of  $\Sigma$  can be written as a composition of Dehn twists about non-separating curves and boundary-parallel curves; we defer the discussion of specific presentations of  $\Gamma_\Sigma$  to Section 7.2.

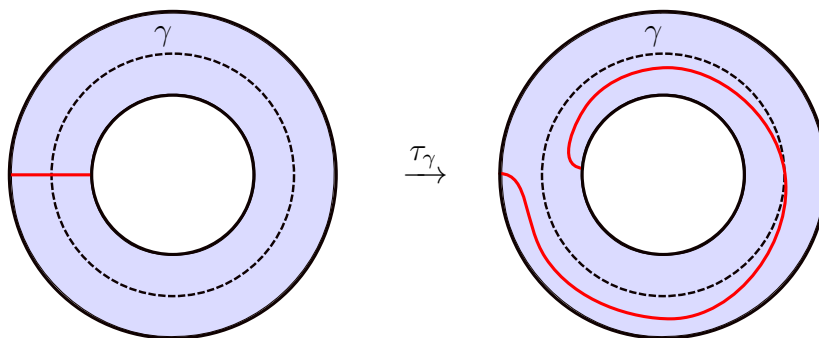


Figure 6.1: The effect of a Dehn twist about a curve  $\gamma$  on an arc across the neighbourhood of  $\gamma$ , shown in red.

Of particular interest to us will be the positive elements of  $\Gamma_\Sigma$ . Precisely, given  $\varphi \in \Gamma_\Sigma$ , we say that  $\varphi$  admits a *positive factorisation*, or simply is *positive*, if it can be written as a product of (positive) Dehn twists about essential simple closed curves in  $\Sigma$ . We denote by  $\Gamma_\Sigma^+$  the sub-monoid of  $\Gamma_\Sigma$  consisting of isotopy classes of positively factorisable maps.

**Remark 6.1.1.** Note that  $\Gamma_\Sigma^+$  can only be non-trivial when  $\partial\Sigma$  is non-empty: as pointed out in [FM11, Section 5.1.4], when  $\partial\Sigma = \emptyset$ , every element of  $\Gamma_\Sigma$  can be written as a product of positive Dehn twists.

Now let  $Y$  be a closed 3-manifold. We say that an *open book decomposition* (or simply *open book*) of  $Y$  is a pair  $(L, \pi)$  where  $L \subset Y$  is an oriented link, called the *binding*, and  $\pi : Y \setminus L \rightarrow S^1$  is a fibration such that for any  $s \in S^1$ ,  $\pi^{-1}(s)$  is the interior of a compact orientable surface  $\Sigma_\pi$  with  $\partial\Sigma_\pi = L$ ; the surface  $\Sigma_\pi$  is called

the *page*. Any locally trivial bundle over oriented  $S^1$  with the fibre  $\Sigma$  is canonically diffeomorphic to the fibration  $M_\varphi \rightarrow S^1$  for  $M_\varphi = [0, 1] \times \Sigma / (0, \varphi(x)) \sim (1, x)$  and  $\varphi$  an orientation-preserving self-diffeomorphism of  $\Sigma$ , taken up to conjugation. Hence, an open book decomposition  $(L, \pi)$  of a 3-manifold  $Y_{(L, \pi)}$  determines a mapping class  $\varphi_\pi \in \Gamma_{\Sigma_\pi}$ , called the *monodromy*. On the other hand, given a pair  $(\Sigma, \varphi)$  with  $\varphi \in \Gamma_\Sigma$  and  $\partial\Sigma \neq \emptyset$ , we may construct a closed 3-manifold  $Y_{(\Sigma, \varphi)}$  in the following way: take the mapping torus  $M_\varphi$ , identify all its boundary components with  $\bigsqcup_n S^1 \times S^1$  for some  $n > 0$ , where in each  $S^1 \times S^1$  the first factor comes from the quotient of the unit interval and the second from  $\partial\Sigma$ , and glue in solid tori  $\bigsqcup_n D^2 \times S^1$  via the identity map  $\bigsqcup_n \partial D^2 \times S^1 \rightarrow \bigsqcup_n S^1 \times S^1$ . The resultant closed 3-manifold  $Y_{(\Sigma, \varphi)}$  admits an open book decomposition with the binding given by the cores  $\bigsqcup_n \{0\} \times S^1$  of the solid tori, the page  $\Sigma$  and monodromy  $\varphi$ . Hence, we can pass between  $(L, \pi)$  and  $(\Sigma, \varphi)$  to determine an open book decomposition of a closed 3-manifold up to diffeomorphism.

## § 6.2 | Contact structures

We now proceed to discuss the basics of contact geometry in a three-dimensional setting, introducing the notion of a contact structure and establishing the dichotomy between tight and overtwisted contact structures. Our main source for the following standard material is [Gei08, Chapters 1 and 2].

For the rest of the section, let  $Y$  be a smooth orientable 3-manifold. Suppose that  $\xi$  is a smooth codimension one sub-bundle of the tangent bundle  $TY$ , also called a *plane distribution*. It is convenient to think of  $\xi$  as a “plane field” such that the planes attached to corresponding points of  $Y$  twist smoothly as one follows along some path in  $Y$ . One can show that in a small neighbourhood of any point,  $\xi$  is given by the kernel of a differential 1-form  $\alpha \in \Omega^1(Y)$ . Moreover, if  $\xi$  is co-orientable (that is, the line bundle  $\xi^\perp$  is trivial), then  $\xi = \ker \alpha$  globally for some  $\alpha \in \Omega^1(Y)$ . This leads us to the following definition.

**Definition 6.2.1.** A (*positive*) *contact structure*  $\xi = \ker \alpha$  on  $Y$  is a co-orientable plane distribution that is totally non-integrable, that is,  $\alpha \wedge d\alpha > 0$  everywhere.<sup>1</sup>

Every smooth closed orientable 3-manifold admits a contact structure [Mar71]. Call  $Y$  equipped with a contact structure  $\xi$  a *contact manifold*, written  $(Y, \xi)$ ; we will always tacitly assume that a co-orientation is chosen on  $\xi$ . Note that since a contact structure defines a volume form  $\alpha \wedge d\alpha \in \Omega^3(Y)$ , it also defines an orientation of  $Y$ . Consequently, one may need to be careful when considering contact structures on chiral 3-manifolds (that is, those admitting orientation-reversing self-diffeomorphisms), such as lens spaces  $L(p, q)$  with  $q^2 \equiv -1 \pmod p$  [Hem76, Example 3.22].

We are bound by tradition to provide the following two examples of contact structures on  $\mathbb{R}^3$ . Let  $(x, y, z)$  be the Euclidean coordinates on  $\mathbb{R}^3$  and define  $\alpha := dz - ydx$ .

<sup>1</sup>One can also consider *negative* contact structures where  $\alpha \wedge d\alpha < 0$ , however, we will not do that.

Then  $\alpha \wedge d\alpha = dx \wedge dy \wedge dz$  is the standard volume form on  $\mathbb{R}^3$ , so  $\xi_{\text{std}} = \ker \alpha$  is a contact structure; call  $(\mathbb{R}^3, \xi_{\text{std}})$  the *standard contact*  $\mathbb{R}^3$ . Now consider cylindrical coordinates  $(r, \theta, z)$  on  $\mathbb{R}^3$  and define  $\xi_{\text{ot}} := \ker(\cos r dz + r \sin r d\theta)$ , which is also straightforwardly verified to be a contact structure. Some contact planes of  $\xi_{\text{std}}$  and  $\xi_{\text{ot}}$  at  $z = 0$  are illustrated in Figure 6.2, courtesy of Patrick Massot.

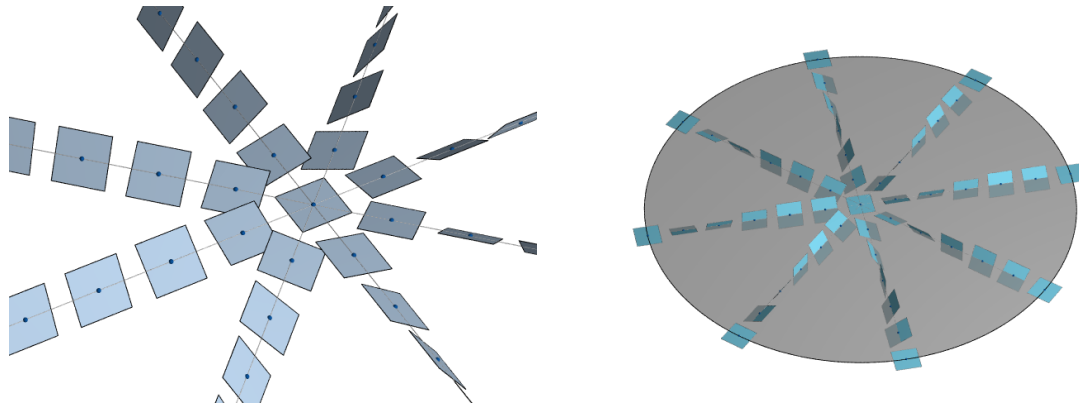


Figure 6.2: Contact planes at  $z = 0$  of  $\xi_{\text{std}}$  (left) and  $\xi_{\text{ot}}$  (right).

Another manifold we will require is the *standard contact 3-sphere*  $(S^3, \xi_{\text{std}})$ . Consider  $S^3 \subset \mathbb{R}^4$  with Euclidean coordinates  $(x_1, y_1, x_2, y_2)$  on  $\mathbb{R}^4$  and define

$$\alpha := x_1 dy_1 - y_1 dx_1 + x_2 dy_2 - y_2 dx_2.$$

Writing  $r$  for the radial coordinate on  $\mathbb{R}^4$  (that is,  $r^2 = x_1^2 + y_1^2 + x_2^2 + y_2^2$ ), we see that  $r dr \wedge \alpha \wedge d\alpha > 0$  for  $r > 0$ . Since  $S^3$  is a submanifold of  $\mathbb{R}^4$  obtained by setting  $r = 1$ , we have that  $\xi_{\text{std}} = \ker \alpha|_{r=1}$  is a contact structure on  $S^3$ . The contact planes of  $\xi_{\text{std}}$  are everywhere perpendicular to the fibres of the Hopf fibration of  $S^3$ .

We say that two contact manifolds  $(Y, \xi)$  and  $(Y', \xi')$  are *contactomorphic* if there exists a diffeomorphism  $f : Y \rightarrow Y'$  such that  $f^* \xi' = \xi$ ; if  $Y = Y'$ , say that  $\xi$  and  $\xi'$  are *isomorphic*. For instance, one can show that  $(S^3, \xi_{\text{std}})$  with one point removed is contactomorphic to  $(\mathbb{R}^3, \xi_{\text{std}})$ . However, it was first shown by Bennequin [Ben83] that  $(\mathbb{R}^3, \xi_{\text{std}})$  and  $(\mathbb{R}^3, \xi_{\text{ot}})$  are not contactomorphic. This is somewhat surprising in view of the well-known *Darboux' theorem* that states that for any point  $p \in (Y, \xi)$  in some contact manifold, there exists a neighbourhood of  $p$  contactomorphic to a neighbourhood of the origin in  $(\mathbb{R}^3, \xi_{\text{std}})$ . In particular, Bennequin's result implies that contact structures may possess non-trivial global properties even though locally they all look the same. One such property possessed by  $(\mathbb{R}^3, \xi_{\text{ot}})$  is the existence of an embedded disc  $D$  such that the tangent planes along  $\partial D$  coincide with the contact planes (for example, consider the disc  $\{r \leq \pi, z = 0\}$  shown in grey in Figure 6.2).

**Definition 6.2.2.** A contact manifold  $(Y, \xi)$  is *overtwisted* if it contains an embedded disc  $D$  with  $\xi|_p = T_p D$  for all  $p \in \partial D$ . Such disc is also called *overtwisted*. If a contact manifold is not overtwisted, then it is *tight*.

No overtwisted discs exist in  $(\mathbb{R}^3, \xi_{\text{std}})$  or  $(S^3, \xi_{\text{std}})$ , so these manifolds are tight. The contraposition of tight and overtwisted contact manifolds is of fundamental importance in contact topology. In broad strokes, for a given closed contact manifold, overtwisted contact structures are easy to classify in view of a result by Eliashberg [Eli89], but tight contact structures might be very diverse, surprising and require a bespoke approach to their study. Let us now briefly lay out some background required to explain Eliashberg's result.

We say that two contact structures  $\xi_0$  and  $\xi_1$  on  $Y$  are *isotopic* if there exists a smooth family of contact structures  $\{\xi_t : t \in [0, 1]\}$ . If  $\xi_0$  and  $\xi_1$  are isotopic and  $Y$  is closed, *Gray's theorem* [Gra59] states that there exists a smooth family  $\{f_t : t \in [0, 1]\}$  of self-diffeomorphisms of  $Y$  with  $f_0 = \text{id}$  and  $(f_t)_*\xi_0 = \xi_t$  for all  $t \in [0, 1]$ . In particular, existence of an isotopy from  $\xi_0$  to  $\xi_1$  on a closed  $Y$  implies the existence of a contactomorphism  $(Y, \xi_0) \rightarrow (Y, \xi_1)$ .

**Theorem 6.2.3** ([Eli89]). Let  $\Xi_{\text{ot}}(Y)$  be the space of overtwisted contact structures on a closed smooth orientable 3-manifold  $Y$  and let  $\text{Distr}(Y)$  be the space of co-oriented plane distributions on  $Y$ . Then the inclusion map  $\Xi_{\text{ot}}(Y) \hookrightarrow \text{Distr}(Y)$  induces a bijection on path components.

This statement implies that every co-oriented plane field on a closed  $Y$  is homotopic to an overtwisted contact structure, and any two overtwisted contact structures which are homotopic as plane fields, are homotopic (hence, by an application of Gray's theorem and some additional results from differential topology<sup>2</sup>, isotopic) via overtwisted contact structures. Hence, the task of classifying overtwisted contact structures up to isotopy can be reduced to considering homotopy classes of appropriate plane fields. Specifically, homotopy classes of such plane fields for  $Y$  with chosen orientation correspond to homotopy classes of maps  $Y \rightarrow S^2$ . Thus, for example, the space of non-isotopic overtwisted contact structures on  $S^3$  is parameterised by  $\pi_0(\text{Map}(S^3 \rightarrow S^2)) = \pi_3 S^2 \cong \mathbb{Z}$ .

On the other hand, tight contact structures generally are harder to approach. To begin with, not all 3-manifolds admit tight contact structures: a counterexample is  $\overline{\Sigma(2, 3, 5)}$ , the Poincaré homology sphere with reversed orientation [EH99]. Moreover, it is not sufficient for the purposes of classifying tight contact structures to know their homotopy type as plane fields: Giroux has shown that there exist tight contact structures on the 3-torus  $T^3$  that are homotopic as plane fields but not isomorphic [Gir94], while Eliashberg and Polterovich exhibited further examples on  $T^3$  that are homotopic as plane fields and isomorphic, but not isotopic [EP94]. Here is a collection of some important results concerning the classification of tight contact structures up to isotopy that are currently available:

- each one of  $S^3$ ,  $\mathbb{R}^3$  and  $S^1 \times S^2$  carries a unique tight contact structure;

---

<sup>2</sup>Cf. footnote on [Gei08, p. 206]

- there exists a classification of tight contact structures on  $S^1 \times D^2$ ,  $T^2 \times I$  and lens spaces  $L(p, q)$  [Hon00a], as well as torus bundles over the circle and circle bundles over closed surfaces [Hon00b];
- classification results have been obtained for various small Seifert fibred spaces [Ghi05b; GLS06; Mat18; Tos20].

In Section 6.4 we will see that a contact manifold being tight is a particularly important property for its symplectic fillability. Before that, however, we seek to marry contact structures and open book decompositions via a crucial result of Giroux.

### § 6.3 | Giroux correspondence

Let  $Y$  be a closed smooth orientable 3-manifold and fix an open book  $(L, \pi)$  of  $Y$ . We say that a contact structure  $\xi = \ker \alpha$  on  $Y$  is *supported* by  $(L, \pi)$  if  $d\alpha$  induces a positive area form on the interior of every page that, in turn, induces the given orientation of  $L$ , and  $\alpha$  induces a positive volume form on  $L$ . As first shown by Thurston and Winkelnkemper [TW75], one can always construct a contact structure supported by  $(L, \pi)$ . For example, a page–monodromy representation of an open book supporting  $(S^3, \xi_{\text{std}})$  is given by  $(H_+, \tau_\alpha)$ , where  $H_+$  is the oriented planar surface spanned by the positive Hopf link and  $\tau_\alpha$  is the Dehn twist about its core. A natural question to ask now is if contact structures similarly give rise to open books. The following theorem of Giroux gives the affirmative answer up to certain notions of equivalence.

**Theorem 6.3.1** ([Gir02]). There exists a bijective correspondence

$$\left\{ \frac{\text{contact structures on } Y}{\text{isotopy}} \right\} \longleftrightarrow \left\{ \frac{\text{open book decompositions of } Y}{\text{positive stabilisation}} \right\}.$$

Here by *(positive) stabilisation* we mean the following operation: represent the open book by a page–monodromy pair  $(\Sigma, \varphi)$ , add a 1-handle to  $\Sigma$  and pre-compose  $\varphi$  with a (positive) Dehn twist  $\tau_\gamma$  about some simple closed curve  $\gamma \subset \Sigma$  that intersects the co-core of the 1-handle exactly once.

The easier direction of the proof is showing that if a stabilisation of  $(\Sigma, \varphi)$  yields an open book  $(\Sigma', \varphi')$ , then they support respective contact manifolds  $(Y, \xi)$  and  $(Y, \xi')$  with  $\xi$  isotopic to  $\xi'$ . The opposite direction that involves the construction of open books supporting a given contact structure, however, is rather non-trivial and depends on the theory of convex surfaces. Expository accounts of the proof can be found in [Etn04] and [Goo05].

The main consequence of the Giroux correspondence is that it enables us to consider questions of contact and symplectic geometry through a powerful lens of surface mapping class groups that on many occasions yields remarkable insights, hardly accessible by geometric methods alone.

## § 6.4 | Symplectic fillability

We have already seen in the case of links and their Seifert surfaces that considering our objects of interest as boundaries of other objects may be fruitful in the study of both. Thus, a natural question when faced with a contact manifold is whether it is a boundary of a symplectic manifold in some compatible way. We now discuss some of the ways of making that question precise.

Recall that a *symplectic manifold*  $(X, \omega)$  is an oriented 4-manifold  $X$  together with a closed 2-form  $\omega$ , called a *symplectic form*, that satisfies the condition  $\omega \wedge \omega > 0$ . A contact manifold  $(Y, \xi)$  is (*weakly*) *symplectically fillable* if there exists a compact symplectic manifold  $(X, \omega)$  such that  $Y = \partial X$  and  $\omega|_{\xi} > 0$ . For all types of fillability considered, we often omit the adverb ‘symplectically’ and call the respective  $(X, \omega)$  bounded by  $(Y, \xi)$  a (*symplectic*) *filling*. A crucial property of fillable contact manifolds is that they must be tight, as proved by Gromov [Gro85] and Eliashberg [Eli90a].

Say that  $(Y, \xi)$  is *strongly symplectically fillable* if its filling  $(X, \omega)$  also satisfies the condition that there exists a vector field  $v$  defined near  $\partial X$  such that  $v$  points transversely outwards from  $\partial X$ , and the flow of  $v$  dilates  $\omega$  (that is, the Lie derivative of  $\omega$  along  $v$  gives a positive multiple of  $\omega$ ). If, moreover,  $v$  is defined everywhere on  $(X, \omega)$ , then  $(Y, \xi)$  is *exactly symplectically fillable*. Now recall that a *Stein surface* is a complex surface  $W$  endowed with a Morse function  $f : W \rightarrow \mathbb{R}$  such that for any non-critical point  $c$  of  $f$ , the level set  $f^{-1}(c)$  inherits a contact structure  $\xi_c$ , induced by the complex tangencies, that orients  $f^{-1}(c)$  as when  $f^{-1}(c)$  is viewed as the boundary of the complex manifold  $X = f^{-1}((-\infty, c])$ ; the manifold  $X$  is called a *Stein domain* (for a discussion of equivalent definitions, see [Gom98]). A Stein surface admits a symplectic form  $\omega$  that induces  $\xi_c$  on  $f^{-1}(c)$  for all non-critical  $c$ . We say that a contact manifold  $(Y, \xi)$  is *Stein-fillable* if  $Y$  is orientation-preserving diffeomorphic to such  $f^{-1}(c)$  and  $\xi$  is isotopic to  $\xi_c$ .

We have the following sequence of implications:

$$\begin{aligned}
 & (Y, \xi) \text{ is Stein-fillable} \\
 & \xrightarrow{\text{(a)}} (Y, \xi) \text{ is exactly fillable} \\
 & \xrightarrow{\text{(b)}} (Y, \xi) \text{ is strongly fillable} \\
 & \xrightarrow{\text{(c)}} (Y, \xi) \text{ is weakly fillable} \\
 & \xrightarrow{\text{(d)}} (Y, \xi) \text{ is tight.}
 \end{aligned}$$

These different notions of fillability pointedly illustrate the diversity of symplectic fillings since none of the converses of implications (a)–(d) hold: for (b), Ghiggini has exhibited contact structures on  $1/(n+1)$  surgeries on the trefoil in  $S^3$  that are strongly but not exactly fillable [Ghi05a]; for (a), Bowden built on Ghiggini’s examples to show that there exist exactly fillable contact manifolds that are not Stein-fillable [Bow12];

for (c), Eliashberg has exhibited weakly but not strongly fillable contact structures on  $T^3$  [Eli96]; and for (d), Etnyre and Honda were the first to prove the existence of tight non-fillable contact manifolds [EH02].

Being the strongest common notion of fillability, Stein fillability is also the one most accessible with the tools of surface mapping class group theory. In order to see precisely how, we briefly digress to discuss Lefschetz fibrations.

Let  $X$  be an orientable 4-manifold and  $S$  a compact connected surface, with  $\partial S$  possibly non-empty. A *Lefschetz fibration* on  $X$  is a singular fibre bundle  $\pi : X \rightarrow S$  with finitely many critical points  $\{x_1, \dots, x_n\} \subset X$  such that near each critical point,  $\pi$  is given, in complex coordinates, by  $\pi(z_1, z_2) = z_1^2 + z_2^2$ . Each fibre containing a critical point  $\pi^{-1}(\pi(x_i))$  is an immersed surface called a *singular fibre*; all other fibres are *regular*. If the complex orientation in the local model near a critical point  $x_i$  agrees with that of  $X$ , call  $x_i$  a *positive singularity*, and call it a *negative singularity* otherwise; say that  $\pi$  is *positive* if all singularities are positive. There is a convenient way of describing singular fibres in a Lefschetz fibration: Suppose that  $x_i$  is the only critical point in a singular fibre  $\Sigma'$ , take an arc  $\gamma \subset S$  from a nearby regular fibre  $\Sigma$  to  $\Sigma'$ , and consider a totally real disc  $D$  containing  $x_i$  and lying over  $\gamma$  in a local chart around  $x_i$ ; the disc  $D$  is called the *Lefschetz thimble* of  $x_i$ , and  $v := \partial D \subset \Sigma$  is the *vanishing cycle* of  $x_i$ . Then  $\Sigma'$  is obtained from  $\Sigma$  by collapsing  $v$  to a point. Further, let  $X_{x_i}$  be the preimage of a small neighbourhood of  $\gamma \subset S$  under  $\pi$ . Then the preimage of  $\partial X_{x_i}$  is a fibre bundle over  $S^1$  with fibre  $\Sigma$  and monodromy  $\varphi_i$  given by a single positive Dehn twist about  $v$  if  $x_i$  is positive, or a negative Dehn twist if  $x_i$  is negative. If  $S = D^2$  and  $p_i = \pi(x_i)$  are distinct for all  $i$ , choose a regular fibre  $\pi^{-1}(p_0)$  and embedded arcs  $a_1, \dots, a_n \subset D^2$  joining  $p_0$  to  $p_1, \dots, p_n$ , ordered anticlockwise and disjoint except at  $p_0$ . The total monodromy of the Lefschetz fibration is then  $\varphi = \varphi_n \circ \dots \circ \varphi_1$ ; furthermore, the fibration is fully determined, up to diffeomorphism, by the collection  $(\varphi_1, \dots, \varphi_n)$ , up to cyclic permutation, conjugation of all  $\varphi_i$  by a fixed element of  $\Gamma_\Sigma$ , and different choices of arcs (which, in turn, are related by so-called *Hurwitz moves*). Finally, we say that a Lefschetz fibration is *allowable* if the associated vanishing cycle of every critical point is homologically essential in  $\Sigma$ .

Now, given a positive allowable Lefschetz fibration (PALF)  $\pi : X \rightarrow D^2$  with regular fibre  $\Sigma$  satisfying  $\partial \Sigma \neq \emptyset$ , and monodromy  $\varphi$ , we can realise it by attaching 2-handles to  $D^2 \times \Sigma$  along knots given by the vanishing cycles with framing  $-1$  with respect to the page framing. Then  $\partial X$  admits an open book decomposition  $(\Sigma, \varphi)$ . Moreover, by work of Eliashberg [Eli90b] and Gompf [Gom98],  $X$  is a Stein domain. Loi and Piergallini [LP01] and, independently, Akbulut and Özbağcı [AÖ01], have shown that the converse holds: every Stein domain admits a PALF structure over  $D^2$ . Also, Plamenevskaya has proved that for a given Stein domain  $X$ , the contact structure induced on  $\partial X$  by the Stein structure is supported by the open book on  $\partial X$  induced by the corresponding PALF structure over  $D^2$  [Pla04]. Note that if the monodromy of

an open book contains Dehn twists about null-homologous curves in the page  $\Sigma$ , we can replace them with positive twists about homologically essential curves via relations in  $\Gamma_\Sigma$  (see Section 7.2). A combination of these facts implies the following theorem of Giroux, originally derived somewhat differently.

**Theorem 6.4.1** ([Gir02]). A contact manifold  $(Y, \xi)$  is Stein-fillable if and only if it is supported by an open book  $(\Sigma, \varphi)$  with  $\varphi \in \Gamma_\Sigma^+$  (that is,  $\varphi$  factorises as a product of positive Dehn twists).

Even in view of this result, however, the outlook for classifying Stein-fillable manifolds is complicated: for example, proving that a contact manifold is not Stein-fillable this way entails the usually intractable task of obstructing positive factorisability of *all* monodromies of supporting open books. A tempting but untrue strengthening of Theorem 6.4.1 would be the claim that the monodromy of *every* open book  $(\Sigma, \varphi)$  supporting a Stein-fillable contact manifold  $(Y, \xi)$  factorises positively. Indeed, a result of Wendl [Wen10] implies that if the genus  $g(\Sigma) = 0$ , then Stein fillings of  $(Y, \xi)$ , up to symplectic deformation, are in one-to-one correspondence with positive factorisations of  $\varphi$ , up to conjugation. However, if  $g(\Sigma) \geq 2$ , it follows from the work of Wand [Wan15] and Baker, Etnyre and Van Horn-Morris [BEVHM10] that  $\varphi$  need not admit any positive factorisation. As noted in the opening of the chapter, the case of  $g(\Sigma) = 1$  has been studied by Lisca [Lis14] who has shown that if  $\Sigma$  has one boundary component and  $Y$  is a Heegaard Floer  $L$ -space, then  $(Y, \xi)$  is Stein-fillable if and only if  $\varphi$  admits a positive factorisation. The following chapter is dedicated to showing that there exists no correspondence between Stein fillings and positive factorisations of the monodromy for  $g(\Sigma) = 1$ , ultimately demonstrating that the above strengthening does not hold for all genera  $g(\Sigma) \geq 1$ .

# Non-positive Stein-fillable open books of genus one

---

In this chapter we construct an infinite family of Stein-fillable contact 3-manifolds  $(Y_n, \xi_n)$  for  $n \geq 0$  that are supported by genus one open books  $(\Sigma_{1,2}, \varphi_n)$  such that  $\varphi_n$  does not admit a factorisation into a product of positive Dehn twists. Our starting point will be the open book  $(\Sigma_{1,2}, \varphi_0)$  for a Stein-fillable contact manifold  $(Y_0, \xi_0)$ , with  $Y_0$  diffeomorphic to the lens space  $L(5, 1)$ , which we are going to obtain using Conway's techniques from [Con19b]. The rest of  $(Y_n, \xi_n)$  are consequently obtained by Legendrian surgery on a binding component of  $(\Sigma_{1,2}, \varphi_0)$ . The proof that  $\varphi_n$  does not positively factorise for any  $n \geq 0$  then hinges on some observations about lantern relations in the mapping class group of  $\Sigma_{1,2}$  together with results of Lisca and Lecuona [LL11] on Stein fillability of contact Seifert fibred spaces.

Section 7.1 is devoted to constructing all  $(Y_n, \xi_n)$  via transverse contact surgery and demonstrating their Stein fillability. Then, in Section 7.2, we show that none of the  $\varphi_n$  have any positive factorisations.

## § 7.1 | The family $(Y_n, \xi_n)$

Recall that an oriented knot  $K \subset (Y, \xi)$  is *Legendrian* (respectively, *transverse*) if its oriented tangent vector is everywhere contained in the contact planes (respectively, is everywhere positively transverse to the contact planes). *Contact  $r$ -surgery* on a Legendrian knot  $K \subset (Y, \xi)$  amounts to first performing Dehn surgery along  $K$  with surgery coefficient  $r$  given with respect to the contact framing, then extending the contact structure over the surgery torus to obtain another contact manifold.<sup>1</sup> The special case of  $r = -1$  is called *Legendrian surgery*. Analogously, by *transverse surgery* on  $K$  we mean an extension of topological surgery to the contact category, defined by Gay [Gay02], in which we first cut out, then re-glue a contact neighbourhood of a transverse knot  $K$  to obtain a new contact manifold; *admissible* transverse surgery is characterised by 'removing the twisting' near the knot, while *inadmissible* transverse

---

<sup>1</sup>The result of contact surgery is fully determined by  $(Y, \xi)$ ,  $K$  and  $r$  when  $r = 1/k$  for  $k \in \mathbb{Z}$ ; otherwise, there are choices involved.

surgery ‘adds the twisting’. In this section, we first introduce these two varieties of transverse surgery with the purpose of constructing the  $(Y_n, \xi_n)$  family. Then, we follow [Con19b, Section 3] to carry out the construction and show that all resultant contact manifolds are Stein-fillable.

### § 7.1.1 | Transverse contact surgery

This subsection is based on the accounts of transverse contact surgery in [BE13, Section 2] and [Con19a, Section 2.3]. Consider  $S^1 \times \mathbb{R}^2$  endowed with the contact structure  $\xi_{\text{rot}} = \ker(\cos r \, dz + r \sin r \, d\theta)$ , where  $z$  is the  $S^1$ -coordinate and  $(r, \theta)$  are standard polar coordinates on  $\mathbb{R}^2$ . For short, we write  $\{r \leq R\}$  for the solid torus  $S^1 \times \{(r, \theta) : r \leq R\}$ . Similarly, write  $\{r = R\}$  for the torus of radius  $R$ . Let  $K \subset (Y, \xi)$  be a transverse knot in some closed contact manifold. By the contact neighbourhood theorem [Gei08, Theorem 2.5.8], a tubular neighbourhood of  $K$  can be identified with a contactomorphic  $\{r \leq a\}$  inside  $(S^1 \times \mathbb{R}^2, \xi_{\text{rot}})$  for some  $a > 0$ , where  $K$  maps onto the  $z$ -axis and a framing of  $K$  against which all slopes will be measured is given by  $\lambda = S^1 \times \{(a, 0)\}$ . Fixing  $r_0 > 0$ , we find that  $\{r = r_0\}$  is a torus of slope  $-\cot r_0/r_0$ , that is, the foliation induced on  $\{r = r_0\}$  by  $\xi_{\text{rot}}$  is given by parallel lines with slope  $-\cot r_0/r_0$ . (Note that multiple  $r_0$  can yield the same slope.)

To perform *admissible transverse  $p/q$ -surgery*, take a torus of slope  $p/q \in \mathbb{Q}$  inside  $\{r \leq a\}$ , remove the interior of the corresponding solid torus of the same slope, and perform a *contact cut* on the boundary (that is, quotient the boundary by the  $S^1$ -action of translation along the leaves of slope  $a$ ; see [Ler01] for more details) to obtain a smooth manifold with a well-defined contact structure. For *inadmissible contact surgery*, first remove  $\{r < b\}$  for some  $b \leq a$ , then glue in a thickened torus layer  $T^2 \times I = \{r_0 \leq r \leq b + 2\pi\}$  via the identification of  $\{r = b + 2\pi\}$  with  $\partial(Y \setminus \{r < b\})$ , choosing  $r_0$  such that the new boundary  $\{r = r_0\}$  has slope  $p/q$ . A contact cut on this new boundary gives the result of inadmissible transverse  $p/q$ -surgery.

### § 7.1.2 | Open books for transverse-surgered manifolds

Now, we collect necessary ingredients from [Con19b] to describe open books supporting the result of inadmissible transverse surgery on a knot that is a component of the binding of some open book supporting the original manifold.

Suppose  $(\Sigma, \varphi)$  is an open book and  $\Sigma$  has a boundary component  $K$ , forming a part of the binding. In the following, by ‘stabilising  $K$ ’ we mean adding a 1-handle with the attaching sphere on  $K$  and pre-composing the monodromy with a positive Dehn twist about a curve that is boundary-parallel to one of the two boundary components into which  $K$  was split. After that, we continue denoting by  $K$  the other boundary component, without a twist about it.

Recall that given a rational number  $r < 0$ , we can write it as a negative continued

fraction  $[a_1 + 1, a_2, \dots, a_n]^-$ , where

$$r = a_1 + 1 - \frac{1}{a_2 - \frac{1}{\dots - \frac{1}{a_n}}}$$

and  $a_i \leq -2$  for all  $i$ . The following two propositions give the desired procedure for passing from transverse surgery descriptions of contact manifolds to their open books.

**Proposition 7.1.1** ([Con19b, Proposition 3.9]). Let  $r < 0$  be a rational number such that  $r = [a_1 + 1, a_2, \dots, a_n]^-$ . The open book supporting admissible transverse  $r$ -surgery with respect to the page slope on the binding component  $K$  is obtained by, for each  $i = 1, \dots, n$  in order, stabilising  $K$  positively  $|a_i + 2|$  times and adding a positive Dehn twist about  $K$ .

**Proposition 7.1.2** ([Con19b, Proposition 3.12]). Let  $r = p/q > 0$  be a rational number, fix a positive integer  $n$  such that  $1/n < r$ , and set  $r' = p/(q - np)$ . The open book supporting inadmissible transverse  $r$ -surgery with respect to the page slope on the binding component  $K$  is obtained by first adding  $n$  negative Dehn twists about  $K$ , and then performing admissible transverse  $r'$ -surgery on  $K$ .

**§ 7.1.3 | Transverse +5-surgery on a right-handed trefoil**

Consider a transverse right-handed trefoil knot  $T$  in  $(S^3, \xi_{\text{std}})$ , where  $\xi_{\text{std}}$  is the standard tight contact structure on  $S^3$ . By stabilising the standard open book for  $(S^3, \xi_{\text{std}})$  given by the positive Hopf band, we can take  $T$  to be the binding of an open book  $(\Sigma_{1,1}, \tau_\alpha \tau_\beta)$  with one-holed torus pages supporting  $(S^3, \xi_{\text{std}})$ ; this open book is shown on the left of Figure 7.1.

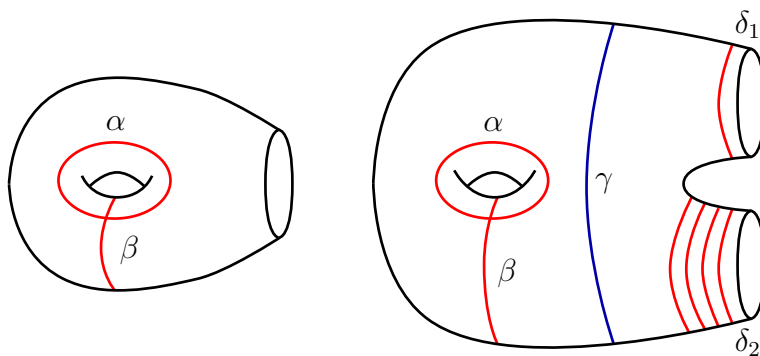


Figure 7.1: On the left: an open book  $(\Sigma_{1,1}, \tau_\alpha \tau_\beta)$  that supports  $(S^3, \xi_{\text{std}})$ . On the right: an open book  $(\Sigma_{1,2}, \tau_\alpha \tau_\beta \tau_\gamma^{-1} \tau_{\delta_1} \tau_{\delta_2}^4)$  that supports  $(Y_0, \xi_0)$ , the result of inadmissible transverse +5-surgery on a right-handed trefoil in  $(S^3, \xi_{\text{std}})$ .

In the notation of Proposition 7.1.2, we have  $r = p/q = 5/1$ . Choosing  $n = 1$ , we get that  $r' = -5/4 = [-3 + 1, -2, -2, -2]^-$ . Hence, an open book supporting

$(Y_0, \xi_0)$ , the product of inadmissible transverse  $+5$ -surgery on  $T$ , is obtained by adding a negative boundary twist  $\tau_\gamma^{-1}$  to the monodromy, stabilising once, adding a twist about  $K$ , then adding three more twists about  $K$ . Renaming  $K$  to  $\delta_2$  and the other boundary component to  $\delta_1$ , we conclude that  $(Y_0, \xi_0)$  is supported by the open book  $(\Sigma_{1,2}, \varphi_0)$  shown in Figure 7.1 with  $\varphi_0 = \tau_\alpha \tau_\beta \tau_\gamma^{-1} \tau_{\delta_1} \tau_{\delta_2}^4$ . Now, since  $r > 2g(\Sigma_{1,1}) = 2$  and  $(\Sigma_{1,1}, \tau_\alpha \tau_\beta)$  supports the Stein-fillable contact manifold  $(S^3, \xi_{\text{std}})$  with the *Ozsváth–Szabó contact invariant*  $c(\xi_{\text{std}}) \neq 0$  [OS05], we have that  $c(\xi_0) \neq 0$  and hence  $(Y_0, \xi_0)$  is tight [HP13, Theorem 1.2].

Figure 7.2 shows via a sequence of blow-ups, isotopies and blow-downs of Kirby diagrams (see [GS99, Chapter 5]), that  $Y_0$  can be obtained by topological  $-5$ -surgery on the unknot in  $S^3$  and thus is diffeomorphic to the lens space  $L(5, 1)$ . (We remark that Moser has classified all topological surgeries on torus knots yielding lens spaces in [Mos71].) By work of McDuff [McD90] and Plamenevskaya and Van Horn-Morris [PVHM10], any tight contact structure on  $L(p, 1)$  with  $p \neq 4$  has a unique Stein filling, hence so does  $(Y_0, \xi_0)$ .

Finally, recall from, for example, [Etn04, Theorem 5.7], the following fact about Legendrian surgery: if  $K$  is a knot in a contact manifold that lies in a page of some supporting open book  $(\Sigma, \varphi)$  and  $K$  is boundary-parallel to the binding component  $\delta$ , then the contact manifold obtained by Legendrian surgery on  $K$  is supported by the open book  $(\Sigma, \varphi \circ \tau_\delta)$ . Thus, we observe that  $(Y_n, \xi_n)$ , the product of  $n$ -fold Legendrian surgery on the  $\delta_2$  component of  $(\Sigma_{1,2}, \varphi_0)$ , is supported by the open book  $(\Sigma_{1,2}, \varphi_n)$ , where  $\varphi_n = \tau_\alpha \tau_\beta \tau_\gamma^{-1} \tau_{\delta_1} \tau_{\delta_2}^{4+n}$ . Since Legendrian surgery preserves Stein fillability [Eli90b; Wei91], this yields an infinite family of Stein-fillable contact manifolds  $\{(Y_n, \xi_n) : n \geq 0\}$  with each  $(Y_n, \xi_n)$  supported by  $(\Sigma_{1,2}, \varphi_n)$ .

## § 7.2 | Non-positivity of $\varphi_n$

The purpose of this section is to show that the mapping classes  $\varphi_n \in \Gamma_{\Sigma_{1,2}}$  do not admit positive factorisations into Dehn twists for  $n \geq 0$ .

Luo, building on work of Gervais [Ger96], showed in [Luo97] that the mapping class group  $\Gamma_\Sigma$  of a compact oriented surface  $\Sigma$  admits a presentation in which generators are Dehn twists, and all relations are supported in sub-surfaces homeomorphic to either  $\Sigma_{1,1}$  or  $\Sigma_{0,4}$ . Precisely, let  $\mathcal{S}(\Sigma)$  be the set of isotopy classes of simple loops in  $\Sigma$  and write  $I(\alpha, \beta) = \min\{|a \cap b| : a \in \alpha, b \in \beta\}$ , where  $\cap$  denotes geometric intersection. Also, write  $\partial(\alpha, \beta)$  for the boundary of a small regular neighbourhood  $N(a \cup b)$  of the union of minimally intersecting curves  $a \in \alpha$  and  $b \in \beta$ . We have  $N(a \cup b)$  homeomorphic to  $\Sigma_{1,1}$  when  $I(\alpha, \beta) = 1$ , and homeomorphic to  $\Sigma_{0,4}$  when  $I(\alpha, \beta) = 2$  with algebraic intersection number  $\alpha \cdot \beta = 0$ ; in the latter case, denote by  $\tau_{\partial(\alpha\beta)}$  the composition of Dehn twists about all boundary components of  $N(a \cup b)$ . Also denote by  $\tau_{\alpha\beta}$  the Dehn twist  $\tau_{\tau_\alpha(\beta)}$ . Then, in Luo's presentation of  $\Gamma_\Sigma$ , generators are given by  $\{\tau_\alpha : \alpha \in \mathcal{S}(\Sigma)\}$  and relations are the following:

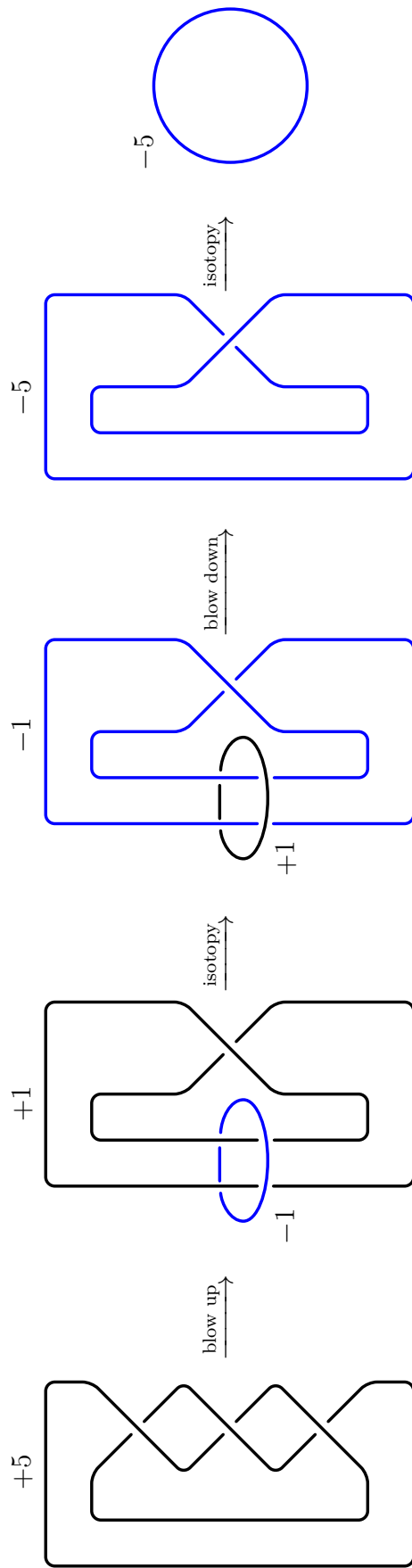


Figure 7.2: A surgery diagram showing that the  $+5$ -surgery on a trefoil and the  $-5$ -surgery on the unknot give diffeomorphic 3-manifolds.

- (I)  $\tau_\alpha = 1$  if  $\alpha$  is the isotopy class of the null-homotopic loop;
- (II)  $\tau_\alpha\tau_\beta = \tau_\beta\tau_\alpha$  if  $I(\alpha, \beta) = 0$ ;
- (III)  $\tau_{\alpha\beta} = \tau_\alpha\tau_\beta\tau_\alpha^{-1}$  if  $I(\alpha, \beta) = 1$ ;
- (IV)  $\tau_\alpha\tau_\beta\tau_{\alpha\beta} = \tau_{\partial(\alpha\beta)}$  if  $I(\alpha, \beta) = 2$  and  $\alpha \cdot \beta = 0$ ;
- (V)  $(\tau_\alpha\tau_\beta\tau_\alpha)^4 = \tau_{\partial(\alpha\beta)}$  if  $I(\alpha, \beta) = 1$ .

The above relations are well-known: (I) and (II) are clearly true; (III), called the *braid relation*, (IV) and (V) were discovered by Dehn in the 1930s [Deh87], with (IV) independently rediscovered and named the *lantern relation* by Johnson [Joh79]. The lantern relation is illustrated in Figure 7.3. Note that if one or more of the boundary curves are homotopically trivial, the lantern relation reduces to the identity. In what follows, given a surface  $\Sigma$ , we accordingly refer to any sub-surface homeomorphic to  $\Sigma_{0,4}$ , none of whose boundary components bound discs in  $\Sigma$ , as a *lantern*.

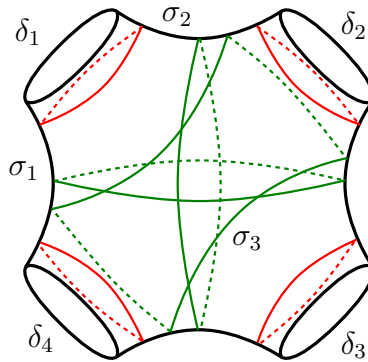


Figure 7.3: The lantern relation on  $\Sigma_{0,4}$  is  $\tau_{\delta_1}\tau_{\delta_2}\tau_{\delta_3}\tau_{\delta_4} = \tau_{\sigma_1}\tau_{\sigma_2}\tau_{\sigma_3}$ , up to cyclic permutation of  $\tau_{\sigma_i}$  and reordering of  $\tau_{\delta_i}$ .

We begin with a simple observation. Letting  $|\epsilon|_w$  denote the total exponent of  $\tau_\epsilon$  in a word  $w$  of Dehn twists, we have:

**Lemma 7.2.1.** Let  $\delta_1$  and  $\delta_2$  denote curves respectively isotopic to the boundary components of  $\Sigma_{1,2}$  and let  $w$  be a word in Dehn twists about curves on  $\Sigma_{1,2}$ . Then the number  $|\delta_2|_w - |\delta_1|_w$  depends only on the mapping class of  $w$ .

*Proof.* Using the above presentation of  $\Gamma_\Sigma$  for  $\Sigma = \Sigma_{1,2}$ , we see that any non-trivial relation which contains either  $\tau_{\delta_i}$  must be a lantern relation; the claim follows immediately by showing that every lantern in  $\Sigma_{1,2}$  has boundary components isotopic to each  $\delta_i$ . To see this, let  $\Lambda \subset \Sigma_{1,2}$  be any lantern, and  $\epsilon$  a curve isotopic to a boundary component of  $\Lambda$  but not isotopic to either  $\delta_i$ . Now, if  $\epsilon$  is non-separating in  $\Sigma_{1,2}$ , then  $\overline{\Sigma_{1,2} \setminus \epsilon}$  is a lantern, so  $\Lambda$  is as claimed. On the other hand, if  $\epsilon$  is separating, then as it is not boundary-parallel in  $\Sigma_{1,2}$  it must cut the surface into  $\Sigma_{0,3} \sqcup \Sigma_{1,1}$ , neither of which contains a lantern, giving a contradiction.  $\square$

We are almost ready to prove that  $\varphi_n$  cannot be written as a product of positive Dehn twists for any  $n \geq 0$ . Before we do that, however, we need some results from [LL11] regarding Stein fillability of Seifert fibred manifolds. Let us recall that a *Seifert fibred* manifold  $M(e_0; r_1, \dots, r_k)$  is a 3-manifold that can be obtained from  $S^3$  by the surgery whose diagram consists of  $k$  unknots with surgery coefficients  $-1/r_1, \dots, -1/r_k$  threaded onto the unknot with the surgery coefficient  $e_0$ ; an illustration is given in Figure 7.4.

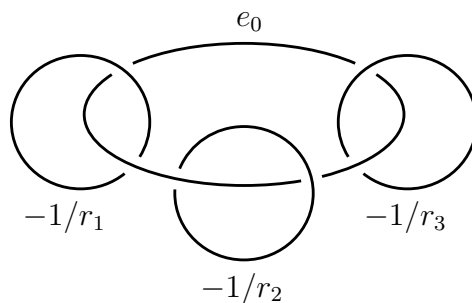


Figure 7.4: A Seifert fibred 3-manifold  $M(e_0; r_1, r_2, r_3)$ .

**Definition 7.2.2** ([LL11, Definitions 1.1 and 1.2]). A  $k$ -tuple  $(r_1, \dots, r_k) \in (\mathbb{Q} \cap (0, 1))^k$  is *realisable* if  $k \geq 3$ ,  $r_1 \geq \dots \geq r_k$  and there exist coprime integers  $m > h > 0$  satisfying

$$\frac{h}{m} > r_1, \quad \frac{m-h}{m} > r_2, \quad \text{and} \quad \frac{1}{m} > \max(r_3, \dots, r_k).$$

A Seifert fibred manifold  $M(-1; r_1, \dots, r_k)$  is *of special type* if  $1 > r_1 \geq r_2 \geq \dots \geq r_k$ ,  $(r_1, \dots, r_k)$  is not realisable, and  $r_1 + \dots + r_k > 1 > r_1 + r_2$ .

**Theorem 7.2.3** ([LL11, Theorem 1.4]). A closed oriented Seifert fibred 3-manifold of special type is not symplectically fillable.

Now we present the desired proof.

**Theorem 7.2.4.** The monodromy  $\varphi_n \in \Gamma_{\Sigma_{1,2}}$  represented by the word  $\tau_\alpha \tau_\beta \tau_\gamma^{-1} \tau_{\delta_1} \tau_{\delta_2}^{4+n}$  does not admit a positive factorisation for any  $n \geq 0$ .

*Proof.* Suppose otherwise, and let  $w$  be a positive factorisation of  $\varphi_n$ . Then  $|\delta_1|_w \geq 0$  and, by Lemma 7.2.1, we have  $|\delta_2|_w \geq 3 + n$ . Since boundary-parallel Dehn twists commute with all other twists, we can write  $w = w' \tau_{\delta_2}^{3+n}$  for  $w'$  a positive factorisation of  $\varphi' = \tau_\alpha \tau_\beta \tau_\gamma^{-1} \tau_{\delta_1} \tau_{\delta_2}$ .

Now, following the procedure used in Section 7.1, we recover that  $(\Sigma_{1,2}, \varphi')$ , shown in Figure 7.5, supports  $(Y', \xi')$ , the result of inadmissible transverse +2-surgery on a right-handed trefoil. (Indeed, setting  $n = 1$  and  $r = 2$  in Proposition 7.1.2, we have  $r' = -2 = [-3 + 1]^-$ , so  $(\Sigma_{1,2}, \varphi')$  is obtained by adding a negative Dehn twist about the boundary  $K$  of  $(\Sigma_{1,1}, \tau_\alpha \tau_\beta)$  in Figure 7.1, stabilising once, and adding a boundary twist about  $K$ .)

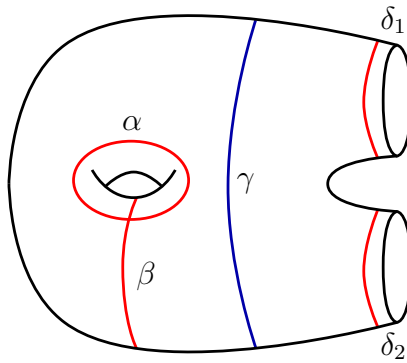


Figure 7.5: An open book decomposition  $(\Sigma_{1,2}, \tau_\alpha \tau_\beta \tau_\gamma^{-1} \tau_{\delta_1} \tau_{\delta_2})$  supporting the result of inadmissible transverse  $+2$ -surgery on a right-handed trefoil in  $(S^3, \xi_{\text{std}})$ .

Now, consider the Seifert fibred manifold  $M(-1; \frac{1}{2}, \frac{1}{3}, \frac{1}{4})$ . Figure 7.6 shows that it is orientation-preserving diffeomorphic to  $Y'$ , the  $(+2)$ -surgery on a right-handed trefoil in  $S^3$ . However,  $(\frac{1}{2}, \frac{1}{3}, \frac{1}{4})$  is not realisable, for the following reason. The condition in Definition 7.2.2 that  $\frac{1}{m} > r_3 = \frac{1}{4}$  implies that  $m \in \{1, 2, 3\}$ . Since  $m > h > 0$  for some integer  $h$ , we have  $m \neq 1$ . If  $m = 2$ , then  $h = 1$  and  $\frac{h}{m} \not> r_1 = \frac{1}{2}$ . Finally, if  $m = 3$ , then  $\frac{h}{m} > r_1 = \frac{1}{2}$  implies that  $h = 2$ , but  $\frac{m-h}{m} \not> r_2 = \frac{1}{3}$ .

Hence, Theorem 7.2.3 implies that  $(M(-1; \frac{1}{2}, \frac{1}{3}, \frac{1}{4}), \xi)$  is not Stein-fillable for any contact structure  $\xi$ . By Giroux [Gir02], it follows that no monodromy of an open book decomposition supporting  $(Y', \xi')$  admits a positive factorisation. Hence no positive factorisation of  $\varphi'$  exists, supplying a contradiction.  $\square$

**Remark 7.2.5.** The open books in our examples have pages  $\Sigma_{1,2}$  with two boundary components, and we note that one can add 1-handles to  $\Sigma_{1,2}$  to obtain any surface  $\Sigma_{g,n}$  with  $g, n \geq 1$  other than  $\Sigma_{1,1}$ . Since adding a 1-handle to the page of an open book amounts to, on the level of 3-manifolds, taking a contact connected sum with  $S^1 \times S^2$  endowed with its unique Stein-fillable contact structure, it also preserves Stein fillability. Moreover, if one attaches a 1-handle while extending the monodromy by the identity on the co-core of the 1-handle, it does not change the property of not being positively factorisable (cf. [Lis14, Remark 5.3]). Hence, the only case where the question of existence of Stein-fillable  $(\Sigma_{g,n}, \varphi)$  with non-positive  $\varphi$  is still open is when  $(g, n) = (1, 1)$ .

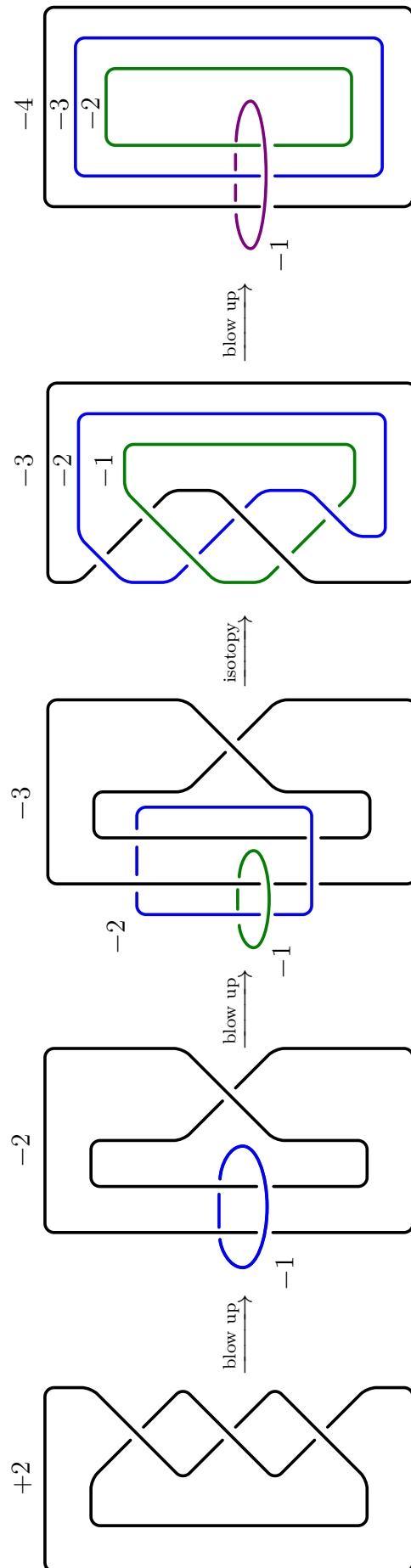


Figure 7.6: A surgery diagram showing that the  $+2$ -surgery on a trefoil is diffeomorphic to  $M(-1; \frac{1}{2}, \frac{1}{3}, \frac{1}{4})$ .

# Appendices

# Script for computing lattice embeddings for ABCs

---

The following Jupyter notebook running the SageMath kernel builds a dictionary of all embeddings of black and white lattices corresponding to non-zero determinant alternating 3-braid closures with up to a desired number of crossings. Cells 1 to 4 define functions that enumerate all lexicographically maximal braid representatives of isotopy classes of such closures and compute corresponding embeddings. Cells 5 and 6 build and explain the structure of the dictionary, while cell 7 contains some examples of working with it.

```
[1]: # PARTITIONS

import itertools

def partitions(n):
    # For a natural number n, returns all ordered partitions of n into natural
    ↪ summands
    s = set()
    s.add((n, ))
    for x in range(1, n):
        for y in partitions(n - x):
            s.add((x, ) + y)
    return s

def even_partitions(n):
    # For a natural number n, returns all ordered partitions of n
    # of even length with sum of even-indexed elements >= sum of odd-indexed elements,
    # split into 2-tuples [(a_1, b_1), (a_2, b_2), ..., (a_k, b_k)]
    p_even = [x for x in sorted(partitions(n))[:-1] if len(x) % 2 == 0]
    p_tuples = [[(x[i], x[i + 1]) for i in range(0, len(x), 2)] for x in p_even]
    p = [x for x in p_tuples if sum([x[i][0] for i in range(0, len(x), 2)]) >= \
        sum([x[i][1] for i in range(0, len(x), 2)])]
    return p
```

```
[2]: # SYMMETRIES

def unique_lists_in_list(l):
    # Takes a list of lists, returns the list of unique lists in the original list
    l_unique = [x for i, x in enumerate(l) if x not in l[:i]]
    return l_unique

def rot(l):
    # Takes a list, returns a list of its cyclic rotations
    l_rot = [[l[k - m] for k in range(len(l))] for m in range(len(l))]
    return l_rot

def ref(l):
    # Takes a list of tuples (a_1, b_1) ... (a_n, b_n) and returns the list of tuples
    # (a_1, b_n) ... (a_2, b_1)
    l_ref = [(l[-i % len(l)][0], l[len(l) - 1 - i][1]) for i in range(len(l))]
    return l_ref

def dual(l):
    # Given a list of tuples (a_1, b_1) ... (a_n, b_n), returns the list of tuples
    # (b_n, a_n) ... (b_1, a_1)
    l_dual = [(x[1], x[0]) for x in l][::-1]
    return l_dual

def symmetries(l):
    # Returns all representations of a list of 2-tuples w.r.t. cyclic rotation and
    # reflection
    l_symmetries = sorted(unique_lists_in_list(rot(l) + rot(ref(l))), reverse =
    True)
    return l_symmetries

def symmetries_with_dual(l):
    # Returns all representations of a list of tuples w.r.t. cyclic rotation and
    # reflection
    # and taking the dual
    l_symmetries_with_dual = sorted(\
        unique_lists_in_list(rot(l) + rot(ref(l)) + rot(dual(l)) + \
            rot(ref(dual(l)))), reverse = True)
    return l_symmetries_with_dual

def all_reps(n):
    # Gives the lexicographically highest representative of each symmetry class in
    # even_partitions(n)
    # w.r.t. cyclic rotation and reflection such that sum a_i >= sum b_i
    ll = even_partitions(n)
    symm_class_reps = []
    ignored_indices = set()
```

```

lens = [len(l1[i]) for i in range(len(l1))]
maxs = [max([l1[i][j][0] for j in range(lens[i])] +\
           [l1[i][j][1] for j in range(lens[i])]) for i in range(len(l1))]
a_sums = [sum([l1[i][j][0] for j in range(lens[i])]) for i in range(len(l1))]
b_sums = [sum([l1[i][j][1] for j in range(lens[i])]) for i in range(len(l1))]

for i in range(len(l1)):
    if i not in ignored_indices:
        if a_sums[i] == b_sums[i]:
            l_symms = symmetries(l1[i])
        else:
            l_symms = symmetries_with_dual(l1[i])
        l_symm_class_rep = list(filter(lambda l:\
                                     sum([l[k][0] for k in range(len(l))]) >=\
                                     sum([l[k][1] for k in range(len(l))]),\
                                     l_symms))[0]
        symm_class_reps.append(l_symm_class_rep)
    for j in range(i + 1, len(l1)):
        if j not in ignored_indices:
            if lens[i] == lens[j] and maxs[i] == maxs[j] and\
                {a_sums[i], b_sums[i]} == {a_sums[j], b_sums[j]}:
                if l1[j] in l_symms:
                    ignored_indices.add(j)

return symm_class_reps

```

```

[3]: # GOERITZ MATRICES
# NB: we invert the convention used in the rest of the thesis
# and flip the signs on all Goeritz matrices, making them
# positive-definite; accordingly, we then consider embeddings
# into positive-definite integral lattices

def goeritz(l):
    # For a given list l = [(a_1, b_1), ..., (a_k, b_k)] representing an
    # alternating 3-braid \beta, generates the white Goeritz matrix
    # (black Goeritz matrix can be obtained by running goeritz(dual(l)))

    a_sum = sum([x[0] for x in l])
    b_sum = sum([x[1] for x in l])

    if len(l) == 1:
        if l[0][0] == 1 and l[0][1] == 1:
            m = [[]]
        elif l[0][0] == 1 and l[0][1] > 1:
            m = [[l[0][1]]]
        elif l[0][0] == 2 and l[0][1] == 1:
            m = [[2]]
        elif l[0][0] == 2 and l[0][1] > 1:

```

```

    m = [[2, -2], [-2, 1[0][1] + 2]]
elif 1[0][0] > 2 and 1[0][1] == 1:
    m = [[0] * (a_sum - 1) for x in range(a_sum - 1)]
    m[0][0] = 2
    m[0][1] = -1
    m[-1][-1] = 2
    m[-1][-2] = -1
    for k in range(1, 1[0][0] - 2):
        m[k][k - 1] = -1
        m[k][k + 1] = -1
        m[k][k] = 2
elif 1[0][0] > 2 and 1[0][1] > 1:
    m = [[0] * a_sum for x in range(a_sum)]
    for k in range(a_sum - 1):
        m[k][(k - 1) % a_sum] = -1
        m[k][(k + 1) % a_sum] = -1
        m[k][k % a_sum] = 2
    m[1[0][0] - 1][0] = -1
    m[1[0][0] - 1][(-2) % 1[0][0]] = -1
    m[1[0][0] - 1][(-1) % 1[0][0]] = 1[0][1] + 2
elif len(1) == 2 and a_sum == 2:
    m = [[1[0][1] + 2, -2], [-2, 1[1][1] + 2]]
else:
    m = [[0] * a_sum for x in range(a_sum)]
    c = 0
    for j in 1:
        if j[0] == 1:
            m[c][(c - 1) % a_sum] = -1
            m[c][(c + 1) % a_sum] = -1
            m[c][c] = j[1] + 2
        else:
            for k in range(j[0] - 1):
                m[c + k][(c + k - 1) % a_sum] = -1
                m[c + k][(c + k + 1) % a_sum] = -1
                m[c + k][(c + k) % a_sum] = 2
            m[c + j[0] - 1][(c + (j[0] - 1) - 1) % a_sum] = -1
            m[c + j[0] - 1][(c + (j[0] - 1) + 1) % a_sum] = -1
            m[c + j[0] - 1][(c + j[0] - 1) % a_sum] = j[1] + 2
            c += j[0]

return m

```

```
[4]: # EMBEDDINGS
```

```
def wu_elt(m):
```

```
# For an embeddable Goeritz matrix, returns the Wu element of the embedding
# (i.e., the image of  $v_0 = -v_1 - \dots - v_n$ )
```

```
wu = []
```

```

n = len(m[0])
for i in range(n):
    t = 0
    for j in range(n):
        t += m[i][j]
for k in range(abs(t)):
    wu.append(i + 1)
return wu

def wu_form(m):
    # Puts the matrix into "Wu form", where the coefficients of the Wu element are
    ↪negative
    n = len(m[0])
    wu_form = [[0] * n] * n
    for i in range(n):
        t = 0
        for j in range(n):
            t += m[i][j]
        if t < 0:
            wu_form[i] = [-x for x in m[i]]
        else:
            wu_form[i] = m[i]
    return wu_form

def are_iso(m1_input, m2_input):
    # Determines whether two matrices represent equivalent embeddings
    # via row and column operations with all possible sign combinations for zero-sum
    ↪rows
    n = len(m1_input[0])
    c = 0
    m1 = wu_form(m1_input)
    m2 = wu_form(m2_input)

    if m1 == m2: return True

    zero_rows = ''
    for j in range(n):
        if sum(m1[j]) == 0:
            zero_rows += '1'
        else:
            zero_rows += '0'

    n_zero_rows = zero_rows.count('1')
    combinations = [str(bin(j))[2:].zfill(len(str(bin(2 ** n_zero_rows - 1))[2:
    ↪])) \
                    for j in range(2 ** n_zero_rows)]

    all_signs = []

```

```

for i in combinations:
    t = []
    c = 0
    for k in range(n):
        if zero_rows[k] == '1' and i[c] == '0':
            t.append(m1[k])
            c += 1
        elif zero_rows[k] == '1' and i[c] == '1':
            t.append([-x for x in m1[k]])
            c += 1
        else:
            t.append(m1[k])
    # print t
    all_signs.append(t)

for i in all_signs:
    m1_rot_ref = []
    for j in range(n):
        t_rot = []
        t_rot_ref = []
        for k in i:
            row_rot = [k[(1 + j) % n] for l in range(n)]
            row_rot_ref = row_rot[::-1]
            t_rot.append(row_rot)
            t_rot_ref.append(row_rot_ref)
        m1_rot_ref.append(sorted(t_rot))
        m1_rot_ref.append(sorted(t_rot_ref))

    m2 = sorted(m2)
    for k in m1_rot_ref:
        if m2 == k:
            return True

    return False

def are_iso_list(ll):
    # Determines all matrices that represent non-equivalent embeddings
    # in a given list of matrices ll
    if len(ll) == 0:
        return []

    iso_indices = []
    iso_embs = []
    n = len(ll[0][0])

    if len(ll) == 1:
        iso_embs.append(ll[0])
        return iso_embs

```

```

for i in range(len(l1)):
    if i not in iso_indices:
        iso_embs.append(l1[i])
        for j in range(i + 1, len(l1)):
            if are_iso(l1[i], l1[j]):
                iso_indices.append(j)
return iso_embs

def embs(l):
    # Returns a list of matrices representing non-equivalent embeddings
    # of the black lattice for an alternating 3-braid closure given by l
    # (returns empty list if there are none)
    g = goeritz(l)
    embs_gap = libgap.OrthogonalEmbeddings(g, len(g[0])).sage()
    if embs_gap["solutions"] == []:
        return []
    else:
        emb_matrices = []
        for s in embs_gap["solutions"]:
            e = []
            for t in s:
                e.append(embs_gap["vectors"][t - 1])
            emb_matrices.append(e)
        return are_iso_list(emb_matrices)

```

[5]: # *DICTIONARY*

```

def emb_dict(max_crossings):
    # Creates a dictionary containing the following info:
    # n: # of crossings in the ABC  $\hat{(\beta)}$ ; runs from 3 to max_crossings
    # l: lexicographically maximal 3-braid whose closure gives  $\hat{(\beta)}$ 
    # g_white: white Goeritz matrix
    # g_black: black Goeritz matrix
    # emb_white: list of matrices representing non-equivalent
    #             embeddings of the black lattice
    # emb_black: list of matrices representing non-equivalent
    #             embeddings of the white lattice
    # is_embeddable: True if  $\hat{(\beta)}$  is embeddable, False otherwise
    d = {}
    for n in range(3, max_crossings + 1):
        abcs = all_reps(n)
        for l in abcs:
            g_white = goeritz(l)
            g_black = goeritz(dual(l))
            emb_white = embs(l)
            emb_black = embs(dual(l))
            if emb_white != [] and emb_black != []:
                d[n] = (emb_white, emb_black, is_embeddable)

```

```

else:
    is_embeddable = False
    d.append({"n": n,
             "l": 1,
             "g_white": g_white,
             "g_black": g_black,
             "emb_white": emb_white,
             "emb_black": emb_black,
             "is_embeddable": is_embeddable})

return d

```

```
[6]: # Building the dictionary with max_crossings = 18;
      # this can take a while...
```

```

max_crossings = 18
d = emb_dict(max_crossings)

```

```
[7]: # We can view all embeddable ABCs (up to rotation, reflection and taking the dual
      # of a respective 3-braid) with a fixed number of crossings (say, 10) as shown
```

```

n = 10
emb_abcs = [x["l"] for x in d if x["is_embeddable"] == True and x["n"] == n]
print("Embeddable ABCs with " + str(n) + " crossings:")
for abc in emb_abcs:
    print(abc)
print("\n")

# Each embedding is represented by a matrix, with the (i, j)
# element corresponding to the coefficient of e_j in
# the image of v_i

# View embeddings for a particular ABC as follows:

abc = [(3, 1), (1, 3), (1, 1)]
embs_white = [x["emb_white"] for x in d if x["l"] == abc][0]
print("Embeddings of the black lattice for", abc)
for e in embs_white:
    for r in e:
        print(r)
    print("***")

```

Embeddable ABCs with 10 crossings:

```

[(5, 5)]
[(4, 3), (1, 2)]
[(3, 4), (2, 1)]
[(3, 1), (1, 3), (1, 1)]
[(2, 2), (1, 2), (2, 1)]
[(2, 2), (1, 1), (1, 1), (1, 1)]
[(1, 1), (1, 1), (1, 1), (1, 1), (1, 1)]

```

Embeddings of the black lattice for  $[(3, 1), (1, 3), (1, 1)]$

$[-1, 1, -1, 1, 0]$

$[1, 0, -1, 1, -1]$

$[0, 1, 0, -1, 0]$

$[0, 0, -1, -1, 1]$

$[0, 0, 0, 1, 1]$

\*\*\*

$[-1, 1, -1, 0, 1]$

$[1, 0, -1, 0, 0]$

$[0, 1, 0, 0, -1]$

$[0, 0, 1, -1, 1]$

$[0, 0, 0, 2, 0]$

\*\*\*

$[-1, 1, -1, 0, 0]$

$[1, 0, -1, 0, -1]$

$[0, 1, 0, 0, 0]$

$[0, 0, -1, 1, 1]$

$[0, 0, 0, -2, 1]$

\*\*\*

$[-1, 1, 0, 1, 0]$

$[1, 0, 0, 1, -1]$

$[0, 1, -1, -1, 0]$

$[0, 0, 1, -1, 1]$

$[0, 0, -1, 1, 1]$

## Appendix B

# Scripts for computing TAPs for $K_1$ , $K_2$ and $K_3$

---

The following Jupyter notebook running the SageMath kernel illustrates the computation of twisted Alexander polynomials that vanish on the metabolisers of  $K_1$ ; the cases of  $K_2$  and  $K_3$  are analogous. Notebooks with computations for all three knots can be found in the .ipynb format in the repository <https://github.com/vbrej/3-braid-tap>.

```
[1]: # Starting with the Seifert matrix for  $K_1$ 
# with exponent sequence (2,-2,2,-2,1,-2,2,-2,2,-1)
# obtained from Julia Collins' calculator:
# https://www.maths.ed.ac.uk/~v1ranick/julia/index.htm

R.<t> = LaurentPolynomialRing(ZZ)
S = Matrix(R, [[-1,0,0,0,0,0,0,0,0,0,0,0,0,0,0,0],
               [1,-1,0,1,0,0,0,0,0,0,0,0,0,0,0,0],
               [0,0,1,-1,0,0,0,0,0,0,0,0,0,0,0,0],
               [0,0,0,1,0,0,-1,0,0,0,0,0,0,0,0,0],
               [0,1,0,0,-1,0,0,0,0,0,0,0,0,0,0,0],
               [0,0,0,-1,1,-1,0,1,0,0,0,0,0,0,0,0],
               [0,0,0,0,0,0,1,-1,0,0,0,0,0,0,0,0],
               [0,0,0,0,0,0,0,1,0,-1,0,0,0,0,0,0],
               [0,0,0,0,0,1,0,-1,-1,0,1,0,0,0,0,0],
               [0,0,0,0,0,0,0,0,0,1,-1,0,0,0,0,0],
               [0,0,0,0,0,0,0,0,0,0,1,0,0,-1,0,0],
               [0,0,0,0,0,0,0,0,0,1,0,0,-1,0,0,0],
               [0,0,0,0,0,0,0,0,0,0,-1,1,-1,0,1,0],
               [0,0,0,0,0,0,0,0,0,0,0,0,0,1,-1,0],
               [0,0,0,0,0,0,0,0,0,0,0,0,0,0,1,0],
               [0,0,0,0,0,0,0,0,0,0,0,0,1,0,0,-1]])

#  $P = t*S - S^T$  is a presentation matrix of the Alexander module

P = t * S - S.transpose()
```

```

# det(P) is the Alexander polynomial
ap = P.determinant()
ap.factor()

```

[1]:  $(1 - 3t + 7t^2 - 10t^3 + 11t^4 - 10t^5 + 7t^6 - 3t^7 + t^8)^2$

[2]: *# Performing column operations on P until we get  
# all possible unit pivots*

```

for i in range(1):
    P.add_multiple_of_column(i, 1, P[0,i])

for i in range(4):
    P.add_multiple_of_column(i, 4, P[1,i])

P.set_col_to_multiple_of_col(3, 3, t^-1)
for i in range(3):
    P.add_multiple_of_column(i, 3, P[2,i])

P.set_col_to_multiple_of_col(6, 6, t^-1)
for i in range(6):
    P.add_multiple_of_column(i, 6, P[3,i])

for i in range(5):
    P.add_multiple_of_column(i, 5, P[4,i])

for i in range(8):
    P.add_multiple_of_column(i, 8, P[5,i])

P.set_col_to_multiple_of_col(7, 7, t^-1)
for i in range(7):
    P.add_multiple_of_column(i, 7, P[6,i])

P.set_col_to_multiple_of_col(9, 9, t^-1)
for i in range(9):
    P.add_multiple_of_column(i, 9, P[7,i])

for i in range(11):
    P.add_multiple_of_column(i, 11, P[8,i])

P.set_col_to_multiple_of_col(10, 10, t^-1)
for i in range(10):
    P.add_multiple_of_column(i, 10, P[9,i])

P.set_col_to_multiple_of_col(13, 13, t^-1)
for i in range(13):
    P.add_multiple_of_column(i, 13, P[10,i])

```

```

for i in range(12):
    P.add_multiple_of_column(i, 12, P[11,i])

for i in range(15):
    P.add_multiple_of_column(i, 15, P[12,i])

P.set_col_to_multiple_of_col(14, 14, t^-1)
for i in range(14):
    P.add_multiple_of_column(i, 14, P[13,i])

P.set_col_to_multiple_of_col(0, 0, t^4)
P.set_col_to_multiple_of_col(2, 2, t^7)
P.add_multiple_of_column(2, 0, t - t^2)
P.add_multiple_of_column(0, 2, -1 + t)
P.add_multiple_of_column(2, 0, t^-3 - t^-2)
P.set_col_to_multiple_of_col(0, 0, t^-4)

# Swapping columns to put P into a nice form

P.swap_columns(1,0)
P.swap_columns(4,1)
P.swap_columns(3,2)
P.swap_columns(6,3)
P.swap_columns(5,4)
P.swap_columns(8,5)
P.swap_columns(7,6)
P.swap_columns(9,7)
P.swap_columns(11,8)
P.swap_columns(10,9)
P.swap_columns(13,10)
P.swap_columns(12,11)
P.swap_columns(15,12)
P.swap_columns(14,13)

for i in range(14):
    P.set_col_to_multiple_of_col(i, i, -1)

```

[3]: *# P now has the form*

```

# [ I | 0 ]
# [ ----- ]
# [ * | p 0 ]
# [ * | 0 p ]

# for p = p(t) the square root of the Alexander polynomial

# Conclude that the Alexander module is generated by
# the lifts of \hat{\alpha}_{15} and \hat{\alpha}_{16}

```

```
show(P[:14,:])
show(P[14:,14:])
```

```
[3]: [1 0 0 0 0 0 0 0 0 0 0 0 0 0 0]
      [0 1 0 0 0 0 0 0 0 0 0 0 0 0 0]
      [0 0 1 0 0 0 0 0 0 0 0 0 0 0 0]
      [0 0 0 1 0 0 0 0 0 0 0 0 0 0 0]
      [0 0 0 0 1 0 0 0 0 0 0 0 0 0 0]
      [0 0 0 0 0 1 0 0 0 0 0 0 0 0 0]
      [0 0 0 0 0 0 1 0 0 0 0 0 0 0 0]
      [0 0 0 0 0 0 0 1 0 0 0 0 0 0 0]
      [0 0 0 0 0 0 0 0 1 0 0 0 0 0 0]
      [0 0 0 0 0 0 0 0 0 1 0 0 0 0 0]
      [0 0 0 0 0 0 0 0 0 0 1 0 0 0 0]
      [0 0 0 0 0 0 0 0 0 0 0 1 0 0 0]
      [0 0 0 0 0 0 0 0 0 0 0 0 1 0 0]
```

```
[3]: [1 - 3*t + 7*t^2 - 10*t^3 + 11*t^4 - 10*t^5 + 7*t^6 - 3*t^7 + t^8
      0]
      [
      0 1 - 3*t +
      7*t^2 - 10*t^3 + 11*t^4 - 10*t^5 + 7*t^6 - 3*t^7 + t^8]
```

```
[15]: # Now computing the Blanchfield pairing and linking form

      # First, pass to PolynomialRing(QQ) so we can use Sage to find
      # the multiplicative inverse mod  $t^3 - 1$  of  $ap(t) = \Delta_K(t) = p^2(t)$ ,
      # as  $\Delta_K(t)$  has no negative powers

      R.<t> = PolynomialRing(QQ)

      p = R(P[15,15])
      q = R(t^3 - 1)

      # We scale the multiplicative inverse of  $p$  mod  $q$  over  $QQ[t]$ 
      # so that  $p * pinv = c \pmod q$  with  $pinv \in ZZ[t]$ ,  $c \in ZZ$ 
      # Then  $ap * apinv = c^2 \pmod q$ 

      pinv = 7 * p.inverse_mod(q)

      #  $P_{FP}$  is the Friedl-Powell matrix  $(t - 1) * (S - t*S^T)^{-1}$ 
      # which will tell us the Blanchfield pairing

      P_FP = (t - 1) * (S - t * S.transpose()).inverse()

      # Entries of the Blanchfield matrix have form
      #  $(1/p) * f(t)$  for  $f(t)$  in  $ZZ[t^{-1}]$ , and since they live in
      #  $QQ(t)/ZZ[t^{-1}]$ , can multiply both numerators and denominators
```

```

# by  $p * \text{pinv} = c * \text{pinv}$ ; then, modulo  $q$  the denominators are
#  $p^2 * \text{pinv} = c^2 = 49$  and the numerators are given by  $c * f(t) * \text{pinv}$ 

# After dividing through by  $c$ , entries of the Blanchfield matrix have form
#  $1/c * f(t) * \text{pinv}$ ; the values  $f(t) * \text{pinv}$  are contained in  $B$ 

B = pinv * Matrix(R, [[P_FP[14, 14] * p, P_FP[14, 15] * p],
                    [P_FP[15, 14] * p, P_FP[15, 15] * p]])

B[0,0] = B[0,0].quo_rem(q)[1]
B[0,1] = B[0,1].quo_rem(q)[1]
B[1,0] = B[1,0].quo_rem(q)[1]
B[1,1] = B[1,1].quo_rem(q)[1]

show(B)

```

```

[15]: [ 2*t^2 + 2*t - 4 -2*t^2 + 4*t - 2]
      [ 4*t^2 - 2*t - 2 -4*t^2 - 4*t + 8]

```

```

[5]: # Now can define the linking pairing of the 3-fold branched cover
# wrt/ ordered basis {a, ta, b, tb}
# L carries the numerators and forgets the 1/c factor in front

L_aa = [B[0,0].monomial_coefficient(t^0), B[0,0].monomial_coefficient(t^2)]
L_ab = [B[1,0].monomial_coefficient(t^0), B[1,0].monomial_coefficient(t^2)]
L_ba = [B[0,1].monomial_coefficient(t^0), B[0,1].monomial_coefficient(t^2)]
L_bb = [B[1,1].monomial_coefficient(t^0), B[1,1].monomial_coefficient(t^2)]
L = Matrix(GF(7), [[L_aa[0], L_aa[1], L_ab[0], L_ab[1]],
                  [L_aa[1], L_aa[0], L_ba[1], L_ab[0]],
                  [L_ba[0], L_ba[1], L_bb[0], L_bb[1]],
                  [L_ab[1], L_ba[0], L_bb[1], L_bb[0]]])

show(L)

```

```

[5]: [3 2 5 4]
      [2 3 5 5]
      [5 5 1 3]
      [4 5 3 1]

```

```

[6]: # Now finding metabolisers by checking on which of the order 49 submodules
# of  $(\mathbb{Z}/7)^4$  generated by {a, ta, b, tb} the linking form vanishes

def unique_lists_in_list(l):
# Takes a list of lists, returns the list of unique lists in the original list

    l_unique = [x for i, x in enumerate(l) if x not in l[:i]]
    return l_unique

n = 7

```

```

cf = []

# Somewhat crudely, we generate all 2- or 4-tuples with entries in Z/7
# to check the vanishing of the linking form -- this can be improved

cf = []
for i in range(n):
    for j in range(n):
        cf.append((i,j))

# N_0
v_0 = []
for c in range(len(cf)):
    v_0.append(Matrix(GF(n), [cf[c][0], cf[c][1], 0, 0]))

v_0 = unique_lists_in_list(v_0)

# N_{k0,k1}
v_k0_k1 = []
for k0 in range(n):
    for k1 in range(n):
        v = []
        for c in range(len(cf)):
            v.append(Matrix(GF(n), [cf[c][0], 0, (k0 * cf[c][0]), (k0 *
↪cf[c][1])]))
            v.append(Matrix(GF(n), [0, cf[c][1], -(k1 * cf[c][1]), (k1 *
↪(cf[c][0] - cf[c][1]))]))

        v_un = unique_lists_in_list(v)
        v_k0_k1.append([(k0, k1)] + v_un)

# Now on to 4-tuples

cf = []
for i in range(n):
    for j in range(n):
        for k in range(n):
            for l in range(n):
                cf.append((i,j,k,l))

# N_0^alpha
v_0_alpha = []
for c in range(len(cf)):
    v_0_alpha.append(Matrix(GF(n), [(-2 * cf[c][0]), cf[c][0], 0, 0]))
    v_0_alpha.append(Matrix(GF(n), [-cf[c][1], (-3 * cf[c][1]), 0, 0]))
    v_0_alpha.append(Matrix(GF(n), [0, 0, (-2 * cf[c][2]), cf[c][2]]))
    v_0_alpha.append(Matrix(GF(n), [0, 0, -cf[c][3], (-3 * cf[c][3]))])
v_0_alpha = unique_lists_in_list(v_0_alpha)

```

```

#  $N_0^{\text{beta}}$ 
v_0_beta = []
for c in range(len(cf)):
    v_0_beta.append(Matrix(GF(n), [(3 * cf[c][0]), cf[c][0], 0, 0]))
    v_0_beta.append(Matrix(GF(n), [-cf[c][1], (2 * cf[c][1]), 0, 0]))
    v_0_beta.append(Matrix(GF(n), [0, 0, (3 * cf[c][2]), cf[c][2]]))
    v_0_beta.append(Matrix(GF(n), [0, 0, -cf[c][3], (2 * cf[c][3])]))

v_0_beta = unique_lists_in_list(v_0_beta)

#  $N_{k0}^{\text{alpha.beta}}$ 
v_k0_alphabeta = []
for k0 in range(n):
    v = []
    for c in range(len(cf)):
        v.append(Matrix(GF(n), [(-2 * cf[c][0]), cf[c][0], 0, 0]))
        v.append(Matrix(GF(n), [-cf[c][1], (-3 * cf[c][1]), 0, 0]))
        v.append(Matrix(GF(n), [(cf[c][2] * k0), 0, (3 * cf[c][2]), cf[c][2]]))
        v.append(Matrix(GF(n), [0, (cf[c][3] * k0), -cf[c][3], (2 * cf[c][3])]))

    v_un = unique_lists_in_list(v)
    v_k0_alphabeta.append([k0] + v_un)

#  $N_{k0}^{\text{beta.alpha}}$ 
v_k0_betaalpha = []
for k0 in range(n):
    v = []
    for c in range(len(cf)):
        v.append(Matrix(GF(n), [(3 * cf[c][0]), cf[c][0], 0, 0]))
        v.append(Matrix(GF(n), [-cf[c][1], (2 * cf[c][1]), 0, 0]))
        v.append(Matrix(GF(n), [(cf[c][2] * k0), 0, (-2 * cf[c][2]), cf[c][2]]))
        v.append(Matrix(GF(n), [0, (cf[c][3] * k0), -cf[c][3], (-3 * cf[c][3])]))

    v_un = unique_lists_in_list(v)
    v_k0_betaalpha.append([k0] + v_un)

```

[7]: # Checking for vanishing of the linking form

```

def is_metaboliser(v, s, L):
    is_met = True
    to_break = False
    for u1 in v:
        if to_break == False:
            for u2 in v:
                if to_break == False:
                    lk = u1 * L * u2.transpose()
                    if lk != 0:

```

```

        is_met = False
        to_break = True

    if is_met == True:# or is_met == False:
        print(s, 'is a metaboliser')

is_metaboliser(v_0, 'N_0', L)
for l in v_k0_k1:
    is_metaboliser(l[1:], 'N_'+str(l[0][0])+',''+str(l[0][1]), L)
is_metaboliser(v_0_alpha, 'N_0^alpha', L)
is_metaboliser(v_0_beta, 'N_0^beta', L)
for l in v_k0_alphabeta:
    is_metaboliser(l[1:], 'N_'+str(l[0])+'^alpha.beta', L)
for l in v_k0_betaalpha:
    is_metaboliser(l[1:], 'N_'+str(l[0])+'^beta.alpha', L)

```

$N_0^{\alpha}$  is a metaboliser  
 $N_0^{\beta}$  is a metaboliser  
 $N_6^{\alpha.\beta}$  is a metaboliser  
 $N_4^{\beta.\alpha}$  is a metaboliser

```

[8]: # We conclude that the metabolisers are
      #  $N_0^{\alpha}$ ,  $N_0^{\beta}$ ,  $N_6^{\alpha.\beta}$ ,  $N_4^{\beta.\alpha}$ 

      # Now to compute the TAPs we first need to work with the Wirtinger presentation
      # to obtain a representation of  $\pi_1(X_K)$ 

      # pres encodes the Wirtinger relations on generators  $g_1, \dots, g_{18}$ ,
      # where  $[i, j, k]$  stands for the relation  $g_i g_j g_i^{-1} g_k^{-1} = 0$ 

pres = [[1,13,12],
        [13,2,1],
        [2,15,14],
        [15,3,2],
        [3,17,16],
        [10,3,4],
        [4,10,11],
        [17,5,4],
        [5,18,17],
        [11,5,6],
        [6,11,12],
        [18,7,6],
        [7,1,18],
        [12,7,8],
        [8,13,14],
        [14,8,9],
        [9,15,16],
        [16,9,10]]

```

```

# If  $v_i$  is the homology class of a lift of  $(\mu_0^{-1} g_i)$  to the
# triple branched cover, from HKL we get that the relation
#  $g_i g_j g_i^{-1} g_k^{-1} = 0$  on  $\pi_1$  induces a relation  $(1 - t) * v_i + t * v_j -$ 
 $\rightarrow v_k = 0$ 

R.<tt> = PolynomialRing(GF(7))
Rq.<t> = QuotientRing(R, R.ideal(tt^2 + tt + 1))
M.<a,b> = CombinatorialFreeModule(Rq)

v1 = 0
v7 = b
v12 = - t * a + b

# Use Wirtinger relations to find the rest of  $v_i$ 's

v8 = (1 - t) * v12 + t * v7
v18 = (1 - t) * v7
v6 = (1 - t) * v18 + t * v7
v13 = t^2 * v12
v2 = t^2 * (v1 - (1 - t) * v13)
v11 = t^2 * (v12 - (1 - t) * v6)
v5 = t^2 * (v6 - (1 - t) * v11)
v17 = (1 - t) * v5 + t * v18
v4 = (1 - t) * v17 + t * v5
v10 = t^2 * (v11 - (1 - t) * v4)
v3 = t^2 * (v4 - (1 - t) * v10)
v16 = (1 - t) * v3 + t * v17
v9 = t^2 * (v10 - (1 - t) * v16)
v15 = t^2 * (v16 - (1 - t) * v9)
v14 = (1 - t) * v2 + t * v15

# Checking the leftover relations -- should all be True

print(v2 == (1 - t) * v15 + t * v3,
v14 == (1 - t) * v8 + t * v13,
v9 == (1 - t) * v14 + t * v8)

vv = [v1, v2, v3, v4, v5, v6, v7, v8, v9, v10, v11, v12, v13, v14, v15, v16, v17,
 $\rightarrow$ v18]

```

True True True

```

[9]: # This is a quick way to get coefficients  $(k_0, k_1, l_0, l_1)$ 
# of  $k_0*a + k_1*t*a + l_0*b + l_1*t*b$  with minimal Sage coercion errors

def indices(v):
    if v == 0:
        return [0] * 4
    else:

```

```

l = v.monomial_coefficients()
i = []

if 'a' in l.keys():
    i += l['a'].list()
else:
    i += [0,0]

if 'b' in l.keys():
    i += l['b'].list()
else:
    i += [0,0]

return i

# Storing (k0, k1, l0, l1) for all v_i, t * v_i and t^2 * v_i, respectively

v_ind = [indices(v) for v in vv]
tv_ind = [indices(t * v) for v in vv]
ttv_ind = [indices(t^2 * v) for v in vv]

```

```

[10]: # We are now ready to compute the TAPS

# This routine for checking if a polynomial
# factorises as a norm is borrowed from SnapPy

def poly_involution(f):
    R = f.parent()
    K = R.base_ring()
    z, t = K.gen(), R.gen()
    bar = K.hom([1/z])
    ans = R(0)
    d = f.degree()
    for e in f.exponents():
        ans += bar(f[e])*t**(d - e)
    return ans

def poly_is_a_norm(g):
    factors = dict(g.factor())
    #print(factors)
    for h in factors:
        assert h.is_monic()
        hbar = poly_involution(h)
        hbar = hbar/hbar.leading_coefficient()
        if hbar == h and factors[h] % 2 != 0:
            return False
        elif hbar not in factors.keys():
            return False

```

```

    elif factors[h] != factors[hbar]:
        return False
    return True

```

[11]: *# This function generates a row of the reduced Fox matrix from  
# Wirtinger presentation in pres (cf. HKL, p.938)*

```

def fox_row(l, reps):
    m1 = I - reps[l[2]-1]
    m2 = reps[l[0]-1]
    m3 = -I
    r = matrix(Rc, 3, 54)
    r.set_block(0, 3*(l[0] - 1), m1)
    r.set_block(0, 3*(l[1] - 1), m2)
    r.set_block(0, 3*(l[2] - 1), m3)
    return r

# This function builds the image of the reduced Fox matrix  
# under the map \Phi from Wirtinger presentation in pres  
# and the representation of v_i's in reps

def fox_mat_image(pres, reps):
    rr = []
    for i in pres:
        rr.append(fox_row(i, reps))

    fox_ext = rr[0]
    for i in range(1, len(rr)):
        fox_ext = fox_ext.stack(rr[i])

    fox_ext_red = fox_ext[[i for i in range(len(pres) * 3) if i not in [0,1,2]],
                          [j for j in range(len(pres) * 3) if j not in [0,1,2]]]
    return fox_ext_red

```

[12]:

```

L.<z> = CyclotomicField(7)
Rc.<t> = PolynomialRing(L)
M = MatrixSpace(Rc, 3)

I = M.identity_matrix()
Z = M.zero_matrix()
Bmat = M([[0,1,0],
          [0,0,1],
          [t,0,0]])

# Note that Bmat is the one taken in HKL (Eqn. 7.2), not in AMMPS!

# Defining characters that vanish on the metabolisers

chars = [(1, 2, 1, 2), (1, -3, 1, -3), (1, 2, 1, -2), (1, -3, 1, -2)]

```

```

for chi in chars:
    chis = [(v_ind[i][0] * chi[0] + v_ind[i][1] * chi[1] + v_ind[i][2] * chi[2] +
↪v_ind[i][3] * chi[3]),\
            tv_ind[i][0] * chi[0] + tv_ind[i][1] * chi[1] + tv_ind[i][2] * chi[2] +
↪tv_ind[i][3] * chi[3]),\
            ttv_ind[i][0] * chi[0] + ttv_ind[i][1] * chi[1] + ttv_ind[i][2] * chi[2] +
↪ttv_ind[i][3] * chi[3])
            for i in range(len(vv))]

    reps = [Bmat * M([z^(chis[i][0]),0,0],
                    [0,z^(chis[i][1]),0],
                    [0,0,z^(chis[i][2])])] for i in range(len(chis))]

    fox_ext_red = fox_mat_image(pres, reps)
    d = fox_ext_red.determinant()
    tap_red = d // ((reps[0] - I).determinant() * (t - 1))

    print('Character:', chi)
    print('Factors of TAP:', dict(tap_red.factor()))
    print('TAP is a norm:', poly_is_a_norm(tap_red // t^(tap_red.exponents()[0])))
    print('-----')

```

Character: (1, 2, 1, 2)

Factors of TAP: {t: 1,  $t^{14} + (2z^4 + 2z^2 + 2z + 1)t^{13} + (8z^4 + 8z^2 + 8z + 3)t^{12} - 15t^{11} + (3z^4 + 3z^2 + 3z - 48)t^{10} + (8z^4 + 8z^2 + 8z - 33)t^9 + (48z^4 + 48z^2 + 48z - 34)t^8 - 199t^7 + (-48z^4 - 48z^2 - 48z - 82)t^6 + (-8z^4 - 8z^2 - 8z - 41)t^5 + (-3z^4 - 3z^2 - 3z - 51)t^4 - 15t^3 + (-8z^4 - 8z^2 - 8z - 5)t^2 + (-2z^4 - 2z^2 - 2z - 1)t + 1$ : 1}

TAP is a norm: False

Character: (1, -3, 1, -3)

Factors of TAP: {t: 1,  $t^{14} + (4z^4 + 4z^2 + 4z - 5)t^{13} + (-24z^4 - 24z^2 - 24z + 15)t^{12} + (93z^4 + 93z^2 + 93z + 14)t^{11} + (-98z^4 - 98z^2 - 98z - 11)t^{10} + (2z^4 + 2z^2 + 2z - 71)t^9 + (11z^4 + 11z^2 + 11z + 154)t^8 - 360t^7 + (-11z^4 - 11z^2 - 11z + 143)t^6 + (-2z^4 - 2z^2 - 2z - 73)t^5 + (98z^4 + 98z^2 + 98z + 87)t^4 + (-93z^4 - 93z^2 - 93z - 79)t^3 + (24z^4 + 24z^2 + 24z + 39)t^2 + (-4z^4 - 4z^2 - 4z - 9)t + 1$ : 1}

TAP is a norm: False

Character: (1, 2, 1, -2)

Factors of TAP: {t: 1,  $t^{14} + (-2z^5 + z^4 - 4z^3 + z^2 + 2z - 5)t^{13} + (3z^5 - 7z^4 + 24z^3 + 3z^2 - 2z + 20)t^{12} + (-7z^5 + 67z^4 - 41z^3 + 8z^2 + 35z - 7)t^{11} + (45z^5 - 52z^4 + 38z^3 - 3z^2 + z - 19)t^{10} + (-68z^5 - 51z^4 - 114z^3 - 24z^2 - 95z - 63)t^9 + (-116z^5 - 121z^4 - 80z^3 - 56z^2 - 124z - 65)t^8 + (-149z^5 + 3z^4 + 3z^3 - 149z^2 - 19)t^7 + (68z^5 + 44z^4 + 3z^3 + 8z^2 + 124z + 59)t^6 + (71z^5 - 19z^4 + 44z^3 + 27z^2 + 95z + 32)t^5 + (-4z^5 + 37z^4 - 53z^3 + 44z^2 - z -$

```
20)*t^4 + (-27*z^5 - 76*z^4 + 32*z^3 - 42*z^2 - 35*z - 42)*t^3 + (5*z^5 + 26*z^4
- 5*z^3 + 5*z^2 + 2*z + 22)*t^2 + (-z^5 - 6*z^4 - z^3 - 4*z^2 - 2*z - 7)*t + 1:
1}
```

TAP is a norm: False

-----

Character: (1, -3, 1, -2)

```
Factors of TAP: {t: 1, t^14 + (-2*z^5 - z^4 - 2*z^3 - z^2 + z - 2)*t^13 + (5*z^5
+ 2*z^4 + 3*z^3 + 6*z^2 + 2*z + 9)*t^12 + (-10*z^5 - 4*z^4 - 9*z^2 - 20)*t^11 +
(35*z^5 + 36*z^4 + 30*z^3 + 35*z^2 + 4*z + 10)*t^10 + (-44*z^5 + 10*z^4 - 8*z^3
- 47*z^2 - 52*z - 85)*t^9 + (57*z^5 + 17*z^4 + 63*z^3 - 29*z^2 + 27*z - 11)*t^8
+ (-7*z^5 - 38*z^4 - 38*z^3 - 7*z^2 + 59)*t^7 + (-56*z^5 + 36*z^4 - 10*z^3 +
30*z^2 - 27*z - 38)*t^6 + (5*z^5 + 44*z^4 + 62*z^3 + 8*z^2 + 52*z - 33)*t^5 +
(31*z^5 + 26*z^4 + 32*z^3 + 31*z^2 - 4*z + 6)*t^4 + (-9*z^5 - 4*z^3 - 10*z^2 -
20)*t^3 + (4*z^5 + z^4 + 3*z^2 - 2*z + 7)*t^2 + (-2*z^5 - 3*z^4 - 2*z^3 - 3*z^2
- z - 3)*t + 1: 1}
```

TAP is a norm: False

## Appendix C

# Reduced TAPs for $K_1$ , $K_2$ and $K_3$

---

The following table contains reduced twisted Alexander polynomials for knots  $K_1$ ,  $K_2$  and  $K_3$  associated to characters  $\chi$  vanishing on the metabolisers of respective knots, as computed in Chapter 5. For brevity, we write  $\zeta = \zeta_7$  and  $\theta = \zeta_7 + \zeta_7^2 + \zeta_7^4$ .

$(K_i, \chi)$	$\tilde{\Delta}_{K_i}^\chi(t)$
$(K_1, \chi_0^\alpha)$	$-t^{15} + (-2\theta - 1)t^{14} + (-8\theta - 3)t^{13} + 15t^{12} + (-3\theta + 48)t^{11} +$ $(-8\theta + 33)t^{10} + (-48\theta + 34)t^9 + 199t^8 + (48\theta + 82)t^7 +$ $(8\theta + 41)t^6 + (3\theta + 51)t^5 + 15t^4 + (8\theta + 5)t^3 + (2\theta + 1)t^2 - t$
$(K_1, \chi_0^\beta)$	$-t^{15} + (-4\theta + 5)t^{14} + (24\theta - 15)t^{13} + (-93\theta - 14)t^{12} + (98\theta + 11)t^{11} +$ $(-2\theta + 71)t^{10} + (-11\theta - 154)t^9 + 360t^8 + (11\theta - 143)t^7 + (2\theta + 73)t^6 +$ $(-98\theta - 87)t^5 + (93\theta + 79)t^4 + (-24\theta - 39)t^3 + (4\theta + 9)t^2 - t$
$(K_1, \chi_6^{\alpha\beta})$	$-t^{15} + (2\zeta^5 - \zeta^4 + 4\zeta^3 - \zeta^2 - 2\zeta + 5)t^{14} +$ $(-3\zeta^5 + 7\zeta^4 - 24\zeta^3 - 3\zeta^2 + 2\zeta - 20)t^{13} +$ $(7\zeta^5 - 67\zeta^4 + 41\zeta^3 - 8\zeta^2 - 35\zeta + 7)t^{12} +$ $(-45\zeta^5 + 52\zeta^4 - 38\zeta^3 + 3\zeta^2 - \zeta + 19)t^{11} +$ $(68\zeta^5 + 51\zeta^4 + 114\zeta^3 + 24\zeta^2 + 95\zeta + 63)t^{10} +$ $(116\zeta^5 + 121\zeta^4 + 80\zeta^3 + 56\zeta^2 + 124\zeta + 65)t^9 +$ $(149\zeta^5 - 3\zeta^4 - 3\zeta^3 + 149\zeta^2 + 19)t^8 +$ $(-68\zeta^5 - 44\zeta^4 - 3\zeta^3 - 8\zeta^2 - 124\zeta - 59)t^7 +$ $(-71\zeta^5 + 19\zeta^4 - 44\zeta^3 - 27\zeta^2 - 95\zeta - 32)t^6 +$ $(4\zeta^5 - 37\zeta^4 + 53\zeta^3 - 44\zeta^2 + \zeta + 20)t^5 +$ $(27\zeta^5 + 76\zeta^4 - 32\zeta^3 + 42\zeta^2 + 35\zeta + 42)t^4 +$ $(-5\zeta^5 - 26\zeta^4 + 5\zeta^3 - 5\zeta^2 - 2\zeta - 22)t^3 +$ $(\zeta^5 + 6\zeta^4 + \zeta^3 + 4\zeta^2 + 2\zeta + 7)t^2 - t$

$(K_1, \chi_4^{\beta\alpha})$	$ \begin{aligned} & -t^{15} + (2\zeta^5 + \zeta^4 + 2\zeta^3 + \zeta^2 - \zeta + 2)t^{14} + \\ & (-5\zeta^5 - 2\zeta^4 - 3\zeta^3 - 6\zeta^2 - 2\zeta - 9)t^{13} + (10\zeta^5 + 4\zeta^4 + 9\zeta^2 + 20)t^{12} + \\ & (-35\zeta^5 - 36\zeta^4 - 30\zeta^3 - 35\zeta^2 - 4\zeta - 10)t^{11} + \\ & (44\zeta^5 - 10\zeta^4 + 8\zeta^3 + 47\zeta^2 + 52\zeta + 85)t^{10} + \\ & (-57\zeta^5 - 17\zeta^4 - 63\zeta^3 + 29\zeta^2 - 27\zeta + 11)t^9 + \\ & (7\zeta^5 + 38\zeta^4 + 38\zeta^3 + 7\zeta^2 - 59)t^8 + \\ & (56\zeta^5 - 36\zeta^4 + 10\zeta^3 - 30\zeta^2 + 27\zeta + 38)t^7 + \\ & (-5\zeta^5 - 44\zeta^4 - 62\zeta^3 - 8\zeta^2 - 52\zeta + 33)t^6 + \\ & (-31\zeta^5 - 26\zeta^4 - 32\zeta^3 - 31\zeta^2 + 4\zeta - 6)t^5 + \\ & (9\zeta^5 + 4\zeta^3 + 10\zeta^2 + 20)t^4 + (-4\zeta^5 - \zeta^4 - 3\zeta^2 + 2\zeta - 7)t^3 + \\ & (2\zeta^5 + 3\zeta^4 + 2\zeta^3 + 3\zeta^2 + \zeta + 3)t^2 - t \end{aligned} $
$(K_2, \chi_0^\alpha)$	$ \begin{aligned} & t^{15} + (-\theta - 2)t^{14} + (-2\theta - 1)t^{13} + (3\theta + 3)t^{12} + (-13\theta - 22)t^{11} + \\ & (-15\theta - 5)t^{10} + (25\theta + 13)t^9 - 82t^8 + (-25\theta - 12)t^7 + \\ & (15\theta + 10)t^6 + (13\theta - 9)t^5 - 3\theta t^4 + (2\theta + 1)t^3 + (\theta - 1)t^2 + t \end{aligned} $
$(K_2, \chi_0^\beta)$	$ \begin{aligned} & t^{15} + (-4\theta - 7)t^{14} + (16\theta + 15)t^{13} + (-41\theta - 26)t^{12} + \\ & (55\theta + 5)t^{11} + (-20\theta - 18)t^{10} + (-25\theta + 114)t^9 - 292t^8 + \\ & (25\theta + 139)t^7 + (20\theta + 2)t^6 + (-55\theta - 50)t^5 + (41\theta + 15)t^4 + \\ & (-16\theta - 1)t^3 + (4\theta - 3)t^2 + t \end{aligned} $
$(K_2, \chi_1^{\alpha\beta})$	$ \begin{aligned} & t^{15} + (-3\zeta^5 + 3\zeta^4 - 2\zeta^3 + \zeta^2 - 4)t^{14} + \\ & (4\zeta^5 - 12\zeta^4 + 6\zeta^3 - 13\zeta^2 + \zeta)t^{13} + \\ & (23\zeta^4 + 9\zeta^3 + 30\zeta^2 - 4\zeta + 17)t^{12} + \\ & (-49\zeta^5 - 17\zeta^4 - 50\zeta^3 - 46\zeta^2 - 33\zeta - 13)t^{11} + \\ & (-48\zeta^5 + 5\zeta^4 + 67\zeta^3 - 34\zeta^2 + 87\zeta - 36)t^{10} + \\ & (164\zeta^5 + 69\zeta^4 + 127\zeta^3 + 39\zeta^2 + 83\zeta + 75)t^9 + \\ & (173\zeta^5 + 32\zeta^4 + 32\zeta^3 + 173\zeta^2 + 166)t^8 + \\ & (-44\zeta^5 + 44\zeta^4 - 14\zeta^3 + 81\zeta^2 - 83\zeta - 8)t^7 + \\ & (-121\zeta^5 - 20\zeta^4 - 82\zeta^3 - 135\zeta^2 - 87\zeta - 123)t^6 + \\ & (-13\zeta^5 - 17\zeta^4 + 16\zeta^3 - 16\zeta^2 + 33\zeta + 20)t^5 + \\ & (34\zeta^5 + 13\zeta^4 + 27\zeta^3 + 4\zeta^2 + 4\zeta + 21)t^4 + \\ & (-14\zeta^5 + 5\zeta^4 - 13\zeta^3 + 3\zeta^2 - \zeta - 1)t^3 + \\ & (\zeta^5 - 2\zeta^4 + 3\zeta^3 - 3\zeta^2 - 4)t^2 + t \end{aligned} $

$(K_2, \chi_1^{\beta\alpha})$	$ \begin{aligned} & t^{15} + (-\zeta^5 - 2\zeta^4 + \zeta^2 - 3\zeta - 7)t^{14} + \\ & (4\zeta^5 + 8\zeta^4 - 4\zeta^3 - 4\zeta^2 + 17\zeta + 28)t^{13} + \\ & (-\zeta^5 - 20\zeta^4 + 21\zeta^3 + 30\zeta^2 - 52\zeta - 78)t^{12} + \\ & (-10\zeta^5 + 38\zeta^4 - 51\zeta^3 - 88\zeta^2 + 122\zeta + 187)t^{11} + \\ & (81\zeta^5 - 15\zeta^4 + 87\zeta^3 + 205\zeta^2 - 155\zeta - 358)t^{10} + \\ & (-256\zeta^5 - 31\zeta^4 - 157\zeta^3 - 312\zeta^2 + 91\zeta + 487)t^9 + \\ & (434\zeta^5 + 146\zeta^4 + 146\zeta^3 + 434\zeta^2 - 430)t^8 + \\ & (-403\zeta^5 - 248\zeta^4 - 122\zeta^3 - 347\zeta^2 - 91\zeta + 396)t^7 + \\ & (360\zeta^5 + 242\zeta^4 + 140\zeta^3 + 236\zeta^2 + 155\zeta - 203)t^6 + \\ & (-210\zeta^5 - 173\zeta^4 - 84\zeta^3 - 132\zeta^2 - 122\zeta + 65)t^5 + \\ & (82\zeta^5 + 73\zeta^4 + 32\zeta^3 + 51\zeta^2 + 52\zeta - 26)t^4 + \\ & (-21\zeta^5 - 21\zeta^4 - 9\zeta^3 - 13\zeta^2 - 17\zeta + 11)t^3 + \\ & (4\zeta^5 + 3\zeta^4 + \zeta^3 + 2\zeta^2 + 3\zeta - 4)t^2 + t \end{aligned} $
$(K_3, \chi_0^\alpha) = (K_3, \chi_2^{\alpha\beta})$	$ \begin{aligned} & t^{15} + (\theta - 3)t^{14} + (-3\theta - 1)t^{13} + (-2\theta - 22)t^{12} + (-73\theta - 8)t^{11} + \\ & (10\theta + 239)t^{10} + (362\theta + 223)t^9 - 675t^8 + (-362\theta - 139)t^7 + \\ & (-10\theta + 229)t^6 + (73\theta + 65)t^5 + (2\theta - 20)t^4 + (3\theta + 2)t^3 + \\ & (-\theta - 4)t^2 + t \end{aligned} $
$(K_3, \chi_0^\beta)$	$ \begin{aligned} & t^{15} - 7t^{14} + (-2\theta + 17)t^{13} + (6\theta - 32)t^{12} + (-26\theta + 26)t^{11} + \\ & (24\theta + 8)t^{10} + (40\theta + 83)t^9 - 178t^8 + (-40\theta + 43)t^7 + \\ & (-24\theta - 16)t^6 + (26\theta + 52)t^5 + (-6\theta - 38)t^4 + (2\theta + 19)t^3 - 7t^2 + t \end{aligned} $
$(K_3, \chi_3^{\beta\alpha})$	$ \begin{aligned} & t^{15} + (-\zeta^5 + 3\zeta^4 + 2\zeta^3 + 2\zeta^2 + 4\zeta - 3)t^{14} + \\ & (18\zeta^5 + \zeta^4 + 3\zeta^3 + 3\zeta^2 - 4\zeta + 11)t^{13} + \\ & (-33\zeta^5 - 17\zeta^4 - 26\zeta^3 - 21\zeta^2 - 11\zeta - 60)t^{12} + \\ & (-5\zeta^5 - 52\zeta^4 - 16\zeta^3 - 3\zeta^2 - 56\zeta + 45)t^{11} + \\ & (-14\zeta^5 + 48\zeta^4 + 66\zeta^3 - 18\zeta^2 + 59\zeta - 5)t^{10} + \\ & (106\zeta^5 + 89\zeta^4 - 10\zeta^3 + 109\zeta^2 + 18\zeta + 101)t^9 + \\ & (-133\zeta^5 - 123\zeta^4 - 123\zeta^3 - 133\zeta^2 - 212)t^8 + \\ & (91\zeta^5 - 28\zeta^4 + 71\zeta^3 + 88\zeta^2 - 18\zeta + 83)t^7 + \\ & (-77\zeta^5 + 7\zeta^4 - 11\zeta^3 - 73\zeta^2 - 59\zeta - 64)t^6 + \\ & (53\zeta^5 + 40\zeta^4 + 4\zeta^3 + 51\zeta^2 + 56\zeta + 101)t^5 + \\ & (-10\zeta^5 - 15\zeta^4 - 6\zeta^3 - 22\zeta^2 + 11\zeta - 49)t^4 + \\ & (7\zeta^5 + 7\zeta^4 + 5\zeta^3 + 22\zeta^2 + 4\zeta + 15)t^3 + \\ & (-2\zeta^5 - 2\zeta^4 - \zeta^3 - 5\zeta^2 - 4\zeta - 7)t^2 + t \end{aligned} $

# References

---

- [AGL18] P. Aceto, M. Golla, and A. G. Lecuona. “Handle decompositions of rational homology balls and Casson-Gordon invariants”. In: *Proceedings of the American Mathematical Society* 146.9 (2018), pp. 4059–4072.
- [AMMMPS20] P. Aceto, J. Meier, A. N. Miller, M. Miller, J. Park, and A. I. Stipsicz. *Branched covers bounding rational homology balls*. 2020. arXiv: [2002.10324 \[math.GT\]](#).
- [AÖ01] S. Akbulut and B. Özbağcı. “Lefschetz fibrations on compact Stein surfaces”. In: *Geometry & Topology* 5.1 (2001), pp. 319–334.
- [Ale23] J. W. Alexander. “A lemma on a system of knotted curves”. In: *Proceedings of the National Academy of Sciences of the United States of America* 9.3 (1923), pp. 93–95.
- [Art25] E. Artin. “Theorie der Zöpfe”. In: *Abhandlungen aus dem Mathematischen Seminar der Universität Hamburg* 4 (1925), pp. 47–72.
- [Aum56] R. Aumann. “Asphericity of alternating knots”. In: *Annals of Mathematics* 64.2 (1956), pp. 374–392.
- [BEVHM10] K. Baker, J. Etnyre, and J. Van Horn-Morris. “Cabling, contact structures and mapping class monoids”. In: *Journal of Differential Geometry* 90.1 (2010), pp. 1–80.
- [BE13] J. Baldwin and J. Etnyre. “Admissible transverse surgery does not preserve tightness”. In: *Mathematische Annalen* 357 (2013), pp. 441–468.
- [Ben83] D. Bennequin. “Entrelacements et équations de Pfaff”. In: *IIIe rencontre de géométrie du Schnepfenried, Vol. 1*. Astérisque 107–108. Société mathématique de France, 1983.
- [Bow12] J. Bowden. “Exactly fillable contact structures without Stein fillings”. In: *Algebraic & Geometric Topology* 12.3 (2012), pp. 1803–1810.
- [BW21] V. Brejevs and A. Wand. *Stein-fillable open books of genus one that do not admit positive factorisations*. 2021. arXiv: [2103.13250 \[math.GT\]](#).

- [Bre20] V. Brejevs. *On slice alternating 3-braid closures*. 2020. arXiv: [2012.00577](https://arxiv.org/abs/2012.00577) [[math.GT](#)].
- [Col16] J. Collins. “An algorithm for computing the Seifert matrix of a link from a braid representation”. In: *Ensaaios Matemáticos* 30 (2016), pp. 246–262.
- [Con19a] J. Conway. “Tight contact structures via admissible transverse surgery”. In: *Journal of Knot Theory and Its Ramifications* 28.04 (2019), p. 1950032.
- [Con19b] J. Conway. “Transverse surgery on knots in contact 3-manifolds”. In: *Transactions of the American Mathematical Society* 372.3 (2019), pp. 1671–1707.
- [Cro89] P. R. Cromwell. “Homogeneous links”. In: *Journal of the London Mathematical Society* s2–39.3 (1989), pp. 535–552.
- [Cro55] R. Crowell. “Invariants of alternating link types”. PhD thesis. Princeton University, 1955.
- [CDGW] M. Culler, N. Dunfield, M. Goerner, and J. Weeks. *SnapPy, a computer program for studying the geometry and topology of 3-manifolds*. Available at <http://snappy.computop.org> (26/02/2021).
- [Deh87] M. Dehn. “Papers on group theory and topology”. In: ed. by J. Stillwell. Berlin–New York: Springer-Verlag, 1987. Chap. The group of mapping classes, pp. 256–362.
- [DO12] A. Donald and B. Owens. “Concordance groups of links”. In: *Algebraic & Geometric Topology* 12.4 (2012), pp. 2069–2093.
- [Don87] S. K. Donaldson. “The orientation of Yang–Mills moduli spaces and 4-manifold topology”. In: *Journal of Differential Geometry* 26.3 (1987), pp. 397–428.
- [Eli89] Y. Eliashberg. “Classification of overtwisted contact structures on 3-manifolds”. In: *Inventiones Mathematicae* 98 (1989), pp. 623–637.
- [Eli90a] Y. Eliashberg. “Filling by holomorphic discs and its applications”. In: *Geometry of low-dimensional manifolds*. Vol. 151. London Mathematical Society Lecture Note Series 2. Cambridge University Press, 1990, pp. 45–67.
- [Eli90b] Y. Eliashberg. “Topological characterization of Stein manifolds of dimension  $>2$ ”. In: *International Journal of Mathematics* 1.1 (1990), pp. 29–46.
- [Eli96] Y. Eliashberg. “Unique holomorphically fillable contact structure on the 3-torus”. In: *International Mathematics Research Notices* 2 (1996), pp. 77–82.

- [EP94] Y. Eliashberg and L. Polterovich. “New applications of Luttinger’s surgery”. In: *Commentarii Mathematici Helvetici* 69.4 (1994), pp. 512–522.
- [Etn04] J. Etnyre. *Lectures on open book decompositions and contact structures*. 2004. arXiv: [math/0409402](https://arxiv.org/abs/math/0409402) [[math.SG](#)].
- [EH99] J. Etnyre and K. Honda. “On the nonexistence of tight contact structures”. In: *Annals of Mathematics* 153 (1999), pp. 749–766.
- [EH02] J. Etnyre and K. Honda. “Tight contact structures with no symplectic fillings”. In: *Inventiones Mathematicae* 148 (2002), pp. 609–626.
- [FM11] B. Farb and D. Margalit. *A Primer on Mapping Class Groups*. Princeton University Press, 2011.
- [FL19] P. Feller and L. Lewark. *Balanced algebraic unknotting, linking forms, and surfaces in three- and four-space*. 2019. arXiv: [1905.08305](https://arxiv.org/abs/1905.08305) [[math.GT](#)].
- [Fox62] R. H. Fox. “A quick trip through knot theory”. In: *Topology of 3-manifolds and related topics (Proceedings of The University of Georgia Institute, 1961)*. Prentice-Hall, Englewood Cliffs, New Jersey, 1962, pp. 120–167.
- [FM66] R. H. Fox and J. W. Milnor. “Singularities of 2-spheres in 4-space and cobordism of knots”. In: *Osaka Journal of Mathematics* 3.2 (1966), pp. 257–267.
- [FP17] S. Friedl and M. Powell. “A calculation of Blanchfield pairings of 3-manifolds and knots”. In: *Moscow Mathematical Journal* 17.1 (2017), pp. 59–77.
- [FV11] S. Friedl and S. Vidussi. “A survey of twisted Alexander polynomials”. In: *The Mathematics of Knots*. Vol. 1. Springer, 2011, pp. 45–94.
- [Gay02] D. Gay. “Symplectic 2-handles and transverse links”. In: *Transactions of the American Mathematical Society* 354 (2002), pp. 1027–1047.
- [Gei08] H. Geiges. *An Introduction to Contact Topology*. Cambridge University Press, 2008.
- [Ger96] S. Gervais. “Presentation and central extensions of mapping class groups”. In: *Transactions of the American Mathematical Society* 348.8 (1996), pp. 3097–3132.
- [Ghi05a] P. Ghiggini. “Strongly fillable contact 3-manifolds without Stein fillings”. In: *Geometry & Topology* 9 (2005), pp. 1677–1687.
- [Ghi05b] P. Ghiggini. “Tight contact structures on Seifert manifolds over  $T^2$  with one singular fibre”. In: *Algebraic & Geometric Topology* 5.2 (2005), pp. 785–833.

- [GLS06] P. Ghiggini, P. Lisca, and A. I. Stipsicz. “Classification of tight contact structures on small Seifert 3-manifolds with  $e_0 \geq 0$ ”. In: *Proceedings of the American Mathematical Society* 134.3 (2006), pp. 909–916.
- [Gir02] E. Giroux. “Géométrie de contact: de la dimension trois vers les dimensions supérieures”. In: *Proceedings of the International Congress of Mathematicians*. 2002, pp. 405–414.
- [Gir94] E. Giroux. “Une structure de contact, même tendue, est plus ou moins tordue”. In: *Annales scientifiques de l’École Normale Supérieure 4e série*, 27.6 (1994), pp. 697–705.
- [Goe33] L. Goeritz. “Knoten und quadratische Formen”. In: *Mathematische Zeitschrift* 36 (1933), pp. 647–654.
- [Gom98] R. E. Gompf. “Handlebody construction of Stein surfaces”. In: *Annals of Mathematics* 148.2 (1998), pp. 619–693.
- [GS99] R. E. Gompf and A. I. Stipsicz. *4-manifolds and Kirby calculus*. American Mathematical Society, 1999.
- [Goo05] N. Goodman. “Overtwisted open books from sobering arcs”. In: *Algebraic & Geometric Topology* 5.3 (2005), pp. 1173–1195.
- [GL78] C. M. Gordon and R. A. Litherland. “On the signature of a link”. In: *Inventiones Mathematicae* 47.1 (1978), pp. 53–69.
- [Gra59] J. Gray. “Some global properties of contact structures”. In: *Annals of Mathematics* 69.2 (1959), pp. 421–450.
- [Gre17] J. E. Greene. “Alternating links and definite surfaces”. In: *Duke Mathematical Journal* 166 (2017), pp. 2133–2151.
- [GJ11] J. E. Greene and S. Jabuka. “The slice-ribbon conjecture for 3-stranded pretzel knots”. In: *American Journal of Mathematics* 133.3 (2011), pp. 555–580.
- [Gro85] M. Gromov. “Pseudoholomorphic curves in symplectic manifolds”. In: *Inventiones Mathematicae* 82 (1985), pp. 307–347.
- [HP13] M. Hedden and O. Plamenevskaya. “Dehn surgery, rational open books and knot Floer homology”. In: *Algebraic & Geometric Topology* 13.3 (2013), pp. 1815–1856.
- [Hem76] J. Hempel. *3-manifolds*. Princeton University Press, 1976.
- [HKL10] C. Herald, P. Kirk, and C. Livingston. “Metabelian representations, twisted Alexander polynomials, knot slicing, and mutation”. In: *Mathematische Zeitschrift* 265 (2010), pp. 925–949.
- [Hon00a] K. Honda. “On the classification of tight contact structures I”. In: *Geometry & Topology* 4.1 (2000), pp. 309–368.

- [Hon00b] K. Honda. “On the classification of tight contact structures II”. In: *Journal of Differential Geometry* 55.1 (2000), pp. 83–143.
- [How17] J. Howie. “A characterisation of alternating knot exteriors”. In: *Geometry & Topology* 21 (2017), pp. 2353–2371.
- [Joh79] D. Johnson. “Homeomorphisms of a surface which acts trivially on homology”. In: *Proceedings of the American Mathematical Society* 75.1 (1979), pp. 119–125.
- [Kau87] L. H. Kauffman. *On knots*. Princeton: University Press, 1987.
- [KL99] P. Kirk and C. Livingston. “Twisted Alexander invariants, Reidemeister torsion, and Casson–Gordon invariants”. In: *Topology* 38.3 (1999), pp. 635–661.
- [Lec12] A. G. Lecuona. “On the slice-ribbon conjecture for Montesinos knots”. In: *Transactions of the American Mathematical Society* 364.1 (2012), pp. 233–285.
- [Lec15] A. G. Lecuona. “On the slice-ribbon conjecture for pretzel knots”. In: *Algebraic & Geometric Topology* 15.4 (2015), pp. 2133–2173.
- [LL11] A. G. Lecuona and P. Lisca. “Stein fillable Seifert fibered 3-manifolds”. In: *Algebraic & Geometric Topology* 11 (2011), pp. 625–642.
- [Ler01] E. Lerman. “Contact cuts”. In: *Israel Journal of Mathematics* 124 (2001), pp. 77–92.
- [Lic62] W. B. R. Lickorish. “A representation of orientable combinatorial 3-manifolds”. In: *Annals of Mathematics* 76.531–540 (1962).
- [Lis07] P. Lisca. “Lens spaces, rational balls and the ribbon conjecture”. In: *Geometry & Topology* 11 (2007), pp. 429–472.
- [Lis17] P. Lisca. “On 3-braid knots of finite concordance order”. In: *Transactions of the American Mathematical Society* 369.7 (2017), pp. 5087–5112.
- [Lis14] P. Lisca. “Stein fillable contact 3-manifolds and positive open books of genus one”. In: *Geometry & Topology* 14 (2014), pp. 2411–2430.
- [LP01] A. Loi and R. Piergallini. “Compact Stein surfaces with boundary as branched covers of  $B^4$ ”. In: *Inventiones Mathematicae* 143 (2001), pp. 325–348.
- [Luo97] F. Luo. “A presentation of the mapping class groups”. In: *Mathematical Research Letters* 4 (1997), pp. 735–739.
- [Mar36] A. Markov. “Über die freie Äquivalenz der geschlossenen Zöpfe”. In: *Recueil Mathématique* 1.43 (1936), pp. 73–78.

- [Mar71] J. Martinet. “Formes de contact sur les variétés de dimension 3”. In: *Proceedings of Liverpool Singularities Symposium II*. Vol. 209. Lecture Notes in Mathematics. Berlin: Springer-Verlag, 1971, pp. 142–163.
- [Mat18] I. Matkovič. “Classification of tight contact structures on small Seifert fibered  $L$ -spaces”. In: *Algebraic & Geometric Topology* 18.1 (2018), pp. 111–152.
- [McD90] D. McDuff. “The structure of rational and ruled symplectic 4-manifolds”. In: *Journal of the American Mathematical Society* 3.3 (1990), pp. 679–712.
- [Mos71] L. Moser. “Elementary surgery along a torus knot”. In: *Pacific Journal of Mathematics* 38 (1971), pp. 737–745.
- [Mur74] K. Murasugi. *On closed 3-braids*. American Mathematical Society, 1974.
- [OS21] B. Owens and F. Swenton. *An algorithm to find ribbon disks for alternating knots*. 2021. arXiv: [2102.11778](https://arxiv.org/abs/2102.11778) [math.GT].
- [ÖS04] B. Özbağcı and A. I. Stipsicz. *Surgery on Contact 3-Manifolds and Stein Surfaces*. Vol. 13. Bolyai Society Mathematical Studies. Berlin: Springer-Verlag, 2004.
- [OS05] P. Ozsváth and Z. Szabó. “Heegaard Floer homology and contact structures”. In: *Duke Mathematical Journal* 129.1 (2005), pp. 39–61.
- [OS03] P. Ozsváth and Z. Szabó. “Knot Floer homology and the four-ball genus”. In: *Geometry & Topology* 7.2 (2003), pp. 615–639.
- [Pla04] O. Plamenevskaya. “Contact structures with distinct Heegaard Floer invariants”. In: *Mathematical Research Letters* 11 (2004), pp. 547–561.
- [PVHM10] O. Plamenevskaya and J. Van Horn-Morris. “Planar open books, monodromy factorizations and symplectic fillings”. In: *Geometry & Topology* 14.4 (2010), pp. 2077–2101.
- [Ple95] W. Plesken. “Solving  $XX^{\text{tr}} = A$  over the integers”. In: *Linear Algebra and its Applications* 226–228 (1995), pp. 331–344.
- [Ras10] J. Rasmussen. “Khovanov homology and the slice genus”. In: *Inventiones Mathematicae* 182.2 (2010), pp. 419–447.
- [Sar10] A. Sartori. “Knot concordance in three manifolds”. MA thesis. University of Pisa, 2010.
- [See14] A. Seeliger. “Symmetrische Vereinigungen als Darstellungen von Bandknoten bis 14 Kreuzungen (Symmetric union presentations for ribbon knots up to 14 crossings)”. MA thesis. Stuttgart University, 2014.

- [Sei35] H. Seifert. “Über das Geschlecht von Knoten”. In: *Mathematische Annalen* 110 (1935), pp. 571–592.
- [Sim20] J. Simone. *Classification of torus bundles that bound rational homology circles*. 2020. arXiv: [2006.14986](https://arxiv.org/abs/2006.14986) [math.GT].
- [Sto03] A. Stoimenow. “The skein polynomial of closed 3-braids”. In: *Journal für die reine und angewandte Mathematik* 564 (2003), pp. 167–180.
- [TW75] W. P. Thurston and H. E. Winkelnkemper. “On the existence of contact forms”. In: *Proceedings of the American Mathematical Society* 52.1 (1975), pp. 345–347.
- [Tos20] B. Tosun. “Tight small Seifert fibered manifolds with  $e_0 = -2$ ”. In: *Algebraic & Geometric Topology* 20.1 (2020), pp. 1–27.
- [Tsu09] T. Tsukamoto. “The almost alternating diagrams of the trivial knot”. In: *Journal of Topology* 2 (2009), pp. 77–104.
- [Wan15] A. Wand. “Factorizations of diffeomorphisms of compact surfaces with boundary”. In: *Geometry & Topology* 19 (2015), pp. 2407–2464.
- [Wei91] A. Weinstein. “Contact surgery and symplectic handlebodies”. In: *Hokkaido Mathematical Journal* 20 (1991), pp. 241–251.
- [Wen10] C. Wendl. “Strongly fillable contact manifolds and  $J$ -holomorphic foliations”. In: *Duke Mathematical Journal* 151.3 (2010), pp. 337–384.